Suboptimal Period Design for a Maneuvering Missile to Evade Tracking Filters

by

Lin-Ying Lai

Dissertation submitted to the Faculty of the

Virginia Polytechnic Institute and State University

in partial fulfillment of the requirements for the degree of

Doctor of Philosophy

in

Aerospace and Ocean Engineering

APPROVED:

Harold L. Stalford, Chairman

Eugene M. Cliff

Frederick H. Lutze

John A. Burns

Scott L. Hendricks

July, 1988

Blacksburg, Virginia

Suboptimal Period Design for a Maneuvering Missile to Evade Tracking Filters

by

Lin-Ying Lai

Harold L. Stalford, Chairman

Aerospace and Ocean Engineering

(ABSTRACT)

The engagement between an antiship missile and a ship's defence system is investigated. The missile is equipped with proportional navigation guidance for homing in on its ship target. The ship's defense system consists of a radar, an estimation system (the extended Kalman filter and the "jump filter" are used), and a gun system.

The performance index is defined as the estimated number of hits (EHITS) of projectiles on the missile. The main objective of this dissertation is to determine maneuvering periods for the missile which minimize the EHITS to evade the ship's gunfire under different engagement conditions. The maneuvering periods are design parameters in the missile's controls of both the vertical and the horizontal planes. The engagement conditions are the follows : the maximum amplitude of the maneuvering functions, the homing in position of the missile on the ship, the measurement noise condition of the ship's radar, and the missile's model assumed in the ship's filters. The missile's control functions considered are periodic and of specific types (sinusoidal, square and sawtooth waveforms); therefore,

the periods which minimize the EHITS in this study are suboptimal for the general engagement problem.

Two methods are used to obtain the suboptimal periods: one is the "brute force" method of computing the EHITS for certain equally spaced periods, the other uses an optimization software to search for the minimum point. The results show that the curve of EHITS vs. period is monotonically decreasing until it reaches a minimum point. The optimal period increases with an increase in measurement noise. Among the three waveforms used, the square wave gives the smallest optimal period and the sawtooth wave gives the largest one. The sinusoidal waveform with the period of 1.9 seconds is recommended. We consider the missile's performance against a perfect radar, a modern radar, and an earlier model radar. The optimum EHITS resulting from the optimal periods are between two and three EHITS for all three radars considered.

Acknowledgements

The author is greatly indebted to Dr. Harold Stalford for the help and guidance he has given. The author wish to extend her sincere appreciation to Dr. J. A. Burns, Dr. E. M. Cliff, Dr. S. L. Hendricks, and Dr. F. H. Lutze for serving on her committee. Special thanks go to Dr. D. W. Mckeon for his correction on part of this dissertation.

The author is especially grateful to her dear husband for his support and encouragement during this period.

Table of Contents

Chapter 1 Introduction and Problem Statement 1

1.1 Introduction and Problem Statement 1

1.2 Dissertation Outline 5

Chapter 2 Model Description 8

2.1 Missile Model 8

2.1.1 Thrust Model 11

2.1.2 Lift Model 12

2.1.3 Drag Model 14

2.1.4 Maneuver Model 15

2.2 Projectile Model 18

2.3 Performance Model 25

2.4 Engagement Model 26

Chapter 3 Extended Kalman Filter 28

3.1 Algorithm for EKF 30

3.1.1 The Propagation Phase 32
3.1.2 The Update Phase 33
3.2 Application of EKF to Our Problem 34
3.3 Jacobian Matrix for R-filter 39
3.4 Jacobian Matrix for E-filter 42
3.5 Jacobian Matrix for A-filter 44

Chapter 4 Jump Filter **47**
4.1 Residual Test for Jump Detection 49
4.2 Δ State Equations 51
4.2.1 The Δx State Equation 51
4.2.2 Δu State Equation 53
4.2.3 Δy State Equation 54
4.3 Estimation of Jump 56
4.4 Moving Window and Reinitialization 60

Chapter 5 Parameters Description **65**
5.1 Parameters That Relate to the Missile 66
5.1.1 Offset Parameter 66
5.1.2 Maneuver Starting Range Parameter 67
5.2 Parameters That Relate to the Ship's Filter 68
5.2.1 Process Noise Parameter 68
5.2.2 Initial Conditions 69
5.2.3 Measurement Noise Values 70
5.2.4 PN Constant Parameter 71
5.3 The Case Number Tables 72
5.4 Comment on Parameters 73

Chapter 6 Program description **80**

6.1 The Main Program 80

6.2 The EHITS Module (The Subroutine EVAL) 83

6.3 The Missile's Trajectory Module 83

6.4 The Filters Module 85

6.4.1 The EKF Module 85

6.4.2 The JTF Module 86

6.5 The Projectile's Trajectory Module 87

6.6 The POH Module 88

6.7 The Optimization Module 89

Chapter 7 Result and Discussion **93**

7.1 Cases Without Maneuvering 94

7.2 PN System Results 98

7.3 NOPN System Results 102

7.3.1 Results from No-Offset Condition 102

7.3.2 Results for the Nonzero Offset Condition 104

7.3.3 Influence of Maneuvering Period on Estimations 106

7.4 Comparison Between Three Maneuvering Functions 107

7.5 Optimization Cases 113

Chapter 8 Conclusion **114**

Bibliography **117**

FIGURES **122**

Appendix A. Program Description 152

Appendix B. Program Input Variables Description 156

Vita 158

List of Illustrations

Figure 1. Cost (EHITS) vs. Period Plot for Case No. 115, Sinusoidal Wave. 122

Figure 2. Cost (EHITS) vs. Period Plot for Case No. 121, Sinusoidal Wave. 123

Figure 3. Cost (EHITS) vs. Period Plot for Case No. 123, Sinusoidal Wave. 124

Figure 4. Cost (EHITS) vs. Period Plot for Case No. 139, Sinusoidal Wave. 125

Figure 5. Cost (EHITS) vs. Period Plot for Case No. 145, Sinusoidal Wave. 126

Figure 6. Cost (EHITS) vs. Period Plot for Case No. 147, Sinusoidal Wave. 127

Figure 7. Cost (EHITS) vs. Period Plot for Case No. 163, Sinusoidal Wave. 128

Figure 8. Cost (EHITS) vs. Period Plot for Case No. 169, Sinusoidal Wave. 129

Figure 9. Cost (EHITS) vs. Period Plot for Case No. 171, Sinusoidal Wave. 130

Figure 10. Cost (EHITS) vs. Period Plot for Case No. 123, Square Wave. 131

Figure 11. Cost (EHITS) vs. Period Plot for Case No. 147, Square Wave. 132

Figure 12. Cost (EHITS) vs. Period Plot for Case No. 171, Square Wave. 133

Figure 13. Cost (EHITS) vs. Period Plot for Case No. 123, Sawtooth Wave. 134

Figure 14. Cost (EHITS) vs. Period Plot for Case No. 147, Sawtooth Wave. 135

Figure 15. Cost (EHITS) vs. Period Plot for Case No. 171, Sawtooth Wave. 136

Figure 16. EHITS Points for Optimization Process, Case No. 147, Sinusoidal Wave. 137

Figure 17. EHITS Points for Optimization Process, Case No. 147, Square Wave. 138

Figure 18. EHITS Points for Optimization Process, Case No. 147, Sawtooth Wave. 139

Figure 19. Probability of Hits vs. Range, Case No. 123, Period = 0.9, Sinusoidal Wave. 140

Figure 20. Accumulated Probability of Hits vs. Range, Case No. 123, Period = 0.9, Sinusoidal Wave. 141

Figure 21. True and Estimated y vs. x, Case No. 123, Period = 0.9, Sinusoidal Wave. 142

Figure 22. True and Estimated z vs. R, Case No. 123, Period = 0.9, Sinusoidal Wave. 143

Figure 23. Probability of Hits vs. Range, Case No. 123, Period = 1.9, Sinusoidal Wave. 144

Figure 24. Accumulated Probability of Hits vs. Range, Case No. 123, Period = 1.9, Sinusoidal Wave. 145

Figure 25. True and Estimated y vs. x, Case No. 123, Period = 1.9, Sinusoidal Wave. 146

Figure 26. True and Estimated z vs. R, Case No. 123, Period = 1.9, Sinusoidal Wave. 147

Figure 27. Probability of Hits vs. Range, Case No. 123, Period = 2.9, Sinusoidal Wave. 148

Figure 28. Accumulated Probability of Hits vs. Range, Case No. 123, Period = 2.9, Sinusoidal Wave. 149

Figure 29. True and Estimated y vs. x, Case No. 123, Period = 2.9, Sinusoidal Wave. 150

Figure 30. True and Estimated z vs. R, Case No. 123, Period = 2.9, Sinusoidal Wave. 151

List of Tables

Table 1. Parameters Values for the PN System as a Function of the Case No. 74

Table 2. Parameters Values for the NOPN System as a Function of the Case No. 77

Table 3. EHITS for the No-Maneuver cases for the PN System 94

Table 4. EHITS for the No-Maneuver cases for the NOPN System 94

Table 5. EHITS at optimal period for cases EHITS at optimal period for cases No. 1-12 : PN System, No Offset, No Noise. 98

Table 6. EHITS at optimal period for cases No. 25-36 : PN System, No Offset, Small Noise. 98

Table 7. EHITS at optimal period for cases No. 49-60 : PN System, No Offset, Large Noise. 98

Table 8. EHITS at optimal period for cases No. 101-112 : NOPN System, No Offset, No Noise. 101

Table 9. EHITS at optimal period for cases No. 125-136 : NOPN System, No Offset, Small Noise. 102

Table 10. EHITS at optimal period for cases No. 149-160 : NOPN System, No Offset, Large Noise. 102

Table 11. EHITS at optimal period for cases No. 113-124 : NOPN System, Offset, No Noise. 104

Table 12. EHITS at optimal period for cases No. 137-148 : NOPN System, Offset, Small Noise. 104

Table 13. EHITS at optimal period for cases No. 161-172 : NOPN System, Offset, Large Noise. 104

Table 14. Parametric Values and Case No. for the Redo Cases for the Sinusoidal Maneuvering Function 107

Table 15. Comparison Between Three Maneuvering Functions 109

Chapter 1 Introduction and Problem Statement

1.1 Introduction and Problem Statement

We investigate the engagement between an anti-ship missile and a ship's defense system. The ship is equipped with a fire control system consisting of a radar, a filter and a gun system to track the missile's trajectory, to predict the missile's future path, and to bombard it with projectiles. The objective of the ship is to maximize the "estimated number of hits" (EHITS) of projectiles on the missile. In order to meet this objective, the ship needs to filter radar data, estimate the missile's states, predict the missile's future path, and intercept it with a steady stream of projectiles by aiming a gun with the proper coordinates. On the other side, the missile is equipped with proportional navigation (PN) guidance for homing in on the ship and two control variables for maneuvering to evade the ship's gunfire. The objective of the missile is to maximize its survivability while

en route to its ship target. It desires, therefore, to minimize the EHITS. In order to meet this objective, the missile needs to optimally shape its trajectory using the two control variables while homing in on the ship. One control variable shapes the missile trajectory in the vertical plane, and the other shapes it in the horizontal plane. An optimal shape is the one which minimizes the EHITS.

The problem investigated in this dissertation deals with the design of the missile's two open-loop control histories which the missile can use optimally to evade gunfire. Periodic controls are considered. Sinusoidal, square and sawtooth waveforms are investigated. The specific problem addressed is what period will yield a minimum number of EHITS, how will the period vary from waveform to waveform, and how will the period depend on various parameters of the engagement. Since the waveforms considered are periodic and of specific types, the periods that minimizes the EHITS in this dissertation are suboptimal for the general engagement problem.

The cost function is the EHITS as a function of the period. It is reasonable to seek a period which minimizes the EHITS. For small periods the cost value is very high since the missile's trajectory maneuvers vary little from an easily predicted path and, consequently, the ship is able to place projectiles within a small miss distance radius of the missile's path. As the period is increased from zero the cost will decrease since the ship has difficulty in estimating small maneuvers that are masked by radar errors and undetected maneuvers generate larger miss distances. As the period is increased still further, the EHITS will reach a mini-

mum and then increase as the ship detects the maneuvers and predicts projectile interceptions more accurately. This study is conducted to determine the period yielding the minimum EHITS.

We use a point mass model for the missile. Proportional navigation (PN) is used to home the missile in on its ship target. One PN constant, N_1 is for homing in the vertical direction, and the other, N_3 is for the azimuth direction. N_1 and N_3 are set at 3.15 and 3.0, respectively. The missile has two control variables for generating maneuvers to evade the ship's gunfire. One control variable shapes the missile trajectory in the vertical plane, and the other shapes it in the horizontal plane. In the vertical direction, maximum maneuver g level of 1.5, 2.5, and 3.5 are considered. In the azimuth direction, the maximum maneuver g level considered are 1.0 and 2.0. The two control signals are considered to be periodic-sinusoidal, square, and saw-tooth waveforms. The main objective of this dissertation is to find the optimal period that minimizes the estimated number of projectile hits that the ship can place on the missile.

The ship measures the position of the missile using radar. It measures the missile's range, elevation and azimuth. We consider three different radars. The first is perfect. The second has the standard deviation radar errors of 15 ft in range, 0.003 rad. in elevation, and 0.001 rad. in azimuth. The third has 15 ft in range, 0.009 rad. in elevation, and 0.003 rad. in azimuth. The radar data is measured at the rate 20 samples per second. The radar data is filtered with a two-level filtering system. In the first level, an extended Kalman filter (EKF) is used to es-

timate the state vector of the missile. The state vector consists of three position coordinates, three velocity coordinates and three guidance parameters that govern the acceleration of the missile. The second level is used when the EKF diverges. This usually occurs when the missile maneuvers which it does by changing the values of its three guidance parameters. In the second level, a filter called the jump filter (JF) is used to estimate the change in the three guidance parameters by processing the residuals of the diverging EKF. The estimated states of the missile are used to predict its future path. A projectile intercept point on the predicted future path is determined by aiming a gun with the proper elevation and azimuth coordinates. The projectile flyout satisfies a bullet drag model and the law of gravity. The miss distance between the projectile's trajectory and the true missile's trajectory is computed. This miss distance, the relative velocity vector between the missile and the projectile, and the geometrical size of the missile are used to compute the probability of a hit. Projectiles are fired at a rate of 3000 rounds per minute. The accumulated probability of hits for the entire missile's trajectory is denoted as the estimated number of hits (EHITS). This is the cost function that the missile wishes to minimize by selecting an "optimal" period for the two periodic control functions that will evade optimally the ship's gunfire.

For use in its filtering system the ship must assume some model of the missile that it desires to track and to engage with a projectile. Two distinct models are used. They are both nonlinear point mass models. The first model which we term the PN system includes (1) proportional navigation which allows the missile to home in on the location of the ship's radar site and (2) three control parameters which

may take jumps to account for the missile's maneuvering to evade the ship's gunfire. This model assumes knowledge of the missile's PN constants. But this assumption is not a serious problem. The problem with this model is that it assumes that the missile's aim point on the ship is known. This is not the case and it cannot be estimated accurately enough until the missile impacts on the ship. The second model which we term the NOPN system consists only of the three guidance parameters to handle the acceleration of the missile as it maneuvers and homes in on its ship target. Proportional navigation is not a part of this model. Therefore, no assumption about the missile's PN constants are needed. Consequently, the NOPN system is a better model for the ship's filtering process since it involves quantities which are actually available to the ship. We use both systems and compare the results.

1.2 Dissertation Outline

This dissertation is arranged as follows : In chapter 2, the models used in our simulation are defined. Section 2.1 gives the various sub-models of the missile, including the dynamic model, the models of the thrust, the lift, and the drag, and the maneuvering guidance model. Section 2.2 gives a discretized equation of motion for the projectiles which are fired by the ship. Section 2.3 presents the performance index, or the cost function, used for the optimization process, while section 2.4 provides a description of the whole engagement model.

In chapter 3, the EKF technique is described. A literature review of the KF and the EKF is given. First, an algorithm for the EKF is given in section 3.1. The application of the EKF to our problem is then presented in section 3.2. Finally, the Jacobian matrices needed in the three filters in our application are derived in the remaining three sections.

In chapter 4, the JF technique is described. A literature review of the estimation problem on tracking of a maneuvering target is given. To trigger the execution of the JF, a jump detection function is required. This is presented in section 4.1. A diverging EKF posesses errors in the state which we denote as the Δ-state. Theses are govern by Δ-state equations. Three kinds of Δ-state equations, the Δx, the Δy, and the Δu states, are given in section 4.2. The jump time and the jump magnitude estimation, which uses the generalized likelihood ratio approach, is given in section 4.3. A moving window technique for storing data is discussed in section 4.4. In this section, a reinitialization technique is also provided to reset the stored data values to prevent them from excessively large values after a detected jump and after every certain interval.

In chapter 5, some parameters that we investigated in the period design are described. Parameters that relate to the missile's part are presented in section 5.1, and those that relate to the ship's filters are given in section 5.2. Two tables are given in section 5.3 to show the correspondence between these parameters and the case numbers which are referenced in the discussion. Some parameters that are

not listed in these two tables but mentioned in section 5.2 are discussed further in section 5.4 to show the values we use.

In chapter 6, a description of the simulation program is given. A flow chart is given to show the structure of the program. The main program description is given in section 6.1. Section 6.2 gives the description of the EHITS module (the subroutine EVAL). Section 6.3 gives the description of the missile's trajectory module. Section 6.4 gives the description of the filters' modules, which contains the EKF module and the JTF module. Section 6.5 gives the description of the projectile's trajectory module. Section 6.6 gives the description of the POH module, which computes the probability of a hit on the missile by a projectile. The optimization module is described in section 6.7.

Chapter 7 contains the discussion of the numerical results. The first three sections describe the results using the sinusoidal maneuvering function. Some observations on the no-maneuver cases are given in section 7.1. The PN system results and the NOPN system results are presented in sections 7.2 and 7.3, respectively. Here, the PN system denotes the cases that the proportional navigation (PN) guidance constants are known to the ship's filters and are used in the filters' model of the missile. On the other hand, the NOPN system denotes the cases not using the PN constants. Additional results come from the square wave and the sawtooth wave maneuvering functions as discussed in section 7.4. Some results using the optimization process are shown in section 7.5. At last, some conclusions are given in chapter 8.

Chapter 2 Model Description

2.1 *Missile Model*

The model given below for the missile uses a coordinate reference frame located on the ship with the origin at the ship's radar. There are 6 state variables, i.e. R, E, A, V, ϕ, and ψ and 3 control variables, i.e. N_2, N_4 and P_{3_g}.

$$\dot{R} = V[\sin\phi \sin E + \cos(\psi - A)\cos\phi \cos E] \tag{2.1}$$

$$\dot{E} = \frac{V}{R}[\sin\phi \cos E + \cos(\psi - A)\cos\phi \sin E] \tag{2.2}$$

$$\dot{A} = \frac{V}{R\cos E}[\sin(\psi - A)\cos\phi] \tag{2.3}$$

$$\dot{V} = \frac{T\cos\alpha - D}{m} - g\sin\phi \tag{2.4}$$

$$\dot{\phi} = -N_1\dot{E} + \frac{g}{V}\,[N_2 - \cos\phi\,] \tag{2.5}$$

$$\dot{\psi} = N_3\dot{A} + \frac{N_4 g}{V\cos\phi} \tag{2.6}$$

x-z Vertical Plane

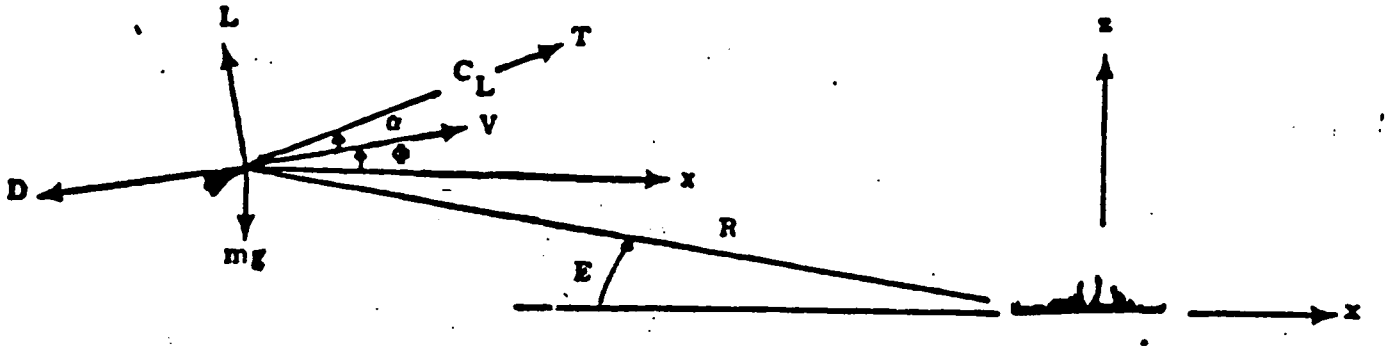

x-y Horizontal Plane

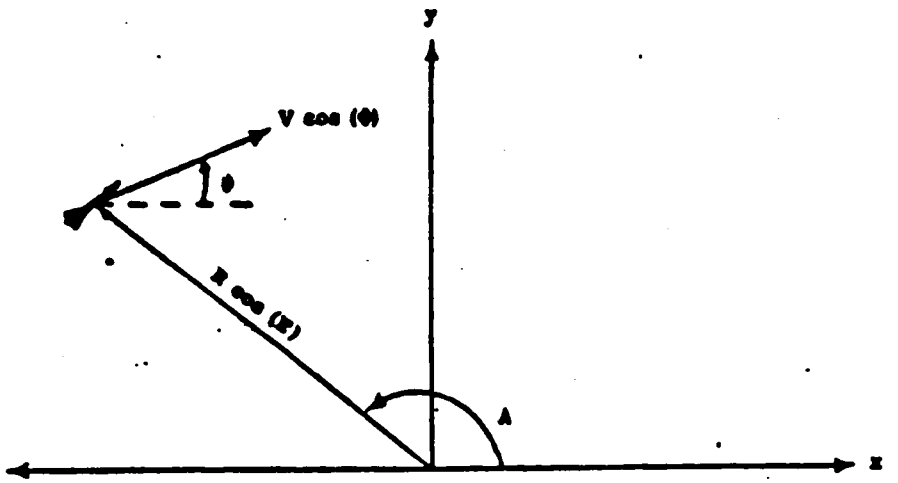

where

R is the range from the ship to the missile; (ft)

E is the elevation of the missile above the ship's radar site; (rad)

A is the azimuth (or bearing) of the missile relative to the heading of the ship; (rad)

V is the speed of the missile; (ft/sec)

ϕ is the flight path angle of the missile; (rad)

ψ is the azimuth heading angle of the missile; (rad)

T is the thrust; (lb-f)

D is the aerodynamic drag; (lb-f)

α is the angle of attack, which is assumed to be small; (rad)

P_{3_g} is a parameter representing thrust over weight;

N_1 is the proportional navigation parameter in elevation;

N_2 is the vertical maneuver (gravity bias) parameter (pop-up);

N_3 is the proportional navigation parameter in azimuth;

N_4 is the horizontal maneuver parameter (pop-over).

The first three equations can be replaced by

$$\dot{x} = V \cos\phi \cos\psi \tag{2.7}$$

$$\dot{y} = V \cos\phi \sin\psi \tag{2.8}$$

$$\dot{z} = -V \sin\phi \tag{2.9}$$

by using the following transformation :

$$x = R \cos E \cos A \tag{2.10}$$

$$y = R \cos E \sin A \tag{2.11}$$

$$z = R \sin E \tag{2.12}$$

or

$$R = \sqrt{x^2 + y^2 + z^2} \tag{2.13}$$

$$E = \sin^{-1} \frac{z}{R} \tag{2.14}$$

$$A = \tan^{-1} \frac{y}{x} \tag{2.15}$$

2.1.1 Thrust Model

The thrust is assumed to act along the missile's center line. The thrust-to-weight ratio is treated as a parameter:

$$\frac{T}{W} = P_{3_g} \tag{2.16}$$

or

$$\frac{T}{m} = P_{3_g} g = P_3 \tag{2.17}$$

where

T is the thrust; (lb-f)

m is the mass of the missile; (slug)

$W = mg$ is the gross weight of the missile; (lb-f)

P_3 and P_{3_g} are constants related by

$$P_3 = P_{3_g} g \tag{2.18}$$

2.1.2 Lift Model

The aerodynamic lift model is used :

$$L = \bar{q} S C_L \tag{2.19}$$

or

$$\frac{L}{m} = \bar{q}\left(\frac{S C_{L\alpha}}{m}\right)\alpha \equiv \bar{q} P_2 \alpha \tag{2.20}$$

where

L is the aerodynamic lift; (lb-f)

m is the mass of the missile; (slug)

$\bar{q} = \frac{1}{2}\rho V^2$ is the dynamic pressure; (lbs/ft^2) (2.20.1)

$\rho = \rho_0 e^{-cz}$ is the air density; (slug/ft^3) (2.20.2)

ρ_0 is the sea level air density; (slug/ft^3)

c is a constant; (2.20.3)

z is the altitude of the missile; (ft)

V is the missile velosity; (ft/sec)

S is the aerodynamic reference area of the missile; (ft^2)

$C_L = C_{L_\alpha}\,\alpha$ is the lift coefficient of the missile;

C_{L_α} is the slope of the lift curve of the missile,which essentially is a constant before the stall point;

$P_2 = \dfrac{SC_{L_\alpha}}{m}$ is a parameter treated as a constant; (ft^3/lb-sec^2)

α is the angle of attack, which can be calculated from

$$\alpha = \frac{\sqrt{(N_1 U_1 + N_2 g)^2 + (N_3 U_2 + N_4 g)^2}}{\bar{q} P_2} \tag{2.21}$$

The following two equations are used in practice to smooth the measured line of sight (LOS) rate that is measured by the missile.

$$\dot{U}_1 = \frac{1}{\tau}[-U_1 - \dot{E}V] \tag{2.22}$$

$$\dot{U}_2 = \frac{1}{\tau}[-U_2 + \dot{A}V\cos\phi] \tag{2.23}$$

where $\tau = \dfrac{1}{2}$ second is the time constant.

These rates are noisy in practice due to noisy radar returns from the ship. That is, the radar signals bounce off various parts of the ship and their returns then appear as noisy LOS rates. So, in practice, the missile will integrate these returns and smooth them using equations similar to (2.22) and (2.23). We ignore this noisy LOS rate process and assume that no integration or smoothing of these rates are made. In this case, the equations relating the LOS rates to the values used by the proportional navigation guidance system are the following :

$$U_1 = -\dot{E}V \tag{2.24}$$

$$U_2 = \dot{A}V\cos\phi \tag{2.25}$$

2.1.3 Drag Model

A polar drag model is used :

$$D = \bar{q}SC_D \tag{2.26}$$

$$C_D = C_{D_0} + C_{D_i} = C_{D_0} + C_{L_\alpha}\alpha^2 \tag{2.27}$$

$$\frac{D}{m} = \bar{q}\left(\frac{SC_{D_0}}{m}\right) + \bar{q}\left(\frac{SC_{L_\alpha}}{m}\right)\alpha^2 \tag{2.28}$$

where

D is the aerodynamic drag;

$\bar{q}$ is the dynamic pressure;

S is the aerodynamic reference area of the missile;

C_D is the drag coefficient of the missile;

C_{D_0} is the zero-lift drag coefficient of the missile;

C_{D_i} is the coefficient of drag due to lift, or the induced drag coefficient.

Using the parameters defined as

$$P_1 \equiv \frac{SC_{D_0}}{m}, \quad \text{and} \quad P_2 \equiv \frac{SC_{L\alpha}}{m} \tag{2.29}$$

we get

$$\frac{D}{m} = \bar{q}P_1 + \bar{q}P_2\alpha^2 \tag{2.30}$$

Substituting equations (2.17), (2.28) and $\cos\alpha \cong 1$ into equation (2.4), we get

$$\dot{V} = P_{3_g} g - P_1 \bar{q} - P_2 \bar{q}\alpha^2 - g\sin\phi \tag{2.31}$$

2.1.4 Maneuver Model

The maneuvering characteristics of a missile are governed by airframe, propulsion and guidance parameters, which include thrust, lift, drag, proportional navigation (PN) constants, and acceleration bias parameters. We focus our attention on the guidance parameters. We note that the ship's filters must assume some model

of the missile that it desired to track and to engage with a projectile. It is assumed that the ship has the information of the missile's equations of motion for the 6 states $R, E, A, V, \phi,$ andψ. However, the control functions

P_{3_g}, N_2, and N_4 are unknown to the ship. Therefore, We need two models for the missile's maneuvers. One is needed in the simulation of the missile's trajectory. The other is needed in the the filter's model of the missile for the ship.

The thrust, lift, and drag models have been described in previous sections for the missile, in which P_{3_g} is one of the control variables describing the amount of g's thrust being generated by the missile. Next, we look at the acceleration bias parameters and the PN constants for the missile. There are two acceleration bias parameters, N_2 and N_4. N_2 denotes the number of g's that the missile is pulling in the vertical plane direction. N_4 denotes the number of g's that the missile is pulling in the horizontal plane direction. In the case of zero line-of-sight-rates, a value of $N_2 = 1$ corresponds to level flight (i.e. no-maneuver in the vertical plane), while $N_4 = 0$ corresponds to no-maneuver in the horizontal plane.

$$N_2 = f_c(t)u(t_s) + 1.0 \tag{2.32.1}$$

$$N_4 = f_c(t)u(t_s) \tag{2.32.2}$$

where

$u(t_s)$ is the step function started at the time t_s.

$f_c(t)$ is one of the following periodic functions :

(1) sinusoidal wave; (2) square wave; (3) sawtooth wave.

The above three parameters, P_{3_g}, N_2, and N_4 are three control variables used by the missile to evade gunfire. They also serve as additional states for the ship's filtering process. The three parameters are in the following form as seen by the ship :

$$\dot{P}_{3_g} = 0. \quad (\text{with jump}) \tag{2.33.1}$$

$$\dot{N}_2 = 0. \quad (\text{with jump}) \tag{2.33.2}$$

$$\dot{N}_4 = 0. \quad (\text{with jump}) \tag{2.33.3}$$

There are two PN constants, N_1 and N_3. The constant N_1 is for homing in the vertical direction and N_3 is for the azimuth direction. The PN constants are usually set in the neighborhood of 3.0. We use 3.15 for N_1 and 3.0 for N_3 in the missile's model for its trajectory simulation. Depending on the assumption of whether the missile's impact point on the ship is the ship's radar site or it is any place on the ship, there are two distinct missile's models considered by the ship. One is the PN system and the other is the NOPN system, see section 5.2.4. If the missile's impact point on the ship is known and if it is the radar site then the ship can advantageously use the missile's PN constants in its filters. The resulting equations of motion are called the PN system. If the missile's impact point on the ship is unknown to the ship it is best that the ship not assume that the missile is

homing in on its radar site. Consequently, no PN constants are used in the ship's filtering equations. We call this the NOPN system.

The acceleration in the elevation and azimuth direction respectively, A_e and A_a , are given by

$$A_e = N_1 V_1 + N_2 g \tag{2.34}$$

$$A_a = N_3 V_2 + N_4 g \tag{2.35}$$

and the bank angle, θ , satisfies

$$\theta = \tan^{-1}\left(\frac{A_a}{A_e}\right) \tag{2.36}$$

2.2 *Projectile Model*

We consider the motion of the projectile as a function of gravity and drag. The discretized equations of motion are used in the simulation program to reduce the computation. Let the x-axis denote the direction of the horizontal plane projection of the projectile's trajectory so that the y components are all zeros. Denote R_p as the range of the projectile, x_p and z_p , as its coordinates in the x-axis and z-axis directions, respectively. At the initial time, $t = 0.$ (sec.), the projectile is fired from the origin, $x_p(0) = z_p(0) = 0.$ (ft), and its initial speed is given by

$V_T(0) = 900.$ ft/sec with the x component $V_x(0) = V_T(0)\cos E_p(0)$ and the z component $V_z(0) = V_T(0)\sin E_p(0)$, where $E_p(0)$ is the elevation angle of the projectile. The time increment is Δt.

We consider a 20mm projectile similar to that described in [46]. We approximate the parameters of such a projectile with the following data.

$$W = 0.074\text{lb} \quad \text{(weight)} \tag{2.37.1}$$

$$S = .0034ft^2 \quad \text{(projected reference area)} \tag{2.37.2}$$

$$C_{D_0} = 0.17 \quad \text{(coefficient of drag at zero Mach number)} \tag{2.37.3}$$

Consider the standard atmosphere condition. The temperature at the sea level T_{SL} is 519° R. The temperature decreases linearly as the altitude increases in the troposphere level, from sea level to the altitude $h_S = 36{,}089\,ft$. Right above the troposphere is the stratosphere where the temperature is a constant $T_S = 390°\text{R}$. Suppose the altitude of the projectile at time t is $z_p(t)$ m , which stays within the traposphere, then

$$T(t) = T_{SL} - cz_p(t) \tag{2.38}$$

This can be rewritten in the following nomalized form :

$$T_e(t) = \frac{T(t)}{T_{SL}} = 1 - c_4 z_p(t) \tag{2.39}$$

where

$$c = \frac{T_{SL} - T_S}{h_S} \tag{2.40}$$

$$c_4 = \frac{c}{T_{SL}} = \frac{(519 - 390)^o R}{36089 ft} \frac{1 ft}{519^o R} \frac{1 in}{12 in} \frac{100 cm}{2.54 cm} \frac{1 m}{}$$

$$= 2.26 x 10^{-5} (1/m) \tag{2.41}$$

Let $M_a(t)$ denote the Mach number of the projectile at time t.

$$M_a(t) = \frac{V_T(t)}{V_a} \tag{2.42}$$

$$V_a(t) = a_{SL}\sqrt{T_e(t)} = a_{SL}\sqrt{1 - c_4 z_p(t)} \tag{2.43}$$

The total drag coefficient C_D of the projectile is considered to be Mach number dependent.

$$C_D = C_{D_0} e^{-1/4 M_a(t)} \tag{2.44}$$

where C_{D_0} is drag coefficient at zero Mach number. We define

$$p(t) = -\frac{1}{4} M_a(t) \tag{2.45}$$

By using the definition of Mach number we can show that

$$p(t) = c_2 \frac{V_T(t)}{\sqrt{T_e(t)}} \tag{2.46}$$

where

$$c_2 = -0.00074 \ (m/\sec) \tag{2.47}$$

The velocity V_T of the projectile is assumed to have the heading angle γ_p with respect to x-axis. The speed in the x direction is denoted by V_x and that in the z direction is denoted by V_z. They are given by

$$V_x = V_T \cos \gamma_p \tag{2.48}$$

$$V_z = V_T \sin \gamma_p \tag{2.49}$$

The correspond drag components are

$$D_x = D \cos \gamma_p \tag{2.50}$$

$$D_z = D \sin \gamma_p \tag{2.51}$$

Note that

$$D_x = D \frac{V_x}{V_T} \tag{2.52}$$

$$D_z = D \frac{V_z}{V_T} \tag{2.53}$$

so that the drag coefficients are

$$C_{D_x} = D\frac{V_x}{V_T} \tag{2.54}$$

$$C_{D_z} = D\frac{V_z}{V_T} \tag{2.55}$$

The equations of motion are

$$\dot{V}_x = -\frac{\bar{q}SC_{D_x}}{m} \tag{2.56}$$

$$\dot{V}_z = -\frac{\bar{q}SC_{D_z}}{m} - g \tag{2.57}$$

We approximate the left hand sides of these two equations by

$$\dot{V}_x \cong \frac{V_x(t+\Delta t) - V_x(t)}{\Delta t} \tag{2.58}$$

$$\dot{V}_z \cong \frac{V_z(t+\Delta t) - V_z(t)}{\Delta t} \tag{2.59}$$

With these approximations we have

$$V_x(t+\Delta t) = V_x(t)\left[1 - \frac{\bar{q}SC_D}{m}\frac{\Delta t}{V_T}\right] \tag{2.60}$$

$$V_z(t+\Delta t) = V_z(t)\left[1 - \frac{\bar{q}SC_D}{m}\frac{\Delta t}{V_T}\right] - g\Delta t \tag{2.61}$$

We Define

$$a(t) = -\frac{\bar{q}SC_D}{m}\frac{\Delta t}{V_T} \tag{2.62}$$

with which we have

$$V_x(t+\Delta t) = V_x(t)[1+a(t)] \tag{2.63}$$

$$V_z(t+\Delta t) = V_z(t)[1+a(t)] - g\Delta t \tag{2.64}$$

From the definition of dynamic pressure

$$\bar{q} = \frac{1}{2}\rho V_T{}^2 \tag{2.65}$$

we find that $a(t)$ becomes

$$a(t) = -\frac{1}{2}\rho_0\left(\frac{\rho}{\rho_0}\right)V_T{}^2\frac{SC_{D_0}}{m}\frac{\Delta t}{V_T} \tag{2.66}$$

But

$$\frac{\rho}{\rho_0} = T_e{}^{c_3} \tag{2.67}$$

where c_3 is given by

$$c_3 = \frac{g}{cR} - 1 = \frac{32.2\,ft/\sec^2}{1716.5\,ft^2/(\sec^2{}^oR)}\frac{36{,}089\,ft}{(519-390)^oR} - 1$$

$$= 4.25 \tag{2.68}$$

We define c_1 as follows

$$c_1 = -\frac{1}{2}\frac{\rho_0 S C_{D_0}}{m} \tag{2.69}$$

Evaluating c_1 using the above data we find that

$$c_1 = -0.00098(1/m) \tag{2.70}$$

We see that $a(t)$ satisfies

$$a(t) = c_1 e^{p(t)} T_e^{c_3}(t) V_T(t) \Delta t \tag{2.71}$$

The x and z coordinates of the projectile can be approximated by

$$x_p(t + \Delta t) = x_p(t) + \left[\frac{V_x(t + \Delta t) + V_x(t)}{2} \right] \Delta t \tag{2.72}$$

$$z_p(t + \Delta t) = z_p(t) + \left[\frac{V_z(t + \Delta t) + V_z(t)}{2} \right] \Delta t \tag{2.73}$$

With the speed equations, &spx. and &spz., we get the follows :

$$x_p(t + \Delta t) = x_p(t) + [1 + \frac{1}{2} a(t)] V_x(t) \tag{2.74}$$

$$z_p(t + \Delta t) = z_p(t) + [1 + \frac{1}{2} a(t)] V_z(t) - \frac{1}{2} g \Delta t^2 \tag{2.75}$$

The total magnitude of the velocity is

$$V_T(t) = \sqrt{V_x^2(t) + V_z^2(t)} \tag{2.76}$$

the range of the projectile is

$$R_p(t) = \sqrt{x_p^2(t) + z_p^2(t)} \tag{2.77}$$

the elevation angle of the projectile is

$$E_p(t) = \tan^{-1} \frac{z_p(t)}{x_p(t)} \tag{2.78}$$

2.3 *Performance Model*

The purpose of this study is to find optimal periodic control functions for the missile to evade the tracking and the interception by a ship's gunfire system. Three periodic maneuvering functions are investigated, i. e., sinusoidal, square, and sawtooth waveforms.

Our performance index to be minimized is the estimated number of hits (EHITS) on the missile by the projectiles. For each projectile fired, the probability of a hit is computed based on the relative velocity vector between the missile and the projectile, the miss distance between their trajectories, and the geometric size of

the missile. The value of each probability of a hit is between 0.0 and 1.0. The accumulated probability of hits for the entire missile's trajectory is denoted as the EHITS. Due to bullet dispersion in practice, it is almost impossible to hit any missile or object with our type of projectiles beyond 2500 feet. Also, there is little utility for a projectile to hit the missile when the range of the missile is less than 300 ft. Therefore, the computation of the probability of hits starts at the missile's range of 2500 ft and ends at that of 300 ft. The missile has a speed of around 930 ft/sec, thus, the period for the computation of the EHITS is only about 2.5 seconds. The projectiles are fired at a rate of 50 rounds per second, therefore, the maximum possile EHITS are about 120.

2.4 Engagement Model

On the ship's side of the engagement we use extended Kalman filters (see chapter 3) and jump filters (see chapter 4) synthesized together to optimize the tracking and the prediction of the missile's trajectory. We desire to maximize the estimated number of hits on the missile. A firing rate of 50 Hz (0.02 seconds interval) is used for projectiles.

On the missile's side of the engagement, we seek to design the optimal maneuvering of the missile through changing the magnitude and period of periodic

control functions N_2 and N_4 to minimize the estimated number of hits by the projectiles.

In this engagement model we fix the ship's filtering algorithm and treat it as an optimal control problem in which the missile's trajectory is to be shaped so that it can evade the ship's gunfire.

Chapter 3 Extended Kalman Filter

Estimation theory has been applied to aerospace systems for many years. Several estimation algorithms have been developed for this purpose. Among these the Kalman filter (KF) is a well-known one. The transition of the KF from a relatively abstract theory to applications in many aerospace systems took place within a very short period right after it had been proposed by Kalman, R. E., [1] and [2], in the 1960's. The KF is essentially a recursive solution to Gauss' linear least-square problem. A least-square-fit interpretation of the KF is given in [3]. The KF is a recursive, minimum variance (unbiased), linear optimal estimator for a linear system with gaussian, uncorrelated measurement error, [11]. Since it is recursive there is no need to store past measurements. Since it is linear it requires minimal computation, even in on-line usage. This filter is based on the concept of linear feedback of the estimation error vector, [4], though in practice this vector is not used directly; where the estimation error vector is defined as the difference between the estimated state vector and the true system vector.

$$e = \hat{x} - x \tag{3.1}$$

Furthermore, the KF generates its own error analysis, i. e. the computation of the error covariance matrix P, see equation (3.6) and (3.12), provides an indication of the accuracy of the estimation. The error covariance matrix P is a symmetric matrix containing the variances and the covariances of the estimation error vector. The (i,j)th element of the P matrix is defined as

$$P(i,j) = E[\, e_i\, e_j] = E[\, (\hat{x}_i - x_i)\, (\hat{x}_j - x_j)\,] \tag{3.2}$$

where E is the expectation notation; e_i and e_j are the ith and the jth elements of the estimation error vector, respectively. For the KF the error covariance matrix depends on the covariances of the initial states and the covariances of the radar measurements $\mathscr{R}$ and the dynamics.

The extension of the KF to nonlinear tracking system problems is made possible by successively linearizing about the current estimated states, as has been done by Schmidt and his group at the NASA/AMES Research Center, [5-6]. Their results are formalized in what is now referred to as the "extended Kalman filter" (EKF), [7-9], pp. 272-281 in [10], and pp.180-200 in [11]. The KF, which assumes that all control inputs of the tracking system are known, is optimal for a linear model with Gaussian noise. But an optimal nonlinear estimator requires an infinite dimensional model for its realization, [12]. Consequently, the linearized estimator EKF is a suboptimal but practical estimator for a nonlinear system with

a known maneuver. Schmidt in [13] describes the history of the recognition of the KF's utility and its subsequent development for aerospace applications. Some of the survey work is also available in [7] and [14]. We employ the algorithm called the continuous-discrete extended Kalman filter, Table 6.1-1, Gelb [11].

3.1 Algorithm for EKF

Consider a model of a nonlinear system to be given by :

$$\dot{x} = f(x) + w \tag{3.3}$$

where x is the n-dimensional state vector.

f is a nonlinear function of the state vector.

w is the process noise, which is assumed to be a zero mean, white gaussian sequence with covariance matrix $Q(t)$.

Consider the nonlinear measurement model given by :

$$z = h(x) + v \tag{3.4.1}$$

where z is the measurement.

h is a nonlinear function of the state vector.

v denotes the measurement noise,which is assumed to be a zero mean, white gaussian sequence with covariance matrix $\mathcal{R}$.

In our problem the measurement model is a linear one and the measurement z represents range (R), elevation (E) and azimuth (A) radar measurements. Therefore, the linear measurement model is considered hereinafter as :

$$z = H\,x + v \tag{3.4.2}$$

There are two phases involved in an EKF (or KF) process. One is the propagation phase, which is defined w. r. t. the time interval $[\,t_{k-1}\,,\ t_k\,]$, the other is the update phase, which is defined w. r. t. the measurement time t_k. These are illustrated in the following figure.

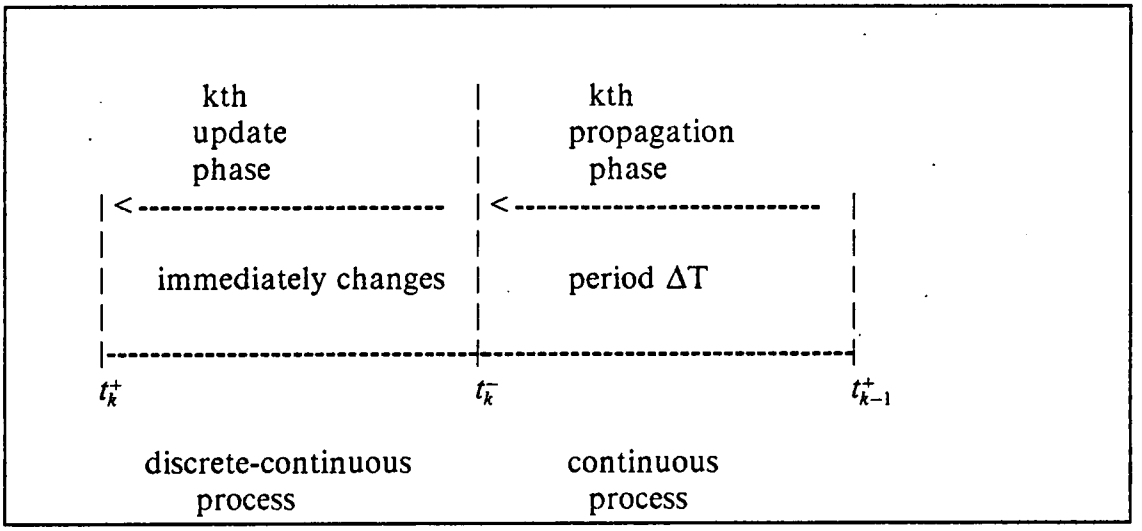

The signs + and - refer to estimated quantities right after and right before the update phase, respectively.

3.1.1 The Propagation Phase

The propagation phase includes state estimate propagation and error covariance propagation from time t_{k-1}^{+} to time t_k^{-}. The propagation of the state estimate uses the known nonlinear equations of motion evaluated at the estimated states. First, we calculate the derivative of the estimated state vector using

$$\dot{\hat{x}}(t_{k-1}^{+}) = f(\hat{x}(t_{k-1}^{+})) \tag{3.5}$$

where $\hat{x}(t_{k-1}^{+})$ is the estimated state vector at the begining time of the kth propagation phase, t_{k-1}^{+}.

We assume that the derivatives of the states remain constant through the kth propagation phase, from t_{k-1}^{+} to t_k^{-} We then use numerical integration to get the estimated states at time t_k^{-} .

In the error covariance propagation calculation we first calculate the derivative of the P matrix using

$$\dot{P} = F(\hat{x})\, P + P\, F(\hat{x})^T + Q \tag{3.6}$$

where Q is the covariance matrix of the process noise, which assumed to be a constant diagonal matrix in our problem.

$F(\hat{x})$ is the Jacobian of the nonlinear dynamics evaluated at the estimated state $\hat{x}$ at the begining time of the kth propagation time

t_k^+ :

$$F(\hat{x}(t_{k-1}^+)) = \left[\frac{\partial f(x)}{\partial x} \right]_{x=\hat{x}(t_{k-1}^+)} \tag{3.7.1}$$

The (i,j)th element of the F matrix is

$$F(i,j) = \frac{\partial f_i}{\partial x_j} \tag{3.7.2}$$

3.1.2 The Update Phase

The update phase consists of the state estimate update and the error covariance update. In order to accomplish these two updates at time t_k , we need to get the Kalman gain matrix, $K(t_k)$ first. The criterion for choosing the Kalman gain matrix is to minimize the sum of the diagonal elements of the error covariance matrix, $P(t_k^+)$. In other words, it minimizes the length of the estimation error vector e, [11]. The equation thus obtained for the K matrix is :

$$K(t_k) = P(t_k^-)\, H^T\, V(t_k)^{-1} \tag{3.8}$$

$$V(t_k) = H\, P(t_k^-)\, H^T + \mathcal{R} \tag{3.9}$$

where $\mathcal{R}$ is the covariance matrix of the measurement noise

$V(t_k)$ is the theoretical value of the predicted measurement residual covariance matrix.

$P(t_k^-)$ is the error covariance matrix obtained right after the k^{th} propagation phase.

With the Kalman gain obtained, the state estimate update uses the following equations :

$$\hat{x}(t_k^+) = \hat{x}(t_k^-) + K(t_k)\gamma(t_k) \tag{3.10}$$

$$\gamma(t_k) = z(t_k) - H\hat{x}(t_k^-) \tag{3.11}$$

where γ is the predicted measurement residual;

z is the measurement vector.

$\hat{x}(t_k^-)$ is the estimated state vector obtained after the k^{th} update phase.

The update of the error covariance matrix is obtained from the following equation :

$$P(t_k^+) = [\, I - K(t_k)H \,]P(t_k^-) \tag{3.12}$$

3.2 Application of EKF to Our Problem

We have a system with 6 states and 3 guidance parameters as additional states (i. e., controls), but the computation cost of a nine states filter system (EKF and JF) is unnecessary. Before entering into the filtering part, it is advantageous to

decouple the system into three smaller systems since in our engagement problem the estimation performance can be accomplished with very littile degradation. We base this on the following observation : The three state variables R, V, and P_{3_g} describe the longitudinal aspects of the state along the velocity vector. The three state variables E, ϕ, and N_2 describe the longitudinal aspects of the state in the vertical plane. The three state variables A, ψ, and N_4 describe the lateral aspects of the state in the horizonal plane. Since the missile's velocity is approximately aligned along the line-of- sight of the missile / ship geometry, we can decouple the state vector into the three state vectors without a loss in estimation performance.

So, even though we use the whole set of equations of motion to simulate the true missile trajectory data, we can use 3 separate filters to estimate the states and controls (i. e., guidance parameters) using the measurements of R, E, and A, respectively. The corresponding filters are called the R-filter, the E-filter, and the A-filter, respectively. Since the states of the system consists of the states of the three filters, we use the estimated values of the states from all three filters in the nonlinear equations of the propagation phase to perform the propagation.

The initial condition for the states of the three filters are :

$$\hat{x}_r(0) = \begin{bmatrix} \hat{R}(0) \\ \hat{V}(0) \\ \hat{P}_{3g}(0) \end{bmatrix} \tag{3.13}$$

$$\hat{x}_e(0) = \begin{bmatrix} \hat{E}(o) \\ \hat{\phi}(0) \\ \hat{N}_2(0) \end{bmatrix} \tag{3.14}$$

$$\hat{x}_a(0) = \begin{bmatrix} \hat{A}(0) \\ \hat{\psi}(0) \\ \hat{N}_4(0) \end{bmatrix} \tag{3.15}$$

The initial condition for the three error covariance matrix P_r , P_e, and P_a are diagonal matrices :

$$P_r(o) = \begin{bmatrix} \sigma_r^2(1) & 0 & 0 \\ 0 & \sigma_r^2(2) & 0 \\ 0 & 0 & \sigma_r^2(3) \end{bmatrix} \tag{3.16}$$

$$P_e(0) = \begin{bmatrix} \sigma_e^2(1) & 0 & 0 \\ 0 & \sigma_e^2(2) & 0 \\ 0 & 0 & \sigma_e^2(3) \end{bmatrix} \tag{3.17}$$

$$P_a(0) = \begin{bmatrix} \sigma_a^2(1) & 0 & 0 \\ 0 & \sigma_a^2(2) & 0 \\ 0 & 0 & \sigma_a^2(3) \end{bmatrix} \tag{3.18}$$

We arrange the three states for each of the three filters in the above order, and the measurement used for each of the three filters is R, E, and A, respectively, which is the first element for each filter. Thus the measurement model at the time t_k for each of these 3 filters can be reduced to the following scalar equation form :

$$z(t_k) = x_1(t_k) + v(t_k) \tag{3.19}$$

where z is the measurement for each filter

x_1 is the first element of the states vector, which is R, E, and A, respectively for each of the three filters.

v is the measurement error for each filter.

From equations (3.4.2) and (3.19) we get

$$H = [1 \quad 0 \quad 0] \tag{3.20}$$

$$\mathcal{R} = E[v \quad v^T] = \sigma_{x_1}^2 \tag{3.21}$$

Therefore, the theoretical value of the predicted measurement residual covariance matrix can be reduced to a scalar as follows :

$$V(t_k) = H P(t_k^-) H^T + \mathcal{R}$$

$$= [1 \quad 0 \quad 0] \begin{bmatrix} P_{11} & P_{12} & P_{13} \\ P_{21} & P_{22} & P_{23} \\ P_{31} & P_{32} & P_{33} \end{bmatrix}_{(t_k^-)} \begin{bmatrix} 1 \\ 0 \\ 0 \end{bmatrix} + \sigma_{x_1}^2$$

$$= P_{11}(t_k^-) + \sigma_{x_1}^2 \tag{3.22}$$

Note that $V(t_k)$ is now simply a scalar.

The EKF gain matrix can be simplified as :

$$K(t_k) = P(t_k^-)\, H(t_k)^T\, V(t_k)^{-1}$$

$$= \frac{1}{V(t_k)} \begin{bmatrix} P_{11} & P_{12} & P_{13} \\ P_{21} & P_{22} & P_{23} \\ P_{31} & P_{32} & P_{33} \end{bmatrix}_{(t_k^-)} \begin{bmatrix} 1 \\ 0 \\ 0 \end{bmatrix}$$

$$= \frac{1}{V(t_k)} \begin{bmatrix} P_{11} \\ P_{21} \\ P_{31} \end{bmatrix}_{(t_k^-)} \tag{3.23}$$

The predicted measurement residual is simply

$$\gamma(k) = z(k) - H\,\hat{x}(t_k^-) = x_1(t_k) - \hat{x}_1(t_k^-) \tag{3.24}$$

We substitute these equations into the state estimate update and error covariance update equations to complete the update phase.

For the propagation phase we need additional work to get the Jacobian matrix, F, for each filter of the EKF.

3.3 *Jacobian Matrix for R-filter*

The state vector for the R-filter is given by

$$x_r^T = [\, R \quad V \quad P_{3_g} \,] \tag{3.25}$$

Define $f_r(1)$ and $f_r(2)$ as the right hand side of equation (2.1) and (2.31), respectively :

$$f_r(1) = RHS(\dot{R}) = V\,[\,\sin\phi \sin E + \cos(\psi - A)\cos\phi\cos E\,] \tag{3.26}$$

$$f_r(2) = RHS(\dot{V}) = P_{3_g} g - P_1 \bar{q} - P_2 \bar{q}\alpha^2 - g\sin\phi \tag{3.27}$$

We assume a constant control P_{3_g}. Therefore,

$$f_r(3) = RHS(\dot{P}_{3_g}) = 0. \tag{3.28}$$

For the R-filter the F matrix in the error covariance propagation phase is calculated as follows :

$$F_r(1,1) = \frac{\partial f_r(1)}{\partial x_r(1)} = 0. \tag{3.29}$$

$$F_r(1,2) = \frac{\partial f_r(1)}{\partial x_r(2)} = \sin\phi \sin E + \cos(\psi - A)\cos\phi \cos E \tag{3.30}$$

$$F_r(1,3) = \frac{\partial f_r(1)}{\partial x_r(3)} = 0. \tag{3.31}$$

$$F_r(2,1) = \frac{\partial f_r(2)}{\partial x_r(1)} = -(P_1 + P_2\alpha^2)\frac{\partial \bar{q}}{\partial R} - P_2\bar{q}\frac{\partial \alpha^2}{\partial R} \tag{3.32.1}$$

where

$$\frac{\partial \bar{q}}{\partial R} = \frac{\partial}{\partial R}\left(\frac{1}{2}\rho V^2\right)$$

Substituting equations (2.20.1), (2.20.2), and (2.12) into the above equation, we get

$$\frac{\partial \bar{q}}{\partial R} = -c\bar{q}\sin E \tag{3.32.2}$$

Define two variables as follows :

$$b = -N_1\dot{E}V + N_2 g \tag{3.32.3}$$

$$c = -N_3 \dot{A} V \cos \phi + N_4 g \tag{3.32.4}$$

then equation (2.21) can be rewritten as :

$$\alpha^2 = (b^2 + c^2)/(\bar{q} P_2^2)$$

Subsequently,

$$\frac{\partial \alpha^2}{\partial R} = \frac{2}{\bar{q} P_2^2} \left[b \frac{\partial b}{\partial R} + c \frac{\partial c}{\partial R} \right] - \frac{b^2 + c^2}{P_2^2 \bar{q}^2} \frac{\partial \bar{q}}{\partial R} \tag{3.32.5}$$

$$\frac{\partial b}{\partial R} = - N_1 V \frac{\partial \dot{E}}{\partial R} = N_1 V \frac{\dot{E}}{R} \tag{3.32.6}$$

$$\frac{\partial c}{\partial R} = N_3 V \cos \phi \frac{\partial \dot{A}}{\partial R} = N_3 V \cos \phi \frac{\dot{A}}{R} \tag{3.32.7}$$

Similarly,

$$F_r(2,2) = \frac{\partial f_r(2)}{\partial x_r(2)} = - (P_1 + P_2 \alpha^2) \frac{\partial \bar{q}}{\partial V} - P_2 \bar{q} \frac{\partial \alpha^2}{\partial V} \tag{3.33.1}$$

where

$$\frac{\partial \bar{q}}{\partial V} = \rho V = \frac{2\bar{q}}{V} \tag{3.33.2}$$

$$\frac{\partial \alpha^2}{\partial V} = \frac{2}{\bar{q} P_2^2} \left[b \frac{\partial b}{\partial V} + c \frac{\partial c}{\partial V} \right] - \frac{b^2 + c^2}{P_2^2 \bar{q}^2} \frac{\partial \bar{q}}{\partial V} \tag{3.33.3}$$

$$\frac{\partial b}{\partial V} = -N_1 \dot{E} - N_1 V \frac{\partial \dot{E}}{\partial V} = -2N_1 \dot{E} \tag{3.33.4}$$

$$\frac{\partial c}{\partial V} = -N_3 \dot{A} \cos\phi - N_3 V \cos\phi \frac{\partial \dot{A}}{\partial V} = -2N_3 \dot{A} \cos\phi \tag{3.33.5}$$

$$F_r(2,3) = \frac{\partial f_r(2)}{\partial x_r(3)} = g \tag{3.34}$$

$$F_r(3,1) = \frac{\partial f_r(3)}{\partial x_r(1)} = 0. \tag{3.35}$$

$$F_r(3,2) = \frac{\partial f_r(3)}{\partial x_r(2)} = 0. \tag{3.36}$$

$$F_r(3,3) = \frac{\partial f_r(3)}{\partial x_r(3)} = 0. \tag{3.37}$$

3.4 Jacobian Matrix for E-filter

The state vector for the E-filter is given by

$$x_e^T = [\, E \quad \phi \quad N_2 \,] \tag{3.38}$$

Define $f_e(1)$and $f_e(2)$ as the right hand side of equations (2.2) and (2.5).

$$f_e(1) = RHS(\dot{E}) = \frac{V}{R}\left[\sin\phi\cos E + \cos(\psi - A)\cos\phi\sin E\right] \tag{3.39}$$

$$f_e(2) = RHS(\dot{\phi}) = \frac{1}{V}\left[N_1(-\dot{E}V) + N_2 g - g\cos\phi\right] \tag{3.40}$$

We assume a constant control N_2. Therefore,

$$f_e(3) = RHS(\dot{N}_2) = 0. \tag{3.41}$$

For the E-filter the F matrix in the error covariance propagation phase is calculated as follows :

$$F_e(1,1) = \frac{\partial f_e(1)}{\partial x_e(1)} = -\frac{V}{R}\left[\sin\phi\sin E + \cos(\psi - A)\cos\phi\cos E\right] \tag{3.42}$$

$$F_e(1,2) = \frac{\partial f_e(1)}{\partial x_e(2)} = \frac{V}{R}\left[\cos\phi\cos E + \cos(\psi - A)\sin\phi\sin E\right] \tag{3.43}$$

$$F_e(1,3) = \frac{\partial f_e(1)}{\partial x_e(3)} = 0. \tag{3.44}$$

$$F_e(2,1) = \frac{\partial f_e(2)}{\partial x_e(1)} = -N_1 F_e(1,1) \tag{3.45}$$

$$F_e(2,2) = \frac{\partial f_e(2)}{\partial x_e(2)} = -N_1 F_e(1,2) + \frac{g\sin\phi}{V} \tag{3.46}$$

$$F_e(2,3) = \frac{\partial f_e(2)}{\partial x_e(3)} = \frac{g}{V} \tag{3.47}$$

$$F_e(3,1) = \frac{\partial f_e(3)}{\partial x_e(1)} = 0. \tag{3.48}$$

$$F_e(3,2) = \frac{\partial f_e(3)}{\partial x_e(2)} = 0. \tag{3.49}$$

$$F_e(3,3) = \frac{\partial f_e(3)}{\partial x_e(3)} = 0. \tag{3.50}$$

3.5 *Jacobian Matrix for A-filter*

The state vector for the A-filter is given by

$$x_a^T = [\, A \quad \psi \quad N_4 \,] \tag{3.51}$$

Define $f_a(1)$ and $f_a(2)$ as the right hand side of equations (2.3) and (2.6).

$$f_a(1) = RHS(\dot{A}) = \frac{V}{R\cos E} [\, \sin(\psi - A) \cos \phi \,] \tag{3.52}$$

$$f_a(2) = RHS(\dot{\psi}) = \frac{1}{V \cos \phi} [N_3 (\dot{A} V \cos \phi) + N_4 g \,] \tag{3.53}$$

We assume a constant control N_4. Therefore,

$$f_a(3) = RHS(\dot{N}_4) = 0. \tag{3.54}$$

For the A-filter the F matrix in the error covariance propagation phase is calculated as follows :

$$F_a(1,1) = \frac{\partial f_a(1)}{\partial x_a(1)} = -\frac{V}{R\cos E}\cos(\psi - A)\cos\phi \tag{3.55}$$

$$F_a(1,2) = \frac{\partial f_a(1)}{\partial x_a(2)} = -F_a(1,1) \tag{3.56}$$

$$F_a(1,3) = \frac{\partial f_a(1)}{\partial x_a(3)} = 0. \tag{3.57}$$

$$F_a(2,1) = \frac{\partial f_a(2)}{\partial x_a(1)} = N_3 F_a(1,1) \tag{3.58}$$

$$F_a(2,2) = \frac{\partial f_a(2)}{\partial x_a(2)} = N_3 F_a(1,2) \tag{3.59}$$

$$F_a(2,3) = \frac{\partial f_a(2)}{\partial x_a(3)} = \frac{g}{V\cos\phi} \tag{3.60}$$

$$F_a(3,1) = \frac{\partial f_a(3)}{\partial x_a(1)} = 0. \tag{3.61}$$

$$F_a(3,2) = \frac{\partial f_a(3)}{\partial x_a(2)} = 0. \tag{3.62}$$

$$F_a(3,3) = \frac{\partial f_a(3)}{\partial x_a(3)} = 0. \tag{3.63}$$

Chapter 4 Jump Filter

The EKF is usually poor at tracking a maneuvering target. In an unknown maneuver case, the performance of the EKF degrades because the actual trajectory model is different from that assumed in the filter. In the case where there is a step change in the control (or input) variable, the EKF will accumulate errors and possibly lose track (diverge) unless the step change is taken into account. For example, the three guidance parameters in our missile system, P_{3_z}, N_2, and N_4, are treated as functions of time to describe the maneuvers of the missile. Any time variation in any of these three parameters is treated as a jump in the filtering system of the ship.

This kind of estimation problem on tracking a maneuvering target has been widely studied since 1970. A number of approaches have been proposed. Most of these approaches have been compared to the EKF. Singer, [15], augmented the filter's system model with a first order zero-mean, time correlated Gaussian

noise process to handle the target's acceleration. However, the statistical process model is not best suited to describe a maneuver. The model used by Fitts, [16], is also affected by this problem.

The multiple model adaptive filtering techinque is used in many papers, [17] - [34]. This approach processes two (or more) independent filters in parallel, each using a particular model of the target's dynamics. The adaptive mechanism is based on some conditional probabilistic computation in real time; the one with the minimum residual is dominant.

Another popular approach uses a mechanism to detect a maneuver, [35] - [43]. When a maneuver is detected, the filter for the no-maneuver case, which is usually the EKF, is compensated by another filter which is designed for the computation of the maneuvering characteristics, such as the magnitude, the time of occurrence, etc. Among these, the 'jump filter' (JF), [36] - [38], is used in the estimation part in our problem. A similar approach is used by Bogler [35]. Therein, the jump filter is called the CHP filter after its developers Chan, Hu and Plant, [39]. The combination of the CHP filter and the Extended Kalmam filter is called the adaptive Kalman filter in [35]. Herein, we refer to it as the Joint filter, JTF. This type of filtering process was first analyzed by Willsky and Jones, [43].

The purpose and function of the JF can be described in the following three steps. First, the jump of each guidance parameters is detected. Second, the jump time

and the jump magnitude is estimated. Third, the EKF states are adjusted accordingly after detection and evaluation of the jump.

Recall that there are three EKF's called the R-filter, the E-filter, and the A-filter, respectively. Therefore, we design three independent JF's for each of the three EKF's. These combinations are called the joint filters (JTF). However, the equations for these JF's are the same except for the different subscripts, r, e, and a. In this chapter we use only one of them to illustrate the JF equations and neglect the subscripts. The index t_k is replaced by k; also t_k^+ by k^+, and t_k^- by k^-. The index $(k-1, k)$ indicate the values used in the propagation phase from t_{k-1}^+ to t_k^- .

4.1 Residual Test for Jump Detection

We use a residual test to detect a jump. It is based on a comparision between the predicted measurement residual and the theoretical error covariance as follows :

$$\Delta(k) = \sigma^2(k) - V(k) \tag{4.1}$$

where

σ is an integrated weighted value of the predicted measurement residual;

V is the theoretical value of the predicted measurement residual with the assumption of no jump as in equation (3.9).

An increasing positive value of $\Delta(k)$ denotes that the EKF process is diverging from its expected performance. When this happens we declare that a jump in states has taken place. This triggers the execution of the JF. No jump is considered when $\Delta(k)$ is non-positive.

The σ in equation (4.1) is an integrated value over weighted predicted measurement residuals, $\gamma(k)$. The integration is described by the following recursive procedure, where λ is an exponential weighting factor.

$$\sigma(k) = \sigma(k-1)[1 - \lambda(k)] + \lambda(k)\ \gamma(k) \tag{4.2}$$

Here note that a heavier weight on the most recent residual is obtained when λ is larger. We use three different values for $\lambda(k)$ which depends on the magnitude of $N(k)$.

$$\lambda(k) = \begin{cases} 0.25 & \text{if} \quad N(k) \leq 3.0 \\ 0.33 & 3.0 < N(k) < 5.0 \\ 0.5 & 5.0 \leq N(k) \end{cases} \tag{4.3}$$

where

$$N(k) = \frac{|\gamma(k)|}{\sqrt{V(k)}} \tag{4.4}$$

is the number of the standard deviations that the most recent residual $\gamma(k)$ is relative to that of the theoretical error covariance $V(k)$ in the case of no jump. The

definitions of equations (4.2) to (4.4) make it possible that a larger weight is put on the predicted measurement residual which has a higher value.

4.2 Δ State Equations

To obtain the jump error state equations, we analyze three different filtering conditions for the EKF first.

H_1 There is no jump in the system states and also no jump is assumed by the EKF.

$\tilde{H}_1$ There is a jump in the system states but no jump is assumed by the EKF. The EKF is not aware of the jump.

H_2 There is a jump in the system states and the jump information is assumed known to the EKF.

Let $\hat{x}_1$, $\tilde{x}_1$, and $\hat{x}_2$ denote the EKF estimate of the states for the conditions H_1, $\tilde{H}_1$, and H_2, respectively. We know that $\hat{x}_1$ and $\hat{x}_2$ are optimal but $\tilde{x}_1$ is not.

4.2.1 The Δx State Equation

The propagation of the state estimate can be rewritten as a discrete linear equation :

$$\hat{x}(k^-) = \Phi(k-1,k)\,\hat{x}(k-1^+) \tag{4.5}$$

where $\Phi(k-1,k)$ is the transition from t_{k-1}^- to t_k^-

In order to simplify the notations, we define

$$\Delta\Phi(k-1,k) = [I - K(k)\,H\,]\,\Phi(k-1,k) \tag{4.6}$$

where

K is the EKF gain matrix as in equations (3.8) and (3.23);

H is the observation matrix as in equations (3.4.2) and (3.20);

Φ is the transition matrix as in equation .

Substituting equation (4.5) into (3.10) and (3.11), and using the definition of $\Delta\Phi$, we get the equations for $\hat{x}_2$ and $\tilde{x}_1$ as follows :

$$\hat{x}_2(k^-) = K(k)z(k) + \Delta\Phi(k-1,k)\hat{x}_2(k-1^+) \tag{4.7}$$

$$\tilde{x}_1(k^-) = K(k)z(k) + \Delta\Phi(k-1,k)\tilde{x}_1(k-1^+) \tag{4.8}$$

We assume that a jump occurs at an unknown time t_q with the magnitude Δx_q. The estimation of $\tilde{x}_1$ and $\hat{x}_2$ are identical before a jump. After a jump occurs, an error, Δx, between these two estimation is given by

$$\Delta x(k) = \hat{x}_2(k) - \tilde{x}_1(k) \qquad t_k > t_q \tag{4.9}$$

The jump error equation for Δx is obtained by subtracting equation (4.8) from (4.7).

$$\Delta x(k) = \Delta\Phi(k-1, k)\, \Delta x(k-1) \tag{4.10}$$

For the nonlinear system model and the measurement model given in chapter 3, equations (3.3) and (3.4.2), the linearlized transition matrix from time t_{k-1} to t_k is

$$\Phi(k-1, k) \;=\; e^{F(t_k - t_{k-1})} \;=\; I + F(t_k - t_{k-1}) \tag{4.11}$$

where

F is the Jacobian matrix in equations (3.7) and is further developed for R-filter E-filter and A-filter for our problem in sections 3.3, 3.4, and 3.5, respectively.

4.2.2 Δu State Equation

When we use the Δx equations we assume that any element of the system states can take a jump, but this is not always true. In our problem, for the system of the missile, we do not expect that the missile takes a jump in its position elements (R, E, A or x, y, z) or in its velocity elements (V, ϕ, ψ). Jumps may occur in the guidance parameters P_{3_g}, N_2, and N_4. For this reason we introduce a lower dimensional vector, Δu, which contains only those states which define the jump states. We can always rearrange the order of the system states so that

$$\Delta x = D\,\Delta u \tag{4.12.1}$$

with

$$D = \begin{bmatrix} 0 \\ I \end{bmatrix} \tag{4.12.2}$$

For example, in reference to our 3 filters we define

$$\Delta u = \begin{cases} \Delta P_{3_g} & \text{for R-filter} \\ \Delta N_2 & \text{for E-filter} \\ \Delta N_4 & \text{for A-filter} \end{cases} \tag{4.13}$$

then

$$D = \begin{bmatrix} 0 \\ 0 \\ 1 \end{bmatrix} \tag{4.14}$$

for each filter according to the state vectors arranged in sections 3.3, 3.4, and 3.5.

4.2.3 Δy State Equation

In order to simplify the computation, Δx is further non-singularly transformed into a constant state Δy.

Define a recursive matrix Ψ

$$\Psi(0) = I \quad \text{(Identity)} \tag{4.15}$$

$$\Psi(k) = \Delta\Phi(k-1, k)\,\Psi(k-1),\ k \geq 0 \tag{4.16.1}$$

equation (4.16.1) can be rewritten as

$$\Delta\Phi(k-1, k) = \Psi(k)\,\Psi^{-1}(k-1),\ k \geq 0 \tag{4.16.2}$$

Substituting equation (4.16.2) into (4.10) and premultiply both sides with $\Psi^{-1}(k)$, we get

$$\Psi^{-1}(k)\,\Delta x(k) = \Psi^{-1}(k-1)\,\Delta x(k-1) \tag{4.17}$$

This motivate the definition of a new Δ state variable, Δy. Let

$$\Delta y(k) = \Psi^{-1}(k)\,\Delta x(k) \tag{4.18}$$

This can be written in terms of Δu as

$$\Delta y(k) = \Psi^{-1}(k) D \Delta u(k) \tag{4.19}$$

substituting equation (4.18) into (4.17) we get

$$\Delta y(k) = \Delta y(k-1)\ ,\ \ t_k > t_q \tag{4.20}$$

This constant Δ state variable, Δy, makes it possible to derive an efficient algorithm for computing the jump magnitude and the jump time. Since Δy stays

constant after the jump time,t_q, we can always get the Δy(k) we need at any time t_k , $t_k \geq t_q$ as Δy(q). That is

$$\Delta y(k) = \Delta y(q) \ , \ t_k > t_q \tag{4.21}$$

We have to store the values for $\Psi(t_i)$, $i = 0, 1, ...,k$ so that after Δy(k) has been found we can use equations (4.18) and (4.19) to get Δx(k) and Δu(k) from Δx(q) and Δu(q).

4.3 Estimation of Jump

To estimate the jump time we utilize the generalized likelihood ratio (GLR) approach, [29], [43]. GLR considers the ratio of the likelihood of a jump vs. no jump,[37]. The estimated jump time is obtained as the time that maximizes the logarithm of the GLR, (LGLR).

$$\hat{q}(k) = \arg \max_q \ell(q, \Delta\hat{y}(q, k); k) \tag{4.22}$$

then the LGLR can be written as

$$\ell(q, \Delta\hat{y}(q, k); k) = \Delta\hat{y}^T(q, k)\, C(q; k)\, \Delta\hat{y}(q, k) \tag{4.23.1}$$

$$= d^T(q; k)\, \Delta\hat{y}(q, k) \tag{4.23.2}$$

$$= d^T(q;k)\, C^{-1}(q;k)\, d(q,k) \tag{4.23.3}$$

where

$$C(q;k) = \sum_{i=q+1}^{k} [\Delta H(i)]^T [\Delta \mathscr{R}(i)]^{-1} [\Delta H(i)] \tag{4.24}$$

$$d(q;k) = \sum_{i=q+1}^{k} [\Delta H(i)]^T [\Delta \mathscr{R}(i)]^{-1} [\Delta z(i)] \tag{4.25}$$

and the maximum likelihood estimate of the jump magnitude is

$$\Delta\hat{y}(\hat{q}(k), k) = C^{-1}(\hat{q}(k);k)\, d(\hat{q}(k);k) \tag{4.26}$$

Look at the summation equation of $C(q,k)$ and $d(q,k)$ we expect to do the calculation in recursive form and make it more efficient by storing the following :

$$C(0,i) = C(0,i-1) + [\Delta H(i)]^T [\Delta \mathscr{R}(i)]^{-1} [\Delta H(i)] \tag{4.27.1}$$

$$d(0,i) = d(0,i-1) + [\Delta H(i)]^T [\Delta \mathscr{R}(i)]^{-1} [\Delta z(i)] \tag{4.27.2}$$

then

$$C(q,k) = C(0,k) - C(0,q) \tag{4.28.1}$$

$$d(q,k) = d(0,k) - d(0,q) \tag{4.28.2}$$

To obtain further reduction in calculation, we define two new series , $\overline{C}$ and $\bar{d}$, which have lower dimensions. Let

$$\overline{C}(q;k) = D^T \Psi^{-T}(q)\, C(q;k)\, \Psi^{-1}(q)\, D \tag{4.29.1}$$

$$\bar{d}(q;k) = D^T \Psi^{-T}(q)\, d(q;k) \tag{4.29.2}$$

Rewrite the LGLR function in terms of Δu by substituting equation (4.19) into equations (4.23.1) and (4.23.2), to get the following expressions :

$$\ell(q, \Delta\hat{u}(q,k);k) = \Delta\hat{u}^T(q,k)\, \overline{C}(q;k)\, \Delta\hat{u}(q,k) \tag{4.30.1}$$

$$= \bar{d}^T(q;k)\, \Delta\hat{u}(q,k) \tag{4.30.2}$$

$$= \bar{d}^T(q;k)\, \overline{C}^{-1}(q;k)\, \bar{d}(q;k) \tag{4.30.3}$$

With the expresions in terms of $\overline{C}$ and $\bar{d}$, We only need to store $\overline{C}(0,i)$, $\bar{d}(0,i)$, instead of storing $C(0,i)$, and $d(0,i)$. By defining

$$U(i) = \Psi^{-1}(i)D \tag{4.31.1}$$

the $\overline{C}$ and $\bar{d}$ series can be caculated from :

$$\overline{C}(0,i) = U(i)^T\, C(0,i)\, U(i) \tag{4.31.2}$$

$$\bar{d}(0,i) = U(i)^T\, d(0,i) \tag{4.31.3}$$

This reduces the storage requirement. For example, in our problem we need a 3x3 matrix for each $C(0,i)$ and a 3x1 vector for each $d(0,i)$, but only a scalar for each $\overline{C}(0,i)$ and $\overline{d}(0,i)$, i = 0, 1, ..., k.

Also we note that the computation requirement is reduced considerably by using $\overline{C}$'s and $\overline{d}$'s when the JF equations are solved to find the jump time and the jump magnitude. We use a numerical linear search scheme to find the maximum of the LGLR function and the associated jump time. For each candidate point within the moving window (see the next section), we have to calculate the value of the LGLR either in terms of C 's and d's by using equations (4.23.1) and (4.23.2), or in terms of $\overline{C}$'s and $\overline{d}$'s by using equations (4.30.1) and (4.30.2). Obviously, the latter equations, which contains only scalar calculation can be performed in less time. The expense of doing the latter compared to the former is that the computation at each EKF time step i is increased slightly. This is due to the additional calculation for $U(i)$, which involves a 3x3 mairix inversion, and for getting $\overline{C}(0,i)$ and $\overline{d}(0,i)$ from $C(0,i)$ and $d(0,i)$, which involves some multiplications. Even so, it is more important to calculate the jump time and the jump magnitude as fast as possible when the JF is triggered so that we can return to the EKF execution without any delay.

4.4 *Moving Window and Reinitialization*

In order to keep the storage requirement within bounds, we introduce a moving window of length L, say L = 50, for storing $\overline{C}(0,i)$ $\overline{d}(0,i)$ and $U(i)$ in a circle fashion. Thus only the most recent L data points are in storage. Those data points which are older than the amount L counted back from the current one are written over.

During the execution of the JF, the first step is to locate the stored data in the moving window. For this we need some indices to do the mapping between the relative time series in the moving window and the absolute time series in the EKF.

The stored data in the moving window is reinitialized after a jump is detected. By reinitialization we mean that the base point values for the summations of C's and d's are reset to zeros at the jump time and the Ψ matrix is reset as the identity matrix again.

Even though we make the reinitialization after the JF has been executed, it is still possible that the interval between two conscutive jump detections creates a problem. The problem is that the values of $C(0,i)$ increase in values with each time point t_k so that $C(q,k)$ or $\overline{C}(q,k)$, which are the differences between two large values, $C(0,q)$ and $C(0,k)$, are no longer accurate. The same thing also happens for $\overline{C}$'s, d 's, and $\overline{d}$'s. For this reason, we do reinitialization at a selected time

interval frequency, say 4 seconds to keep those values in bounds. Unfortunately, by doing so it will introduce a problem for $C(q,k)$ and $d(q,k)$ since we've got different bases for them in the moving window stored data.

We can solve this problem by introducing a transformation matrix between these two bases. First of all, let us define some notations. Let k denotes the time a jump is detected, and let it also be the last data in the moving window. Let w be the reinitialization time, which occurs before k in the moving window. Let everything within the moving window before w have the first subscript 1, and let those after w have the first subscript 2. Let everything calculated before w but transformed to the base after reinitialization has the second subscript 2. Let q denote a point before reinitialization within the moving window. These notations are illustrated in the following figure.

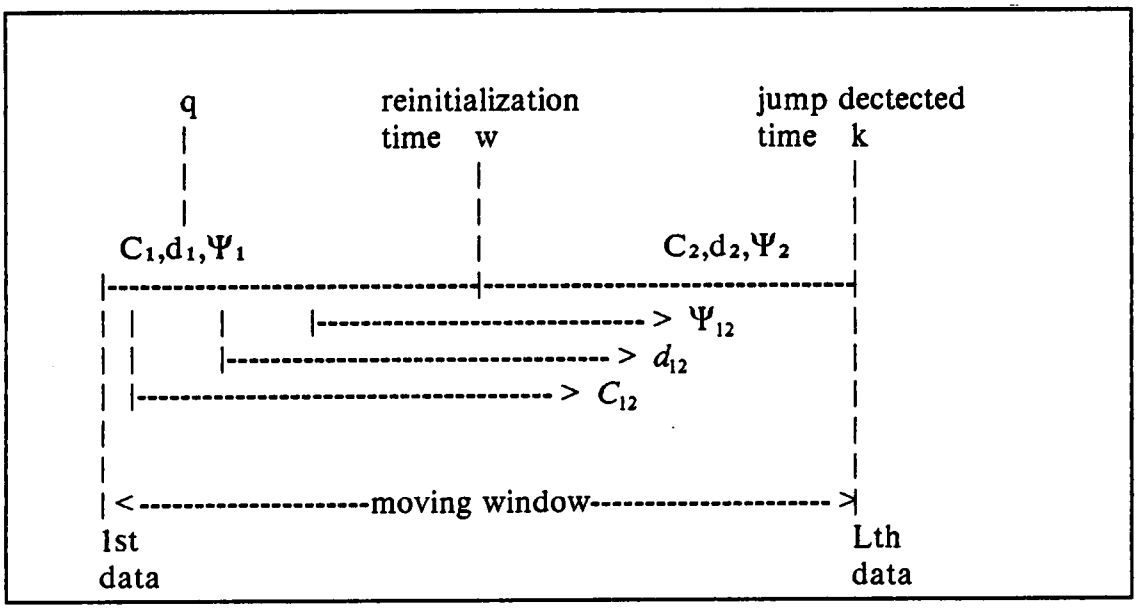

For simplication, suppose there is at most one reinitialization within the moving window. For example, we use 0.05 sec. as the propagation time for the EKF, and there are 50 data points in the moving window. A reinitialization interval of 4 seconds, which contains 80 data points, is used to ensure the above simplified assumption.

The values of $C(q,k)$ and $d(q,k)$ in terms of system 2 can be broken into two parts, one was evaluated in system 2, the other was evaluated in system 1 and needs to be transformed into system 2. With the notations defined, we get the followings :

$$C_2(q,k) = C_2(w,k) + C_{12}(q,w) \tag{4.32.1}$$

$$d_2(q,k) = d_2(w,k) + d_{12}(q,w) \tag{4.32.2}$$

$\bar{C}(q,k)$ and $\bar{d}(q,k)$ in terms of system 2 can then be obtained by using

$$\bar{C}_2(q,k) = U_{12}(q)^T C_2(q,k) U_{12}(q) \tag{4.32.3}$$

$$\bar{d}_2(q,k) = U_{12}(q)^T d_2(q,k) \tag{4.32.4}$$

The transformation between system 1 and system 2 is based on the change of Ψ at the reinitialization time,w :

$$\Psi(w) = \Psi_1(w) \qquad \text{w.r.t. system 1} \tag{4.33.1}$$

$$= \Psi_2(w) = I \qquad \text{w.r.t. system 2} \tag{4.33.2}$$

so

$$\Psi_{12}(q) = \Psi_1(q)\,[\Psi_1(w)]^{-1} \tag{4.34.1}$$

$$U_{12}(q) = [\Psi_{12}(q)]^{-1}\,U_1(q) = \Psi_1(w)\,U_1(q) \tag{4.34.2}$$

From definitions of $C(q,w)$, $d(q,w)$, and ΔH we get the expressions for transforming from system 1 to system 2 :

$$C_{12}(q,w) = [\Psi_1(w)]^{-T}\,C_1(0,w)\,[\Psi_1(w)]^{-1} - [\Psi_1(w)]^{-T}\,C_1(0,q)\,[\Psi_1(w)]^{-1} \tag{4.35.1}$$

$$d_{12}(q,w) = [\Psi_1(w)]^{-T}\,d_1(0,w) - [\Psi_1(w)]^{-T}\,d_1(0,q) \tag{4.35.2}$$

$$\begin{aligned}
\overline{C}_{12}(q,w) &= U_{12}^T(q)\,[\,C_2(0,k) - C_2(0,q)\,]\,U_{12}(q) \\
&= U_{12}^T(q)\,[\,C_2(0,k) - C_2(0,w)\,]\,U_{12}(q) \\
&\quad + U_{12}^T(q)\,[\,C_{12}(0,w) - C_{12}(0,q)\,]\,U_{12}(q) \\
&= U_{12}^T(q)\,C_2(0,k)\,U_{12}(q) \\
&\quad + U_{12}^T(q)\,\Psi_1^{-T}(w)\,[\,C_{11}(0,w) - C_{11}(0,q)\,]\Psi_1^{-1}(w)\,U_{12}(q) \\
&= [\,\Psi_1(w)U_1(q)\,]^T\,C_2(0,k)\,[\,\Psi_1(w)\,U_1(q)\,]
\end{aligned}$$

$$+ \; U_1^T(q)\,\Psi_1^T(w)\,\Psi_1^{-T}(w)\,C_{11}(0,w)\,\Psi_1^{-1}(w)\,\Psi_1(w)U_1(q)$$

$$- \; U_1^T(q)\,\Psi_1^T(w)\,\Psi_1^{-T}(w)\,C_{11}(0,q)\,\Psi_1^{-1}(w)\,\Psi_1(w)U_1(q)$$

$$= [\,\Psi_1(w)U_1(q)\,]^T\,C_2(0,k)\,[\,\Psi_1(w)\,U_1(q)\,]$$

$$+ \; U_1^T(q)\,C_1(0,w)U_1(q) \; - \; \bar{C}_1(0,q) \qquad (4.35.3)$$

$$\bar{d}_{12}(q,w) = U_{12}^T(q)\,[\,d_2(0,k) - d_2(0,q)\,]$$

$$= [\,\Psi_1(w)U_1(q)\,]^T\,d_2(0,k) \; + \; U_1^T(q)\,\Psi_1^T(w)\,d_{12}(q,w)$$

$$= [\,\Psi_1(w)U_1(q)\,]^T\,d_2(0,k)$$

$$+ \; U_1^T(q)\,\Psi_1^T(w)\,\Psi_1^{-T}(w)\,d_1(0,w) \; - \; U_1^T(q)\,d_1(0,q)$$

$$= [\,\Psi_1(w)U_1(q)\,]^T\,d_2(0,k)$$

$$+ \; U_1^T(q)\,d_1(0,w) \; - \; \bar{d}_1(0,q) \qquad (4.35.4)$$

Note that the first terms in equations (4.35.1) and (4.35.2) can be calculated and stored at the reinitialization time w to avoid repeated computation. Note also that the $\bar{C}_1(0,i)$, the $\bar{d}_1(0,i)$ and $U_1(i)$ have been stored at each time step t_i so that the $\bar{C}_1(0,q)$ in equations (4.35.3), the $\bar{d}_1(0,q)$ in equations (4.35.4) and every $U_1(q)$ are ready before the triggering of the JF's execution.

Chapter 5 Parameters Description

In the design of an optimal period for a maneuvering missile, we utilize either the sinusoidal wave, the square wave, or the sawtooth wave, as the maneuvering class of control inputs for the missile. These control inputs are investigated under several different parameters, some of which relate to the missile's side, and others to the ship's side. These parameters are described in sections 5.1 - 5.2. Some parameters are considered to be random so that it is necessary to average, specifically, the maneuver starting range and the measurement noise parameters. The parameters essential for the investigation of the estimated number of hits (EHITS) are presented in two tables. Therein we describe the relationship between these parameter values and the case numbers, section 5.3. Some of the parameters under consideration are easy to get proper values for our purpose, e. g., the process noise and the initial conditions for the ship's filters. The influence of these parameters on the EHITS and the values that we decide to use are given in section 5.4.

5.1 Parameters That Relate to the Missile

There are two important parameters analyzed on the missile's side: one is the offset parameter and the other is the maneuver starting range parameter.

5.1.1 Offset Parameter

The missile may come in and hit the ship along any point. It is not necessary that the missile's impact point coincide with the location of the ship's radar. On the other hand, the ship uses the radar location as its origin in estimating the state vector of the missile. If the missile is homing without offset into the radar position, a filter of the ship can take advantage of this assumption and improve its prediction performance.

To investigate the influence of different impact missile points on the ship, we consider both the zero offset case and a nonzero offset case. By the zero offset case, we mean that the missile is homing into the radar position on the ship. By the nonzero offset case, we prescribe that the missile is homing into an impact point which is 100 ft offset in the positive y-axis direction away from the radar. Here, we are assuming that the y-axis lies along the length of the ship.

5.1.2 Maneuver Starting Range Parameter

The maneuver starting range is the range measured from the ship's radar to the missile at the time when the missile starts its control input maneuver in either the horizontal or the vertical plane.

Although the maneuver starting range is controlled by the missile, the actual range traversed en route to impact in practice depends on the velocity of the missile relative to the ship. Without knowing this relative velocity, the missile can not predict precisely how its trajectory waveform will meet the ship at impact. With such knowledge, the missile could select a maneuver starting range which maximizes its survivability en route to impact. Without such knowledge, it must average its performance over a range of maneuver starting ranges. This is why we consider M different maneuver starting ranges, e. g., M = 24, to evaluate the cost for each run, and then compute the average. The 24 maneuver starting ranges we use are RSTAR = 3250, 3500, ..., 8750, 9000 ft, where the uniform spacing between the starting range points is 250 ft.

5.2 *Parameters That Relate to the Ship's Filter*

There are four parameters governed by the ship's filter. They are the process noise parameter, the initial values for the states, the measurement noise parameter, and the knowledge of the missile's PN constants. Each is described below.

5.2.1 Process Noise Parameter

Theoretically, the error covariance matrix, P, in the EKF should be positive definite. But due to numerical computational error and nonlinear dynamics, some of the diagonal elements of the P matrix can become small and then possibly negative. A view of equation (3.6) reveals that one way to prevent this error is to assume a positive definite Q, which is the covariance matrix of the process noise for each state. Two sets of the process noise have been used, a default one and a larger one. The covariance matrices for the three filters, Q_r, Q_e and Q_a, respectively, with the default process noise are given as follows :

$$Q_r = Q_e = Q_a = 10^{-10} \begin{bmatrix} 1 & 0 & 0 \\ 0 & 1 & 0 \\ 0 & 0 & 1 \end{bmatrix} \tag{5.1}$$

The diagonal elements in these covariance matrices are the auto-covariance values for each corresponding states. The off-diagonal elements are the cross-covariance values, which are assumed to be all zeros.

The covariance matrix for the R-filter remains the same for the second set of the process noise. Those for the E-filter and the A-filter are given in the following :

$$Q_e = Q_a = \begin{bmatrix} 10^{-8} & 0 & 0 \\ 0 & 10^{-8} & 0 \\ 0 & 0 & 0.0625 \end{bmatrix} \tag{5.2}$$

5.2.2 Initial Conditions

Two different sets of initial conditions for the filters have been used to show that it is permissible to start the estimation from any range that is far enough compared with the missile's maneuver starting range. However, the second one, which starts from a smaller range, is preferred since it takes less computations. The first one starts the estimation from a larger range :

$$R = 15200.082, \quad E = 0.00329, \quad A = 3.14159, \tag{5.3.1}$$

$$V = 949.992, \quad \phi = 0., \quad \psi = 0.175, \tag{5.3.2}$$

The second one on the other hand, starts the estimation from a smaller range :

$$R = 9963.258, \quad E = 0.00420, \quad A = 3.09152, \tag{5.4.1}$$

$$V = 936.34919, \quad \phi = -0.00287, \quad \psi = 0.02478, \tag{5.4.2}$$

5.2.3 Measurement Noise Values

We use computer generated, normally distributed random numbers as our measurement noise data. Different measurement noise levels are taken into account : the no measurement noise condition (perfect measurement data), the smaller measurement noise value, and the larger measurement noise value. With the smaller measurement noise we mean that the standard deviations of the radar errors have the values

$$s.t.d.\,(v_r) = 15.\ (ft.) \tag{5.5.1}$$

$$s.t.d.\,(v_e) = 0.003\ (rad.) \tag{5.5.2}$$

$$s.t.d.\,(v_a) = 0.001\ (rad.) \tag{5.5.3}$$

With the larger measurement noise we mean that the standard deviations of the radar errors have the values

$$s.t.d.\,(v_r) = 15.\ (ft.) \tag{5.6.1}$$

$$s.t.d.\,(v_e) = 0.009\ (rad.) \tag{5.6.2}$$

$$s.t.d.(v_a) = 0.003 \ (rad.) \tag{5.6.3}$$

where v is the measurement noise as in equation (3.19) and s.t.d.(v_i) is the standard deviation of the measurement noise of the i-filter, i = R, E, A.

In view of the randomness of measurement noise, it is necessary to compute the cost value by averaging N sets of different runs. Since we have already considered the effect of the maneuver starting range by averaging from M different runs, and since these two effects are independent, we can combine these two effects without additional runs by letting N = M. That is, we generate a set of measurement noise data for each maneuver starting range run. For a different maneuver starting range, we generate a different set of measurement noise data for it. Thus, for either a no noise, maneuvering case or a noise corrupted case, we compute the average cost value from M different runs.

5.2.4 PN Constant Parameter

We also consider different values for the PN constants, N_1 and N_3 in the model of the missile in the filter. One assumes that the PN constants, which is 3.15 for N_1 and 3.0 for N_3, are known exactly; therefore it is called the PN system. The other assumes that no PN constants information is used at all in the filter; therefore it is called the NOPN system. Actually, the PN constants are set to zero in the NOPN system.

For the PN system, the equations of motion used in the filter are the same as those for the missile stated in chapter 2. For the NOPN system, since we do not know the PN constants that the missile is using, it is necessary to define two new states to take the place of N_2 and N_4. We define

$$\tilde{N}_2 = N_2 - \frac{V}{g} N_1 \dot{E} \tag{5.7}$$

$$\tilde{N}_4 = N_4 + \frac{V \cos \phi}{g} N_3 \dot{A} \tag{5.8}$$

so that the effect of N_1 and N_3 can be combined with N_2 and N_4 into $\tilde{N}_2$ and $\tilde{N}_4$, respectively, to compensate for the lack of knowledge of N_1 and N_3. As a result, $\dot{\phi}$ and $\dot{\psi}$ equations can be rewritten without N_1 and N_3 as follows :

$$\dot{\phi} = \frac{g}{V} (\tilde{N}_2 - \cos \phi) \tag{5.9}$$

$$\dot{\psi} = \frac{g}{V \cos \phi} \tilde{N}_4 \tag{5.10}$$

5.3 *The Case Number Tables*

Some parameters described in sections 5.1 - 5.2 are essential for the investigation of the cost value. These include the offset parameter, the PN contant parameter and the measurement noise values. Two tables that describe the relationship be-

tween these parameter values and the case numbers are given in the following pages. Table 1 on page 74 gives all the cases considered for the PN system. Table 2 on page 77 gives all the cases considered for the NOPN system.

5.4 Comment on Parameters

Some cases have been done to compare between the results for different process noise conditions. While the filter's performance is degraded slightly in the PN system when the larger process noise is used, the NOPN system is improved greatly by using the larger process noise. For example, in the NOPN system, the no-maneuvering case, no. 101, the cost value is improved from 0. to 81.2 by just changing the default process noise to the larger one. Similarly, in case no. 113, the cost value is improved from 0. to 93.5. We also get some results which show that the default process noise is better than the larger process noise. For example, by using the default process noise in case no. 25, the mean cost is 70.95 for the EKF and 66.0 for the JTF, whereas the mean cost is 54.85 for the EKF and 56.0 for the JTF by using the larger process noise. From this we say that the adding of the larger process noise is a good tradeoff.

In some cases the results have also been compared for different initial estimation range conditions decribed in section 5.2.2. The results are essentially the same with either initial condition. For example, in case no. 25 of the larger process

Table 1. Parameters Values for the PN System as a Function of the Case No.

Case No	ΔN_2 (g's)	ΔN_4 (g's)	YOFF (ft)	Noise Type	IWIGL
1	0.0	0.	0.	0	0
2	1.5	0.	0.	0	0
3	2.5	0.	0.	0	0
4	3.5	0.	0.	0	0
5	0.0	1.	0.	0	0
6	1.5	1.	0.	0	0
7	2.5	1.	0.	0	0
8	3.5	1.	0.	0	0
9	0.0	2.	0.	0	0
10	1.5	2.	0.	0	0
11	2.5	2.	0.	0	0
12	3.5	2.	0.	0	0
13	0.0	0.	100.	0	0
14	1.5	0.	100.	0	0
15	2.5	0.	100.	0	0
16	3.5	0.	100.	0	0
17	0.0	1.	100.	0	0
18	1.5	1.	100.	0	0
19	2.5	1.	100.	0	0
20	3.5	1.	100.	0	0
21	0.0	2.	100.	0	0
22	1.5	2.	100.	0	0
23	2.5	2.	100.	0	0
24	3.5	2.	100.	0	0

noise, we get 58.57 for the mean cost for the EKF and 58.93 for the JTF at the larger range initial condition. These are very close to those obtained by using the smaller one, which is 54.85 for the EKF and 56.0 for the JTF. By using the smaller one, we reduce the computational time and expenses for the generation and estimation of the missile trajectory by about two thirds that of the larger one.

Table 1. continued

Case No	ΔN_2 (g's)	ΔN_4 (g's)	YOFF (ft)	Noise Type	IWIGL
25	0.0	0.	0.	1	0
26	1.5	0.	0.	1	0
27	2.5	0.	0.	1	0
28	3.5	0.	0.	1	0
29	0.0	1.	0.	1	0
30	1.5	1.	0.	1	0
31	2.5	1.	0.	1	0
32	3.5	1.	0.	1	0
33	0.0	2.	0.	1	0
34	1.5	2.	0.	1	0
35	2.5	2.	0.	1	0
36	3.5	2.	0.	1	0
37	0.0	0.	100.	1	0
38	1.5	0.	100.	1	0
39	2.5	0.	100.	1	0
40	3.5	0.	100.	1	0
41	0.0	1.	100.	1	0
42	1.5	1.	100.	1	0
43	2.5	1.	100.	1	0
44	3.5	1.	100.	1	0
45	0.0	2.	100.	1	0
46	1.5	2.	100.	1	0
47	2.5	2.	100.	1	0
48	3.5	2.	100.	1	0

Table 1. continued

Case No	ΔN_2 (g's)	ΔN_4 (g's)	YOFF (ft)	Noise Type	IWIGL
49	0.0	0.	0.	2	0
50	1.5	0.	0.	2	0
51	2.5	0.	0.	2	0
52	3.5	0.	0.	2	0
53	0.0	1.	0.	2	0
54	1.5	1.	0.	2	0
55	2.5	1.	0.	2	0
56	3.5	1.	0.	2	0
57	0.0	2.	0.	2	0
58	1.5	2.	0.	2	0
59	2.5	2.	0.	2	0
60	3.5	2.	0.	2	0
61	0.0	0.	100.	2	0
62	1.5	0.	100.	2	0
63	2.5	0.	100.	2	0
64	3.5	0.	100.	2	0
65	0.0	1.	100.	2	0
66	1.5	1.	100.	2	0
67	2.5	1.	100.	2	0
68	3.5	1.	100.	2	0
69	0.0	2.	100.	2	0
70	1.5	2.	100.	2	0
71	2.5	2.	100.	2	0
72	3.5	2.	100.	2	0

Table 2. Parameters Values for the NOPN System as a Function of the Case No.

Case No	ΔN_2 (g's)	ΔN_4 (g's)	YOFF (ft)	Noise Type	IWIGL
101	0.0	0.	0.	0	1
102	1.5	0.	0.	0	1
103	2.5	0.	0.	0	1
104	3.5	0.	0.	0	1
105	0.0	1.	0.	0	1
106	1.5	1.	0.	0	1
107	2.5	1.	0.	0	1
108	3.5	1.	0.	0	1
109	0.0	2.	0.	0	1
110	1.5	2.	0.	0	1
111	2.5	2.	0.	0	1
112	3.5	2.	0.	0	1
113	0.0	0.	100.	0	1
114	1.5	0.	100.	0	1
115	2.5	0.	100.	0	1
116	3.5	0.	100.	0	1
117	0.0	1.	100.	0	1
118	1.5	1.	100.	0	1
119	2.5	1.	100.	0	1
120	3.5	1.	100.	0	1
121	0.0	2.	100.	0	1
122	1.5	2.	100.	0	1
123	2.5	2.	100.	0	1
124	3.5	2.	100.	0	1

Table 2. continued

Case No	ΔN_2 (g's)	ΔN_4 (g's)	YOFF (ft)	Noise Type	IWIGL
125	0.0	0.	0.	1	1
126	1.5	0.	0.	1	1
127	2.5	0.	0.	1	1
128	3.5	0.	0.	1	1
129	0.0	1.	0.	1	1
130	1.5	1.	0.	1	1
131	2.5	1.	0.	1	1
132	3.5	1.	0.	1	1
133	0.0	2.	0.	1	1
134	1.5	2.	0.	1	1
135	2.5	2.	0.	1	1
136	3.5	2.	0.	1	1
137	0.0	0.	100.	1	1
138	1.5	0.	100.	1	1
139	2.5	0.	100.	1	1
140	3.5	0.	100.	1	1
141	0.0	1.	100.	1	1
142	1.5	1.	100.	1	1
143	2.5	1.	100.	1	1
144	3.5	1.	100.	1	1
145	0.0	2.	100.	1	1
146	1.5	2.	100.	1	1
147	2.5	2.	100.	1	1
148	3.5	2.	100.	1	1

Table 2. continued

Case No	ΔN_2 (g's)	ΔN_4 (g's)	YOFF (ft)	Noise Type	IWIGL
149	0.0	0.	0.	2	1
150	1.5	0.	0.	2	1
151	2.5	0.	0.	2	1
152	3.5	0.	0.	2	1
153	0.0	1.	0.	2	1
154	1.5	1.	0.	2	1
155	2.5	1.	0.	2	1
156	3.5	1.	0.	2	1
157	0.0	2.	0.	2	1
158	1.5	2.	0.	2	1
159	2.5	2.	0.	2	1
160	3.5	2.	0.	2	1
161	0.0	0.	100.	2	1
162	1.5	0.	100.	2	1
163	2.5	0.	100.	2	1
164	3.5	0.	100.	2	1
165	0.0	1.	100.	2	1
166	1.5	1.	100.	2	1
167	2.5	1.	100.	2	1
168	3.5	1.	100.	2	1
169	0.0	2.	100.	2	1
170	1.5	2.	100.	2	1
171	2.5	2.	100.	2	1
172	3.5	2.	100.	2	1

Chapter 6 Program description

The program is composed of several parts : the main program, the EHITS module (the subroutine EVAL), the missile's trajectory module, the filters module (the EKF and the JTF), the projectile's trajectory module, the POH (probability of a hit) module, and the optimization module. A brief flow chart is given in the next page.

6.1 The Main Program

There are two methods used to obtain the optimal periods that minimize the cost, EHITS. One is the "brute force" method of computing the cost for each period between 0.7 seconds and 6.7 seconds with equally spaced intervals of 0.2 seconds. The other uses the parameter optimization software (SPEYER) to find the period

Computer Program

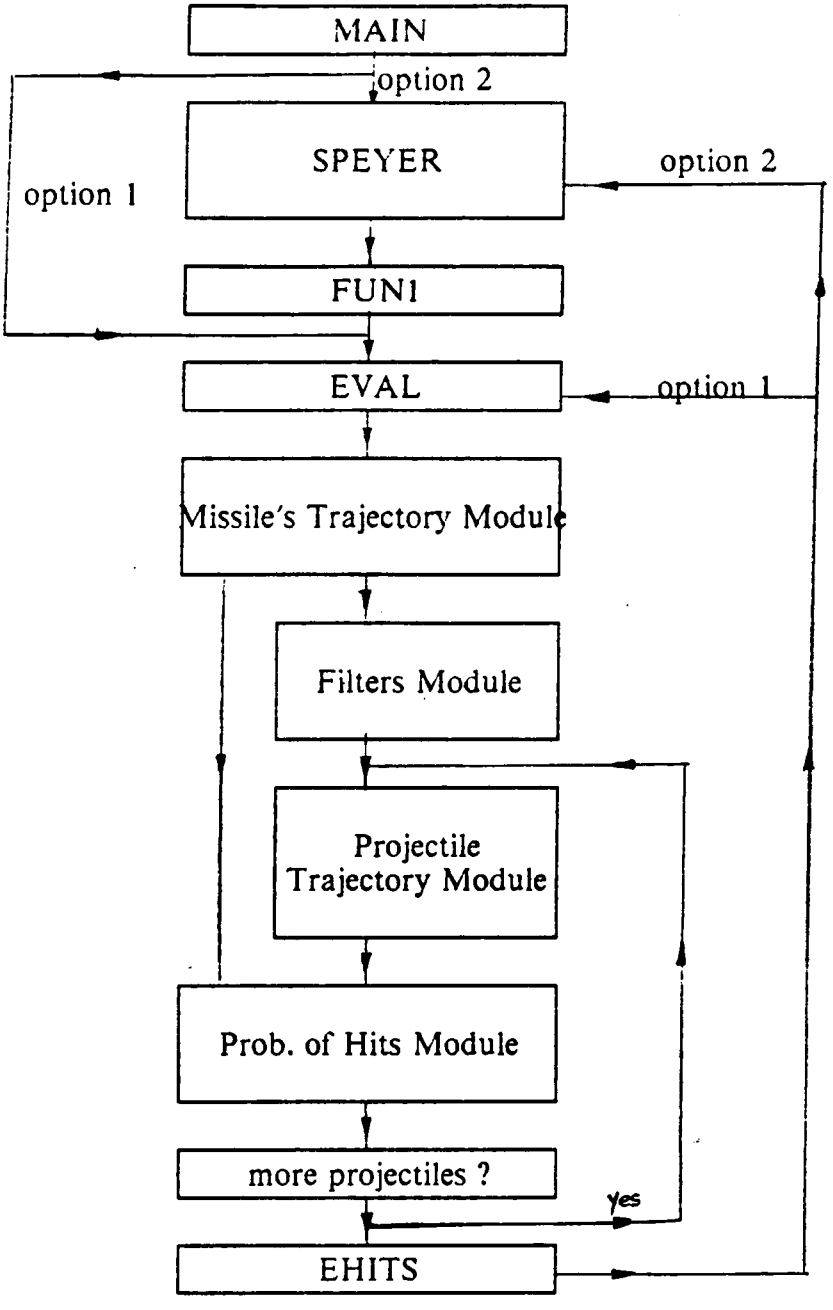

1. **Brute force approach : do for a given period (uniform spacings).**
2. **optimization approach: search for the optimal period.**

with minimum cost. The main program for the first method calls the subroutine EVAL in a DO LOOP to compute costs, cost1 and cost2, for a given trajectory of the missile. Cost1 is obtained by using the EKF as the ship's filter, and cost2 uses JTF as the ship's filters. The main program for the second method calls the subroutine SPEYER to get the optimal period which minimizes the EHITS. The execution of the subroutine SPEYER needs a subroutine, FUN1, which supplies the cost value and its gradients. The subroutine FUN1 calls the subroutine EVAL to compute the EHITS.

Input parameters are read in from the main program. These consists of

DT, IMAP, YOFF, RSTAR, T, R, E,A, V, PHI, PSI, RN1, RN2, RN3, RN4, P1, P2I, P3G, DN2, DN4	for the missile's trajectory module,
DSEED, LP, STD, P, INDP, IWIGL	for the filters module,
EPS1, EPS2, EPSO, SPEPS, LC, ME, MI, N, XOPT, CAYY, PERT, RODG	for the optimization module,
RNEAR, RLAST, TPROJ	for the EHITS module, and
TRAD, TLNGTH, TPROJ	for the POH module.

A description of these parameters is given in Appendix B.

6.2 *The EHITS Module (The Subroutine EVAL)*

The purpose of the subroutine EVAL is to compute the EHITS. First, it calls the missile's trajectory module to get the history of the missile's state vector. Secondly, it calls the filters module twice, the first time for the EKF and the second time for the JTF to get two histories of the estimated trajectory (state vector) of the missile. Thirdly, for each estimated trajectory, the subroutine EVAL calls the projectile module every 0.02 seconds when the missile's range is between 2500 feet and 300 feet. Fourthly, for each projectile fired, the subroutine EVAL further calls the POH module to estimate the probability of a hit on the missile. Finally, the probabilty of hits are accumulated to get the EHITS for each of the EKF result and the JTF result, the higher value is used as the output of this subroutine.

6.3 *The Missile's Trajectory Module*

The missile's trajectory module is made up of the following the subroutines : TRAJ, STOR, CHANGE, LINTP, ASSIGN, MAP, DXDT, IGRAT4, OFFSET. The algorithm is shown in the flow chart in the next page.

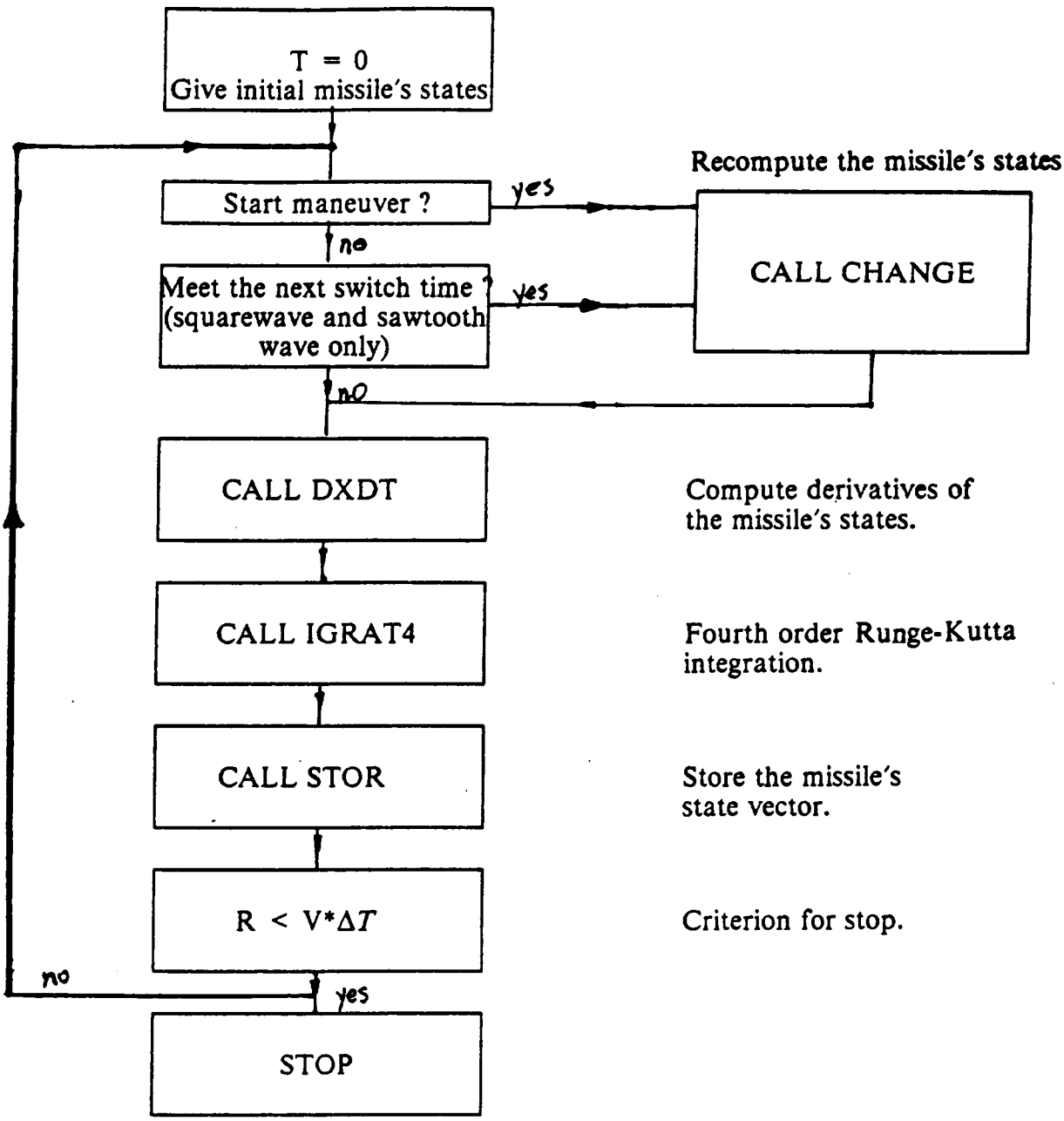
T = 0
Give initial missile's states
Start maneuver ?
yes
Recompute the missile's states
CALL CHANGE
no
Meet the next switch time ?
(squarewave and sawtooth wave only)
yes
no
CALL DXDT
Compute derivatives of the missile's states.
CALL IGRAT4
Fourth order Runge-Kutta integration.
CALL STOR
Store the missile's state vector.
R < V*ΔT
Criterion for stop.
no
yes
STOP

There are three types of periodic functions for both of the vertical plane control (ΔN_2) and the horizontal plane control (ΔN_4). This option is determined by the input parameter IMAP as follows :

IMAP	1 and 2	3 and 4	5 and 6
waveform	sinusoidal wave	square wave	sawtooth wave

6.4 *The Filters Module*

The filters module includes two filter algorithm, the EKF and the JTF. The option of algorithm is determined by the input parameter IW : IW = 1 for the EKF and IW = 2 for the JTF. This module needs the inputs of the first three elements of the missile's state vector for measurements at each time step. An initial guess of the missile's state vector is also required as an input. There are three filters for each of the EKF and the JTF algorithm, the R-filter, the E-filter, and the A-filter.

6.4.1 The EKF Module

The EKF module is made up of the following subroutines : KALMJP2, KALMAIN, UPDATE, XPDATA, XIGRA, and PIGRA. The subroutine KALMJP2 is the entry subroutine of this module. It sets up the initial conditions

for the state vector, the error covariance matrix, P, and the preparation of the calling of an IMSL subroutine, GGNSM, then it calls the subroutine KALMAIN. The IMSL subroutine GGNSM is used to generate vectors of Gaussian distributed random data for the measurement noise. The option of the measurement noise conditions is determined by the input parameter INDP and STD : INDP=1 for the no-measurement noise condition, INDP=2 with STD=15.0, 0.003, 0.001 for the smaller measurement noise condition, and INDP=2 with STD=15.0, 0.009, 0.003 for the larger measurement noise condition.

The subroutine KALMAIN calls the subroutine UPDATE to compute the update phase equations, then it does the propagation phase by calling the subroutine XPDAT to compute the derivatives of x and of P and by calling the subroutines XIGRA and PIGRA to do the integrations.

6.4.2 The JTF Module

The JTF module is made up of the EKF module and the subroutines JUMDET JUMPF and GELG. The values of $\overline{C}(0,i)$, $\overline{d}(0,i)$, and $U(i)$ are calculated for each of the R, E, and A filter and stored in the subroutine UPDATE at each time step t_i. The calculation of the U matrix involves a 3x3 matrix inversion which is computed by the subroutine GELG. These values are stored in a circle fashion and the length of the moving window is 50 time steps. The reinitialization of

these values are executed at a time interval of 4 seconds (every 80 time steps). The subroutine JUMDET for each of the R, E, and A filter are called by the subroutine KALMAIN if IW=2. This subroutine computes the values of $\sigma(k)$, $U(k)$, $\Delta(k)$, see equations (4.1) - (4.4), to determine whether there is a jump. When a jump is declared by the subroutine JUMDET for any filter, the subroutine JUMPF is further called by the subroutine KALMAIN to compute the magnitude of the jump and the corresponding changes of the EKF estimated states. The subroutine JUMPF also reinitialize the values of $\overline{C}(0,i)$, $\overline{d}(0,i)$, and $U(i)$ before it returns to the subroutine KALMAIN.

6.5 The Projectile's Trajectory Module

The projectile's trajectory module is made up of the subroutines PJFC, PJFLT, XGRAT, and EOM. The firing elevation angle of the projectile, E_p , is computed iteratively with an initial guess, E_p (0), in the subroutine PJFLT. The estimated state vector of the missile (which is obtained in the filters module) at the projectile's firing time is needed to simulate the missile's future trajectory. The dynamics of the missile are computed in the subroutine EOM. The subroutine XGRAT is used to do the integrations of the states. Meanwhile, the projectile's trajectory is simulated by calling the subroutine PJFLT and using the current E_p. The adjustment of E_p is then based on the relative range between the missile and the projectile at a future time of the simulation. The estimated elevation

angle of the missile is used as the initial guess of the first projectile's elevation angle $E_p(0)$. For the following projectiles, the E_p of the previous projectile is used as $E_p(0)$. The firing azimuth angle of the projectile is computed after the E_p is obtained.

6.6 *The POH Module*

The purpose of the POH module is to compute the probability of a hit (POH) on the missile by the projectile. It is made up of the following subroutines: TSTPGM, CPAX, XMDATA, PJTM, NHIT, PROB, IOT, and SNVRSN. The subroutine TSTPGM calls the subroutine CPAX to compute the miss distance between the projectile's trajectory and the true missile's trajectory. The history of the missile's states, the elevation and the azimuth angles of the projectile are required as inputs. The position and the velocity vectors of the projectile are computed in the subroutine PJTM, and those for the missile are computed in the subroutine XMDATA. These two subroutines are called iteratively by the subroutine XCPA at the same time step until the closest point of the missile and the projectile (CPA) is found. The position vectors are used to compute the miss distance and the velocity vectors are used to compute the relative velocity between the missile and projectile; both are needed in computing the POH. After the closest point is found, the subroutine TSTPGM then calls the subroutine NHIT to compute the the endpoints of the rectangle over which the probability

is to be estimated. This rectangle is used to take into account the geometrical size of the missile on the POH. The subroutine PROB is called by the subroutine NHIT to compute the probability at a specific point in the rectangle. The probabilities over the whole rectangle points are then accumulated in the subroutine NHITS. This value is the output of the POH module.

6.7 The Optimization Module

The optimization code used is the subroutine package "SPEYER", which is developed by the control group in the Department of Aerospace and Ocean Engineering at VPI&SU, [44]. The optimization algorithm is based on the variable-metric gradient method, which provides a quadratic terminal convergence for finding an unconstrained minimum. It employs a metric which is adjusted during the iteration cycles. This package can be used to solve the optimization problem with multi-parameters and nonlinear constraints. There are two approaches to handle the constraints; one is the gradient projection approach and the other is the penalty function approach. However, our problem consists of only one parameter to be optimized and no constraints at all. There are some simpler gradient methods available for this purpose. We just use 'SPEYER' for future work consideration.

It is assumed that the cost function J to be minimized is smooth to the extent of possessing continuous second order partial derivatives since the gradient vector, J_x , as well as the cost function J itself need to be computed at the starting point. The vector x contains the parameters to be optimized. The update of x is given by following equation :

$$\Delta x = -\alpha H J_x \tag{6.1}$$

where $\alpha > 0$ is a scalar step size parameter, and the H is a variable metric which is selected arbitrarily at the starting point as a positive definite, symmetric matrix. It is updated by

$$H(x + \Delta x) = H(x) + \Delta H \tag{6.2}$$

where ΔH is computed accordingly to either of the following three algorithms :

(1) BFGS

$$\Delta H = \frac{\Delta x \, \Delta x^T}{\Delta x^T \Delta J_x} - \frac{H \Delta J_x \Delta J_x^T H}{\Delta J_x^T H \Delta J_x} + v v^T \tag{6.3.1}$$

where

$$v = \sqrt{\Delta J_x^T H \Delta J_x} \; \frac{\Delta x}{\Delta x^T \Delta J_x} - \frac{H \Delta J_x}{\Delta J_x^T H \Delta J_x} \tag{6.3.2}$$

(2) DFP

$$\Delta H = \frac{\Delta x \, \Delta x^T}{\Delta x^T \Delta J_x} - \frac{H \Delta J_x \, \Delta J_x^T H}{\Delta J_x^T H \Delta J_x} \tag{6.4}$$

(3) Hoshino

$$\Delta H = \frac{\Delta x \, \Delta x^T [\, 2 \Delta J_x^T H \Delta J_x + \Delta x^T \Delta J_x \,]}{\Delta x^T \Delta J_x [\, \Delta J_x^T H \Delta J_x + \Delta x^T \Delta J_x \,]}$$

$$- \frac{H \Delta J_x \, \Delta J_x^T H + \Delta x \, \Delta J_x^T H + H \, \Delta J_x \, \Delta x^T}{\Delta J_x^T H \, \Delta J_x + \Delta x^T \Delta J_x} \tag{6.6}$$

The option for the update of the variable matric is determined by the value of the input parameter MDFP as follows :

MDFP	0	1	2	3
update algorithm	no update	BFGS	DFP	Hoshino

In this dissertation the BFGS update algorithm is used. However, the update algorithm is not critical for one-parameter optimization problem such as ours.

To use the software package, it is necessary to provide a subroutine, FUN1, to calculate the cost function J, and the gradient vector J_x. In our problem the cost function (EHITS) is not analytic; therefore, both the J and J_x are computed numerically. The EHITS can be computed by calling the subroutine EVAL. The gradient vector, which is actually a scalar in our problem, is computed by the centered difference method in the subroutine FUN1. In our problem, the cost

function is the EHITS and the parameter to be optimized is the period used for both N_2 and N_4 maneuvering functions.

Chapter 7 Result and Discussion

All the results discussed in sections 7.1 - 7.3 for both the PN system (cases no. 1 - 72) and the NOPN system (cases no. 101 - 172) are obtained by using the sinusoidal maneuvering function and the conditions described below : (1) the smaller process noise as stated in equation (5.1); (2) the nearer range for the initial condition of state estimation as described in equation (5.4); (3) 8 different maneuver starting ranges from 3250 ft to 5000 ft with equally spaced intervals of 250 ft. Since these results are used only to obtain an approximate value of the optimal period and the minimum cost for each case, only 8 maneuver starting ranges, combined with 8 different sets of generated noise, are used for averaging.

The optimization process has not been used in obtaining these results; only the cost vs. the maneuvering period from 0.7 seconds to 6.7 seconds, with equally spaced intervals of 0.2, are computed. Section 7.3.3 gives some figures to show the influence of maneuvering period on the estimation of trajectories, the proba-

bility of a hit on the missile by each projectile (POH), and the estimated number of hits (EHITS).

In section 7.4 and 7.5, more results for some selected cases are obtained by using the larger process noise as stated in equation (5.2) to improve the performance of the EKF, especially for the shorter period results. Also, 24 maneuver starting ranges, combined with 24 different sets of generated noise are used to cover at least one maneuvering period to get better averages for the larger periods results. However, more maneuver starting ranges have little influence on the shorter period results. The square wave and the sawtooth wave are also used for the maneuvering function. Some plots of the cost vs. the maneuvering period are shown in section 7.4. Some results using the optimization process are shown in section 7.5.

7.1 Cases Without Maneuvering

In order to investigate how the periodic maneuvers reduce the cost, some no-maneuver cases, i.e. cases with $\Delta N_2 = 0$, $\Delta N_4 = 0.$, are checked first. When the missile comes in without any maneuver, the ship's filters perform best since the EKF is designed for the tracking of a no-maneuver target. Therefore we would expect to get a better estimation for the no-maneuver cases as compared to the maneuvering cases under the same filtering conditions.

The cost values (EHITS) for some no-maneuver cases are listed in the following tables :

Table 3. EHITS for the No-Maneuver cases for the PN System

Case No	1	13	25	37	49	61	
Noise Type	0	0	1	1	2	2	
Y Offset	0.	100.	0.	100.	0.	100.	(ft)
EKF	83	0	55	0	30	0	(EHITS)
JTF	83	0	55	0	30	0	(EHITS)

Table 4. EHITS for the No-Maneuver cases for the NOPN System

Case No	101	113	125	137	149	161	
Noise Type	0	0	1	1	2	2	
Y Offset	0.	100.	0.	100.	0.	100.	(ft)
EKF	81	93	34	37	12	13	(EHITS)
JTF	81	93	34	37	12	13	(EHITS)

Concerning the filters used, the EKF and the JTF, we can make the following observation. Comparing the EKF results with the JTF results in these two tables, we see that the cost values obtained by the EKF are the same as those by the JTF. In other words, the jump filter is not triggered for the no-maneuver cases even under measurement noise condition. This implies that the jump filter is not executed due to any measurement noise (or false jumps), which is expected since the JF is designed for the purpose of detecting state jumps but not for the measurement noise

It is shown in Table 3 that for the PN system under the offset condition, cases no. 13, 37, and 61, the cost values are all near zeros. That is, the PN system

totally fails when the missile has its aimpoint 100 ft offset in the y direction. This implies that the performance of the PN system deteriorated whenever the missile comes in with an offset. The reason for this is due to the erroneous assumption of the PN system that the missile is homing in on the radar site. The PN constants are assumed known to the PN system and are used in its model of the missile in the filters. The function of the PN constants in the filters ensures that the estimated trajectory of the missile will end at the radar's origin. However, the origin of the coordinates is placed at the ship's radar (see section 2.1), which is 100 ft away from the aim-point of the missile on the ship in the offset case. Thus, the PN system enhances the filters' performance slightly in the no-offset cases, comparing case no. 1 to no. 101, etc., but it degrades the estimation performance in the offset cases. We note that the missile's aim point on the ship is an unknown quantity to the ship's fire control system.

Conversely, Table 4 shows that the NOPN system can deal effectively with the offset condition as well as the no-offset condition. It is further shown there that the NOPN system performs equally well under both the offset condition and the no-offset condition. For example, among those results obtained with no-measurement noise, case no. 113, which is an offset case, has a higher cost value, EHITS = 93, than that of the corresponding no-offset case no. 101, which has the EHITS of 81. One reason for this is that more uncertainties of the missile's dynamics are taken into account in the filters of the NOPN system. Recall that for the NOPN system, the effects of N_1 and N_2 and that of N_3 and N_4 are merged together into two new variables, $\tilde{N}_2$ and $\tilde{N}_4$. The estimation of $\tilde{N}_2$ and $\tilde{N}_4$ are in-

fluenced by measurement noise more than that of N_2 and N_4, since in the latter case the PN constants N_1 and N_3 are further used as known constants.

For the no-maneuver cases, both the PN and the NOPN systems perform better under the no-measurement noise conditions than under measurement noise existing conditions. Furthermore, as the covariance of the measurement noise increases, the performance degrades. Take as an example the three no-maneuver cases for the NOPN system with no-offset condition, cases no. 101,125, and 149. Among these, case no. 101 (the no measurement noise case) has the highest cost, 81 EHITS, and case no. 149 (the larger measurement noise case) has the lowest cost, 12 EHITS. Therefore the missile has little chance to complete its mission if the measurement condition on the ship is perfect (no measurement noise). However, in the real world, there is always some measurement noise, which increases the chances for the missile to avoid the ship's gunfire and hit the ship. Considering the NOPN system on the ship, the two best no-maneuver cases we obtained for the missile to get fewer hits are those under the larger measurement noise condition, cases no. 149 and 161. The EHITS is 12 and 13, respectively. However, these results cannot be generalized to maneuvering cases.

For those cases with zero-offset but with measurement noise conditions, it is shown in the above tables that the PN system can do better than the NOPN system. For example, case no. 25 (EHITS = 55) vs. case no. 125 (EHITS = 34) show the results under the smaller measurement noise condition, whereas case no. 49 (EHITS = 30) vs. case no. 149 (EHITS = 12) show the results under the

larger measurement noise condition. However, this is not critical for those maneuvering cases, as will be shown in the following two sections.

Finally, Tables 3 and 4 show that the EHITS values are too large for the missile to evade the ship's gunfire. This is a good reason for the missile to maneuver instead of just employing constant controls.

7.2 PN System Results

The PN system cannot handle the offset condition as has been shown in section 7.1. Therefore, we only discuss the no-offset cases for the PN system. The minimum cost and the optimal period for each ΔN_2 and ΔN_4 combination for the PN system under the no-offset and the no-measurement noise conditions are listed in Table 5. Those for the PN system under no-offset but measurement noise conditions are listed in Table 6 and Table 7. The former is under the smaller measurement noise condition and the latter is the larger measurement noise condition.

Table 5. EHITS at optimal period for cases EHITS at optimal period for cases No. 1-12 : PN System, No Offset, No Noise.

$\Delta N_4 \setminus \Delta N_2$	0.0 g's	1.5 g's	2.5 g's	3.5 g's	
0.0	83.	10.	8.	8.	(EHIT)
g's	none	3.8	3.0	2.7	(sec.)
1.0	22.	3.	3.	3.	(EHITS)
g's	3.4	3.5	2.9	2.7	(sec.)
2.0	13.	2.	2.	3.	(EHITS)
g's	2.4	3.5	2.8	2.4	(sec.)

Table 6. EHITS at optimal period for cases No. 25-36 : PN System, No Offset, Small Noise.

$\Delta N_4 \setminus \Delta N_2$	0.0 g's	1.5 g's	2.5 g's	3.5 g's	
0.0	54.5	17.	10.	7.	(EHITS)
g's	none	2.3	2.2	2.2	(sec.)
1.0	26.	10.	6.	3.	(EHITS)
g's	2.1	2.5	2.2	2.1	(sec.)
2.0	14.	6.	3.	3.	(EHITS)
g's	2.0	2.4	2.1	1.9	(sec.)

Table 7. EHITS at optimal period for cases No. 49-60 : PN System, No Offset, Large Noise.

$\Delta N_4 \setminus \Delta N_2$	0.0 g's	1.5 g's	2.5 g's	3.5 g's	
0.0	30.5	9.	8.	5.5	(EHITS)
g's	none	3.4	2.9	2.5	(sec.)
1.0	13.5	4.0	5.	5.	(EHITS)
g's	3.3	3.4	2.9	2.5	(sec.)
2.0	7.5	2.	2.	2.	(EHITS)
g's	2.5	3.5	2.7	2.5	(sec.)

There are two values for each case in these tables. The value in the lower blank is the optimal period in each case. The value in the upper blank is the minimum cost at that optimal period for that specific combination of ΔN_2 and ΔN_4.

From these tables, we can see that the cost is reduced dramatically to a minimum whenever there is a maneuver in the vertical plane (mainly due to the ΔN_2 effect), the horizontal plane (mainly due to the ΔN_4 effect), or both planes. In other words, the higher the maneuvering level of g's, the lower the cost value. For example, the first column of Table 5 shows that when $\Delta N_2 = 0$ the minimum cost decreases as ΔN_4 increases. The same observations are found in Table 6 and Table 7. This implies that the periodic maneuvers really help the missile in its objective to evade the tracking and the gunfire of the ship.

The tables further suggest that we can get a lower cost by maneuvering in both planes. For example, in Table 5, the case with both $\Delta N_2 = 1.5$ g's and $\Delta N_4 = 1.0$ g's has a lower minimum cost than that with only $\Delta N_2 = 2.5$ g's. However, the above observations are true within bounds. The missile cannot use unlimited higher maneuvering levels of g's in both planes. Since the use of the larger ΔN_2 and ΔN_4 values above a certain point does not significantly improve the missile's evasion of tracking, $\Delta N_2 = 1.5$ g's and $\Delta N_4 = 1.0$ g's are a reasonable choice for the missile if the measurement condition for the ship is perfect. With this selection, the EHITS is 2, which is already a very low value. Similarly, picking the minimum effort of ΔN_2 and ΔN_4 to reach the minimum cost value (taking into account the measurement noise for the ship), it is found that $\Delta N_2 = 2.5$ g's and

$\Delta N_4 = 2.0$ g's are suitable for both the larger and the smaller measurement noise conditions. The optimal period is about 2.1 sec. for the former and 2.7 sec. for the latter. Furthermore, the optimal periods in Table 5 are all higher than 2.4 seconds. Specifically, in the case with $\Delta N_2 = 1.5$ g's and $\Delta N_4 = 1.0$ g's, the optimal period is about 3.5 seconds. The optimal periods are all higher than 1.9 sec. for the smaller measurement noise cases in Table 6, and higher than 2.5 sec. for those under the larger measurement noise condition in Table 7.

Comparing the corresponding cases in these tables, we see that most of the minimum costs in Tables 6 and 7 are not lower than those in Table 5, the no-maneuver cases not been considered. This implies that the estimation job is not degraded too much due to measurement noise conditions.

Here, we compare two cases : the one in Table 5 with $\Delta N_2 = 1.5$ g's $\Delta N_4 = 0.$, which has the cost value 10, and the one with $\Delta N_2 = 0$, $\Delta N_4 = 2.0$ g's, which has the cost value 13 We might conclude that the ΔN_2 maneuver is more effective than the ΔN_4 maneuver in the sense that it can get a lower cost value by maneuvering at a lower level of g's. However, we have used different initial conditions for the error covariance matrices, $P_E(0)$ for the E filter and $P_A(0)$ for the A filter, which makes them incomparable. Also, the previous results imply that the larger error covariance values in the P matrix is beneficial to the EKF. This effect is not significant under the influence of the measurement noise condition.

7.3 NOPN System Results

7.3.1 Results from No-Offset Condition

The minimum cost and the optimal period for each ΔN_2 and ΔN_4 combination for the NOPN system under no measurement noise and no-offset conditions are listed in Table 8. Those for the NOPN system under the no-offset but with the measurement noise conditions are listed in Table 9 and Table 10. The former is under the smaller measurement noise condition, and the latter is under the larger one.

Table 8. EHITS at optimal period for cases No. 101-112 : NOPN System, No Offset, No Noise.

$\Delta N_4 \setminus \Delta N_2$	0.0 g's	1.5 g's	2.5 g's	3.5 g's	
0.0	82.3	10.	7.	6.	(EHITS)
g's	none	2.9	2.4	2.2	(sec.)
1.0	20.	3.	3.	3.	(EHITS)
g's	3.1	2.5	2.3	2.1	(sec.)
2.0	10.	1.	1.	2.	(EHITS)
g's	2.1	2.3	2.1	2.1	(sec.)

Table 9. EHITS at optimal period for cases No. 125-136 : NOPN System, No Offset, Small Noise.

$\Delta N_4 \setminus \Delta N_2$	0.0 g's	1.5 g's	2.5 g's	3.5 g's	
0.0	34.	8.	5.5	4.0	(EHITS)
g's	none	2.9	2.5	2.3	(sec.)
1.0	11.	3.5	2.	1.2	(EHITS)
g's	1.9	2.1	2.3	2.3	(sec.)
2.0	5.	1.	0.5	0.5	(EHITS)
g's	1.9	2.1	2.1	2.1	(sec.)

Table 10. EHITS at optimal period for cases No. 149-160 : NOPN System, No Offset, Large Noise.

$\Delta N_4 \setminus \Delta N_2$	0.0 g's	1.5 g's	2.5 g's	3.5 g's	
0.0	12.5	4.0	2.6	2.8	(EHITS)
g's	none	4.3	2.9	3.3	(sec.)
1.0	1.0	1.2	1.0	2.0	(EHITS)
g's	4.3	3.3	3.3	2.5	(sec.)
2.0	2.0	0.4	0.3	1.2	(EHITS)
g's	2.5	5.1	3.3	2.3	(sec.)

The results show many similarities to the PN system, such as : the rapid reduction to a minimum cost by maneuvers; the lower cost by maneuvering in both planes; the higher the maneuvering level of g's, the lower the cost value within some bounds.

Comparing Table 8 to Table 5, Table 9 to Table 6, and Table 10 to Table 7, we see that the results obtained by the PN system and the NOPN system are close for each maneuvering case under no-offset condition. For example, cases with

$\Delta N_2 = 2.5$ g's and $\Delta N_4 = 2.0$ g's in both Table 6 (PN system) and Table 9 (NOPN system) have the same optimal period (2.1 sec.). Besides, the minimum cost is 3 for the former and 0.5 for the latter under the smaller measurement noise condition.

Picking the minimum effort of ΔN_2 and ΔN_4 to reach the minimum cost value, it is recommended that $\Delta N_2 = 2.5$ g's and $\Delta N_4 = 2.0$ g's be used for the no-offset condition with the PN system used on the ship. With this choice, the optimal periods are 2.1 seconds for no measurement noise and the smaller measurement noise conditions, and is 3.3 seconds for the larger measurement noise condition.

7.3.2 Results for the Nonzero Offset Condition

The minimum cost and the optimal period for each ΔN_2 and ΔN_4 combination for the NOPN system under the no-measurement noise and the offset conditions are listed in Table 11 Those for the NOPN system under the offset condition and the measurement noise conditions are listed in Tables 12 and 13. The former is under the smaller measurement noise condition, and the latter is under the larger one.

Table 11. EHITS at optimal period for cases No. 113-124 : NOPN System, Offset, No Noise.

$\Delta N_4 \setminus \Delta N_2$	0.0 g's	1.5 g's	2.5 g's	3.5 g's	
0.0	94.	9.	7.	6.	(EHITS)
g's	none	3.0	2.4	2.3	(sec.)
1.0	20.	4.	2.5	2.5	(EHITS)
g's	3.1	2.5	2.3	2.1	(sec.)
2.0	18.	1.	2.	2.	(EHITS)
g's	1.5	2.3	2.	2.1	(sec.)

Table 12. EHITS at optimal period for cases No. 137-148 : NOPN System, Offset, Small Noise.

$\Delta N_4 \setminus \Delta N_2$	0.0 g's	1.5 g's	2.5 g's	3.5 g's	
0.0	37.	8.5	6.0	4.0	(EHITS)
g's	none	2.9	2.5	2.3	(sec.)
1.0	12.	4.0	2.	1.	(EHITS)
g's	1.9	2.5	2.3	2.3	(sec.)
2.0	6.	2.	0.5	0.5	(EHITS)
g's	1.9	2.2	2.3	2.1	(sec.)

Table 13. EHITS at optimal period for cases No. 161-172 : NOPN System, Offset, Large Noise.

$\Delta N_4 \setminus \Delta N_2$	0.0 g's	1.5 g's	2.5 g's	3.5 g's	
0.0	13.5	4.2	3.0	2.8	(EHITS)
g's	none	4.3	3.5	2.7	(sec.)
1.0	3.8	1.2	1.5	1.2	(EHITS)
g's	3.3	5.5	3.3	3.2	(sec.)
2.0	2.5	0.5	0.3	1.2	(EHITS)
g's	2.5	4.3	3.2	2.3	(sec.)

Again, similar results are found as previously described. Picking the minimum effort of ΔN_2 and ΔN_4 to reach the minimum cost value, it is recommended that $\Delta N_2 = 2.5$ g's and $\Delta N_4 = 2.0$ g's be used for the offset condition with the PN system used on the ship. With this choice, the optimal periods are found at 2.0 seconds, 2.3 seconds, and 3.2 seconds, respectively for the no measurement noise, the smaller and the larger measurement noise conditions.

The results for the NOPN system under the offset condition are close to those under no-offset condition. This can be shown by comparing Table 8 to Table 11, Table 9 to Table 12, and Table 10 to Table 13. Therefore, the NOPN system is less sensitive to the offset condition, unlike the PN system, which totally fails in the nonzero offset condition.

It is recommended that the ship use the NOPN system. The reasons are : (1) under the no-offset condition, the PN and the NOPN systems have close results; (2) under offset conditions, the PN system fails but the NOPN system performs as well as under the no-offset condition; (3) we do not have to know the PN constants as we do in the PN system, which are seldom known precisely.

7.3.3 Influence of Maneuvering Period on Estimations

Some plots are given to show the estimated number of hits versus the range of the missile, see figure 19, 23, and 27 for case no. 123 for the period of 0.9, 1.9, and

2.9 seconds, respectively. The coresponding plots for the accumulated estimated number of hits vs. missile's range are figures 20, 24, and 28. The comparisons between the true and the estimated trajectories for each case are given by figures 21, 25, and 29 for y-coordinate vs. x-coordinate, and figures 22, 26, and 30 for z-coordinate vs. missile's range.

It is shown in figures 21 and 22 that for a maneuvering period like 0.9 sec. or less, the JF is not triggered for execution, and the smoothing-out effect of the EKF makes the estimated trajectory close to the true one. From figure 19, we see that the probability of a hit increases oscillatorily as the missile's range decreases, which implies that the closer the missile's range, the higher the probability of hit except for some dead zones where the projectiles totally miss the missile.

The function of the JF is shown clearly in figures 26 and 30. Before the JF detects a jump, the JTF estimation is exactly the same the EKF's. These estimated trajectories begin to deviate far from the true one when the missile starts its maneuver. The JTF brings the estimated trajectory back to the true one whenever the JF is triggered for execution.

7.4 Comparison Between Three Maneuvering Functions

We have recommended the NOPN system for the ship. The NOPN system performs equally well under the no-offset and offset conditions, which depends on

the aim point of the missile on the ship. Since the aim point of the missile in unknown to the ship, offset conditions would be preferred. Therefore, some NOPN system cases under offset conditions are selected for redoing to get some improvements for the ship's filtering process.

In order to improve the estimation performance for the ship, these selected cases use the larger process noise as in equation equation (5.2). In these cases 24 runs of different maneuver starting ranges are used to get the averaged cost instead of just using 8 runs. More maneuver starting ranges are found to have some influences on large periods results but little for short periods results. This is because more maneuver starting ranges are needed to cover at least one period for the longer periods cases to get unbiased averages. A cost vs. period plot is given for each of these cases, see figures 1-9. The following table shows the correspondence between the plot numbers, the case numbers, and some parametric values.

Table 14. Parametric Values and Case No. for the Redo Cases for the Sinusoidal Maneuvering Function

Plot No	Case No	ΔN_2 (g's)	ΔN_4 (g's)	Noise Type	optimal period (sec.)	EHITS
1	115	2.5	0.	0	2.2	9
2	121	0.0	2.	0	1.6	17
3	123	2.5	2.	0	1.9	2
4	139	2.5	0.	1	2.1	8
5	145	0.0	2.	1	1.6	10.5
6	147	2.5	2.	1	1.9	2
7	163	2.5	0.	2	3.5	2.8
8	169	0.0	2.	2	2.4	3.5
9	171	2.5	2.	2	2.7	1

Again, Table 14 shows that the missile should maneuver in both the horizontal and the vertical planes to get a lower EHITS. Therefore, only cases no. 123, 147, and 171 are chosen further for redoing for the square wave and the sawtooth wave maneuvering functions. These are shown in figures 10 - 12 for the square wave maneuvering cases, and figures 13-15 for the sawtooth wave maneuvering cases.

There are two lines for each plot. The dotted line denotes the EKF results and the solid line denotes the JTF results. It is shown that the dotted line has high cost when the period is small, and the cost drops very rapidly as the period increases. This implies that the EKF performs better for small maneuvering periods of the missile, and the performance deteriates very soon as the periods increases. This is due to the smoothing-out effect of the EKF as described previously. For small periods the cost value is very high since the missile's trajectory maneuvers vary little from an easily predicted path and, consequently, the ship is able to place projectiles within a small miss distance radius of the missile's path. As the period is increased from zero the cost will decrease since the ship has difficulty in estimating small maneuvers that are masked by radar errors and those undetected maneuvers generate larger miss distances. As the period is increased still further, the EHITS reaches a minimum and then increases as the ship detects the maneuvers and predicts projectile interceptions more accurately.

The jump filter (JF) is not triggered until the solid line separates from the dotted line. In most figures the solid line goes below the dotted line when they first separate, but it stays there for only a very short period interval before going above. This observation is due to the delay of the detection of the JF for a jump, which means that in smaller maneuvering period cases, the JF cannot catch up with the maneuvers. We remark that the JF needs a time delay to accumulatd error residuals before it detects a jump, and also that there is a time delay in intercept due to the projectile flyout. The time delays make the estimated trajectory worse when the missile starts an opposite-direction motion soon after the previous jump is estimated. Nevertheless, the JF does perform better than the EKF for larger maneuvering periods.

Both the EKF and the JTF have been used to do the estimation job. Each filter gives a cost value. We take the higher cost value as the final cost value for the EHITS. It is shown in figures 1 - 15 that the EHITS decreases monotonically until it reaches the minimum point.

Table 15. Comparison Between Three Maneuvering Functions

Measurement Noise Type Wave Form \ Case No.	0(no) 123	1(small) 147	2(large) 171	
sin.	2.0	2.0	1.0	(EHITS)
wave	1.9	1.9	2.7	(sec.)
square	2.0	2.0	1.9	(EHITS)
wave	1.6	1.6	1.9	(sec.)
sawtooth	4.0	4.0	1.0	(EHITS)
wave	2.2	2.4	3.3	(sec.)

Table 15 is given to show the comparative results between three periodic maneuvering functions. Suppose the missile uses a square wave maneuvering function, we expect that the JF would be triggered earlier to execute than other waveforms. This is because that the maneuver is a constant between switches and the EKF accumulates larger residules caused by the square waveform than others at the beginning of the maneuvering. In contrast, the JF would be triggered the latest for the sawtooth waveform among the three waveforms investigated. Thus, it is shown in Table 15 that by using the square wave form the optimal period is the smallest one, and by using the sawtooth wave the optimal period is the largest one. However, the earlier detection of a jump does not necessarily imply the best estimation for the entire missile's trajectory and higher EHITS. Similarly, the later detection of a jump does not necessarily imply lower EHITS. For example, in case no. 147, the optimal period is 1.6 sec. for the square wave, which is the smallest, and that for the sawtooth wave is 2.4 seconds, which is the largest among these three wave form results. In these cases, the square wave result has 2.0 EHITS, which is not the best case for the ship, and the sawtooth has 4.0 EHITS, which is not the worse case for the ship, neither. Since these optimal periods obtained by using different periodic waves are different, the dissertation warrants the title "suboptimal period design" instead of "optimal period design".

We select the best control waveform that has the minimum EHITS with the longest optimal period from Table 15. For example, we observe that for case no. 147 (the small measurement noise condition) in Table 15, both the sinusoidal and the square wave have the minimum EHITS of 2.0, but the optimal period for the

sinusoidal waveform (1.9 sec.) is larger than that (1.6 sec.) of the square waveform. Therefore, we select the sinusoidal waveform with the period of 1.9 sec. as the best control waveform under the small measurement noise condition.

With the minimum EHITS, the missile has the highest survivability . With the largest optimal period, the missile needs least maneuvering. Based on these criterions, from Table 15, the optimal waveforms under different measurement noise conditions are recommended as follows : (1) for the no-measurement noise and the small measurement noise conditions, cases no. 123 and 147, respectively, the sinusoidal wave with the period of 1.9 sec. has the EHITS of only 2.0. (2) for the large measurement noise condition, case no. 171, the sawtooth wave with the period of 3.3 sec. has the EHITS of only 1.0. Furtherfore, for case no. 171 the sinusoidal wave with the period of 2.7 sec. is also a good choice since the EHITS is as low as the minimum one (1.0 EHITS), and the optimal period (2.7 sec.) is not too short.

When the ship's radar noise condition is not known to the missile, the best waveform among these three types is the sinusoidal wave with the period of 1.9 seconds. This is an optimal choice for the no-measurement noise and the small measurement noise condition, which have the minimum EHITS 2.0. Although this is not optimal for the large measurement noise condition, but it only has 3.0 EHITS in this case.

7.5 *Optimization Cases*

Case No 147 is chosen to go through the optimization process for the three periodic maneuvering functions. This is an offset case under the smaller measurement noise condition for the NOPN system with $\Delta N_2 = 2.5$ g's and $\Delta N_4 = 2.0$ g's. The initial guess for the optinization process should be selected carefully to reduce the computation time and ensure convergence to the global minimim point. As described in the previous section, the curves of the cost function vs. the maneuvering period monotonically decrease until they reach the minimum point. With this feature, we can always start with a small value period, for example, around 1.0 second, as an initial guess for the optimization process.

The perturbation step for the computation of the cost gradient should be selected properly. It should be small enough so that the central difference equations approximate the differential equations. However, it should be large enough so that the two perturbed points have two different costs, which yield a nonzero gradient.

The optimal periods obtained are 1.894 sec. for the sinusoidal maneuvering function, 1.567 sec. for the square wave, and 2.359 sec. for the sawtooth wave. The corresponding minimum costs are 2.270, 2.130, and 3.079 EHITS, respectively. Figures 16 - 18 show the points which are selected automatically by the program to be calculated during the optimization process for these three cases.

Chapter 8 Conclusion

The period design for the maneuvering control function of the missile to evade the tracking and the prediction capability of the EKF and the JTF (EKF+JF) has been studied.

Our results show that the ship should not use the PN system in its filters. For, if it does then the EHITS on the missile are almost always zero. The reason for this is that the PN system assumes that the missile impacts on the ship at the location of the radar. The survivability is low, however, if the missile's aim point coincide with the ship's radar site. When this is not the case, a filter using the PN system will have large errors in its estimate of the missile's guidance parameters. The result is large miss distances of the ship's projectiles and almost zero EHITS on the missile. For this reason the ship should employ the NOPN system which makes no erroneous assumption about where the missile will impact on the ship.

For the case that the ship uses the NOPN system (i. e., it does not use the PN constants in its filtering process), three kinds of maneuvering control function for the missile have been investigated for the optimal periods. It has been shown as expected that the curve of the cost function vs. the maneuvering period is monotonically decreasing until it reaches a minimum point.

It has been found that the magnitudes of the maneuvering function, ΔN_2 and ΔN_4, have some effects on the period design. We recommend that the missile uses 1.5 g's $< \Delta N_2 <$ 2.5 g's and 1.0g's $< \Delta N_4 <$ 2.0 g's.

The radar measurement capability of the ship has some influence on the estimated number of hits on the missile by the projectiles. In most cases investigated, we found that the optimal period increases with an increase in measurement noise. This is to be expected since the filtering system of the ship cannot detect maneuvers which are masked by the ship's radar errors. The missile's period can be increased without detection until the changes in the missile's position relative to the no-maneuver case matches the radar errors.

The shape of the maneuvering function is also essential to the period design. Comparing the result obtained using the three wave forms, we found that by using a square wave the optimal period is the smallest and by using a sawtooth wave the optimal period is the largest.

When the measurement noise condition is known to the missile, the optimal waveforms under different measurement noise conditions are recommended as follows : (1) for the no-measurement noise and the small measurement noise conditions, cases no. 123 and 147, respectively, the sinusoidal wave with the period of 1.9 sec. has the EHITS of only 2.0. (2) for the large measurement noise condition, case no. 171, the sawtooth wave with the period of 3.3 sec. has the EHITS of only 1.0. The sinusoidal wave with the period of 2.7 sec. is also a good choice since the EHITS is as low as the minimum one (1.0 EHITS), and the optimal period (2.7 sec.) is not too short. When the ship's radar noise condition is not known to the missile, some tradeoff should be made. We recommend that the missile uses the sinusoidal wave with the period of 1.9 seconds. The EHITS thus obtained are 2.0 for the no-measurement noise and the small measurement noise condition and is 3.0 for the large measurement noise condition.

Bibliography

1. Kalman, R. E. "A New Approach to Linear Filtering and Predition Problems," Journal of Basic Enginerring (1960) 35-46.

2. Kalman, R. E. and Bucy, R. S. "New results in Linear Filtering and Prediction Theory," Journal of Basic Enginerring (1961) 95-108.

3. Bryson, Jr. A. E., and Ho, Y. C. "Applied Optimal Control," Hemisphere, Washton, D. C., 1975.

4. Bryson, Jr. A. E., and Ho, Y. C. "New Concepts in Control Theory," Journal on Guidance and Control (1985), 417-425.

5. Smith, G. L., and Schmidt, S. F. "The Application of Statistical Filter Theory to Optimal Trajectory Determination on Board a Circumlunar Vehicle," Reprint 61-92, American Academy of Science Meeting, 1961.

6. McLean, J. D., and Schmidt, S. F. "Optimal Filtering and Linear Prediction Applied to an On-Board Navigation System for the Circumlunar Mission," Reprint 61-93, American Academy of Science Meeting, 1961.

7. Hutchinson, C. E. "The Kalman Filter Applied to Aerospace and Electronic Systems," IEEE Transactions on Aerospace and Electronic Systems (1984) 500-504.

8. Maybeck, P. S. *Stochastic Model, Estimation and Control*, 1 (1979) New York, Academic Press.

9. Maybeck, P. S. *Stochastic Model, Estimation and Control*, 2 (1982) New York, Academic Press.

10. Jazwinski, A. H. *Stochastic Processes and Filtering Theory*, (1970) New York, Academic Press.

11. Gelb, A. *Applied Optimal Estimation*, (1974) Cambridge, Mass., MIT Press.

12. Kushner, H. J. "Approximations to Optimal Nonlinear Filters," Proceedings of 8th Joint Automatic Control Conference (1967) 613-623.

13. Schmidt, S. E. "The Kalman Filter: Its Recognition and Development for Aerospace Applications," Journal on Guidance and Control, Vol.4 No.1 (1981), 4-7.

14. Maybeck, P. S. "Advanced Applications of Kalman Filters and Nonlinear Estimators in Aerospace Systems" in Leondes,C.T.(Ed.),*Control and Dynamic Systems* 20 (1983) 67-154, New York, Academic Press.

15. Singer, R. A. "Estimating Optimal Tracking Filter Performance for Manned Maneuvering Targets," IEEE Transactions on Aerospace and Electronic Systems, AES-6, (July 1970), 473-483.

16. Fitts, J. M. "Aided Tracking as Applied to High Accuracy Pointing Systems," IEEE Transactions on Aerospace and Electronic Systems, AES-9, (May 1973).

17. Maybeck, P. S. "Adaptive Tracker Field-of-View Variation via Multiple Model Filtering," IEEE Transactions on Aerospace and Electronic Systems (1985) 529-539.

18. Chang, C. B. and Tabaczynski, J. A. "Application of State Estimation to Target Tracking," IEEE Transactions on Automatic Control, AC-29, 2(Feb. 1984), 98-109.

19. Brown, R. G. "A New Look at the Magill Adaptive Filter as a Practical Means of Multiple Hypothesis Testing," IEEE Transactions on Circuits and Systems, CAS-30, 10(Oct. 1983), 765-768.

20. Bar-Shalom, Y., and Birmiwal, K. "Variable Dimension Filter for Maneuvering Target Tracking," IEEE Transactions on Aerospace and Electronic Systems, AES-18 5(Sept. 1982), 621-629.

21. Kendrick, J. D., Maybeck, P. S., and Reid, J. G. "Estimation of Aircraft Target Motion Using Pattern Recognition Orientation Measurements,"

IEEE Transactions on Aerospace and Electronic Systems, AES-17 2(Mar. 1981), 254-260.

22. Kenelic, R. J. "Optimal Tracking of a Maneuvering Target in Clutter" IEEE Transactions on Automatic Control, AC-26, 2(June 1981), 750-753.

23. Maybeck, P. S., Jensen, R. I., and Harnly, D. A. "An Adaptive Extended Kalman Filter for Target Image Travking," IEEE Transactions on Aerospace and Electronic Systems AES-17, 2(Mar. 1981), 172-180.

24. Moose, R. L. "Applications of Adaptive State Estimation Theory," Proceedings of the 19th IEEE Conference on Decision and Control, Albuquerque NM (1980) 568-575.

25. Moose, R. L., Van Landingham, H. F. and McCabe, D. H. "Modeling and Estimation for Tracking Maneuvering Targets," IEEE Transactions on Aerospace and Electronic Systems, AES-15 3(May 1979) 448-456.

26. Tenney, R. R., Hebbert, R. S. and Sandell, N. R., Jr. "A Tracking Filter for Maneuvering Sources," IEEE Transactions on Automatic Control, AC-22, 2(Mar. 1977), 246-261.

27. Chang, C. B. and Athans, M. "Hypothesis Testing and State Estimation for Discrete Systems with Finite-Valued Switching Parameters," ESL-P-758, Lincoln Lab., Lexington, MA, (June 1977).

28. Moose, R. L. "An Adaptive State Estimation Solution to the Maneuvering Target Problem," IEEE Transactions on Automatic Control, AC-20, 3(June 1975), 359-362.

29. McAulay, R. J., and Denlinger, E. "A Decision-Directed Adaptive Tracker," IEEE Transactions on Aerospace and Electronic Systems AES-9, 2(Mar. 1973), 229-236.

30. Moose, R. L. and Wang, P. P. "An Adaptive Estimator with Learning for a Plant Containing Semi-Markov Switching Parameters," IEEE Transactions on Systems, Man, and Cybernetics (May 1973), 277-281.

31. Thorp, J. S. "Optimal Tracking of Maneuvering Targets," IEEE Transactions on Aerospace and Electronic Systems, AES-9 4(July 1973), 512-519.

32. Nahi, N. E., and Schaefer, B. M. "Decision Derected Adaptive Recursive Estimators, Divergence Prevention," IEEE Transactions on Automatic Control, AC-17, 1(Feb. 1972), 61-67.

33. Demetry, J. S., and Titus, H. A. "Adaptive Tracking of Maneuvering Targets," Technical Report NPS-52DE8041A, Naval Postgraduate School, Monterey, CA, (Apr. 1968)

34. Magill, R. L. "Optimal Adaptive Estimation of Sampled Stochastic Processes," IEEE Transactions on Automatic Control, AC-10, 5(Oct. 1965), 434-439.

35. Bogler, P. L. "Tracking a Maneuvering Target Using Input Estimation," IEEE Transactions on Aerospace and Electronic Systems (1987) 298-310.

36. Stalford, H. L. "A Friedland-Like Filtering Technique for Estimating Piecewise Constant Controls in Discrete Linear Stochastic Systems," Proceedings American Control Conference , Arlington Virginia (1982) 603-607.

37. Stalford, H. L. "A Computationally Efficient GLR Algorithm for Detecting and Estimating Jumps in Linear Systems," IFAC Identification and System Parameter Estimation, Washington D.C. (1982) 927-932.

38. Stalford, H. L. "An Adaptive Filter for the Track Prediction of Highly Maneuvering Anti-Ship Cruise Missiles," Proceedings of the 19th IEEE Conference on Decision and Control, Albuquerque NM (1980) 544-553.

39. Chan, Y. T., Hu, A. G. C., and Plant, J. B. "A Kalman-Filter Based Tracking Scheme with Input Estimation," IEEE Transactions on Aerospace and Electronic Systems AES-15 (1979) 237-244.

40. Ricker, G. G., and Williams, J. R. "Adaptive Tracking Filter for Maneuvering Targets," IEEE Transactions on Aerospace and Electronic Systems, AES-14, (Jan. 1978), 185-193.

41. Gholson, N. H., and Moose, R. L. "Maneuvering Target Tracking Using Adaptive State Estimation," IEEE Transactions on Aerospace and Electronic Systems, AES-13, (May 1977), 310-317.

42. Chang, C. B., Whiting, R. H., and Athans, M. "On the State of Parameter Estimation for Maneuvering Reentry Targets," IEEE Transactions on Automatic Control, AC-22, (Feb. 1977), 99-105.

43. Willsky, A. S., and Jones, H. L. "A Generalized Likelihood Ratio Approach to the Detection and Estimation of Jumps in Linear Systems," IEEE Transactions on Automatic Control, AC-21, 2(Feb. 1976), 108-112.

44. Cliff, E. M., Kelley, H. J., Lutze, F. H., and Stalford, H. L. "Evasive Maneuvering Modeling and Program Description," Report NSWC/SRC N60921-83G-A165-B022-AMD#1, (Dec. 1986).

45. Pastrick, H. L., Seltzer, S. M., and Warren, M. E. "Guidance Laws for Short-Range Tactical Missiles," Journal on Guidance and Control, (1981), 98-108.

46. "A Shouted Alarm, A Fiery Blast - The Stark Hardly Knew What Hit Her," Time, (June 1, 1987), 20-22.

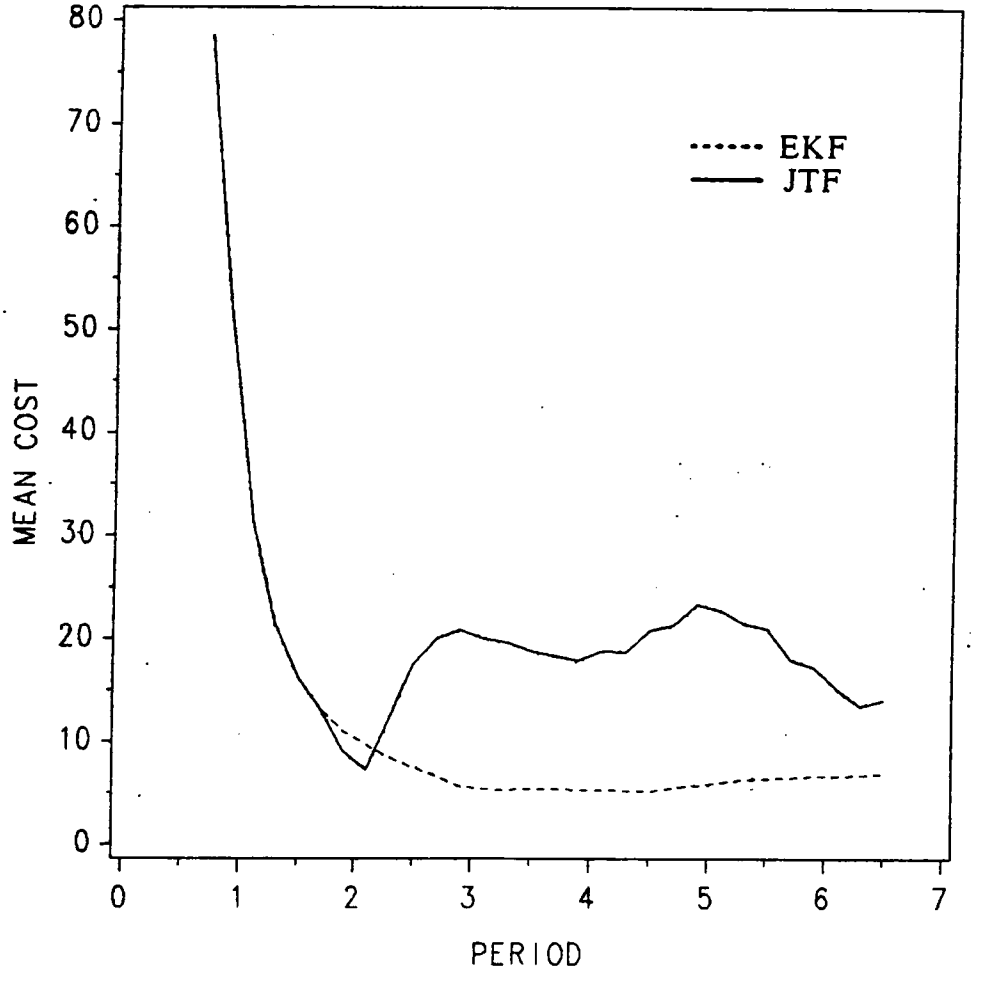

Figure 1. Cost (EHITS) vs. Period Plot for Case No. 115, Sinusoidal Wave.

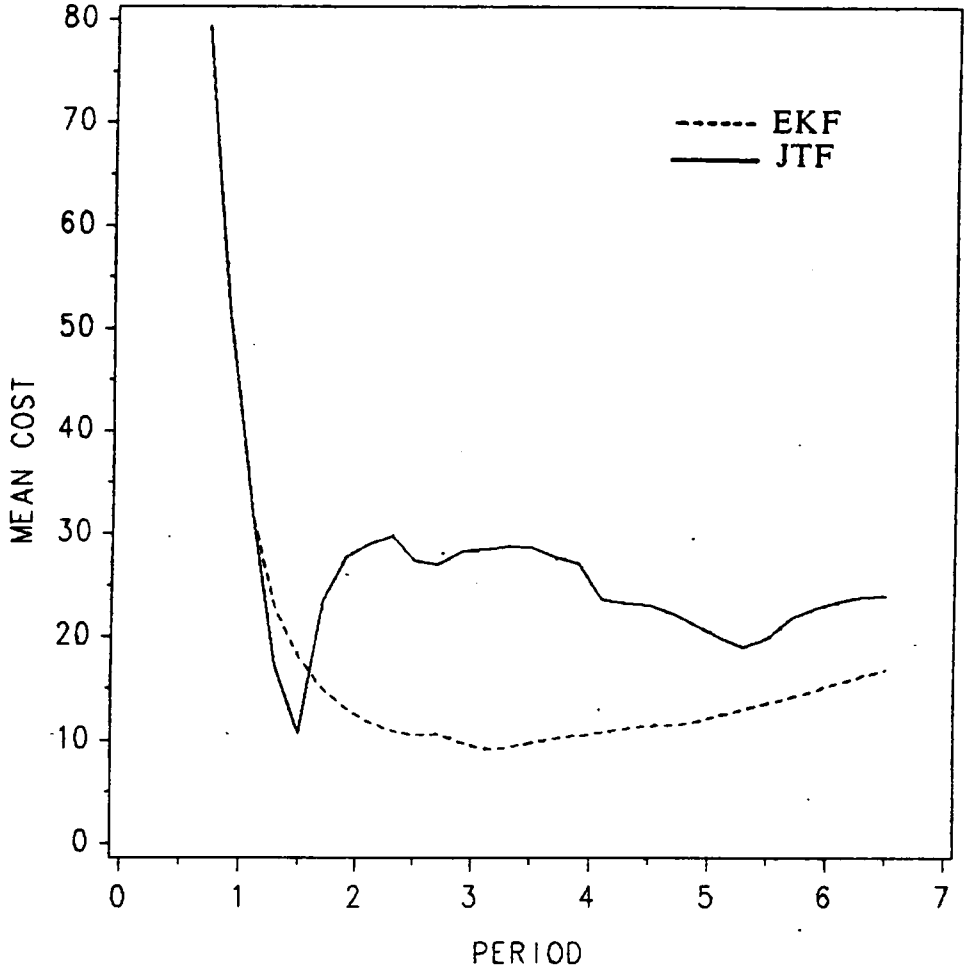

Figure 2. Cost (EHITS) vs. Period Plot for Case No. 121, Sinusoidal Wave.

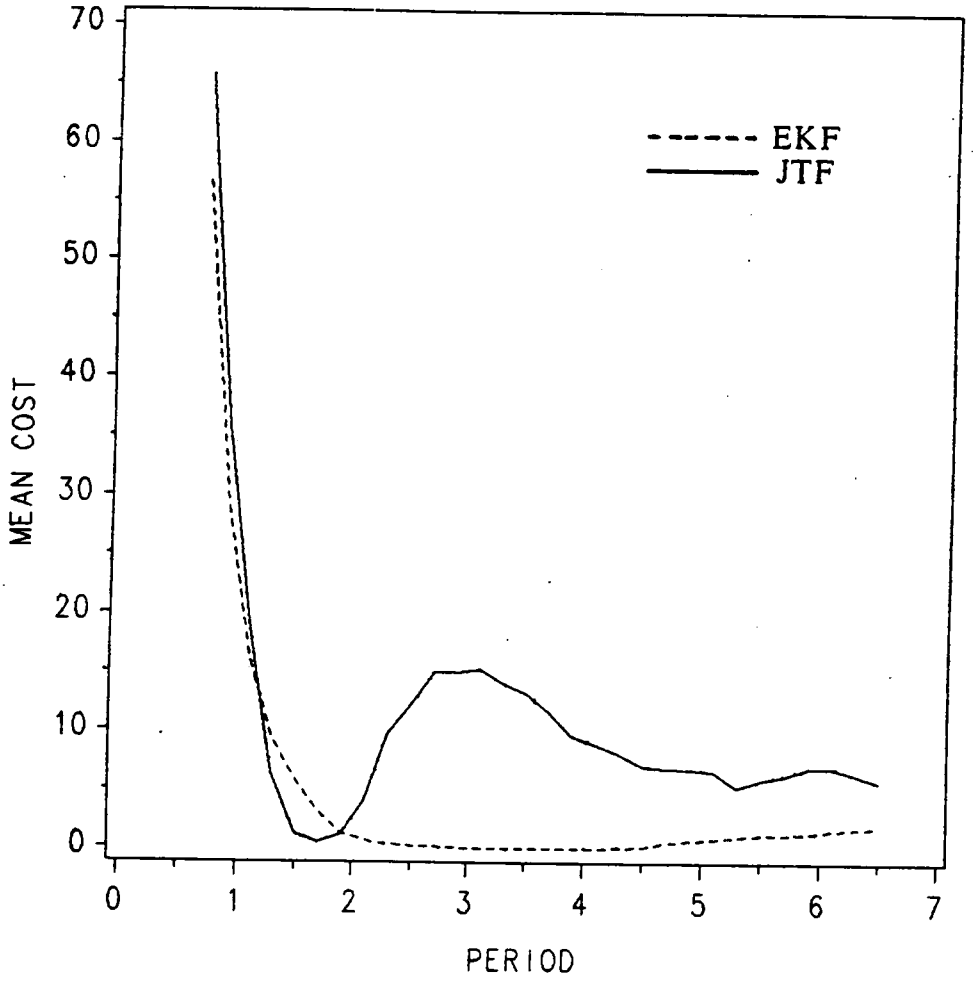

Figure 3. Cost (EHITS) vs. Period Plot for Case No. 123, Sinusoidal Wave.

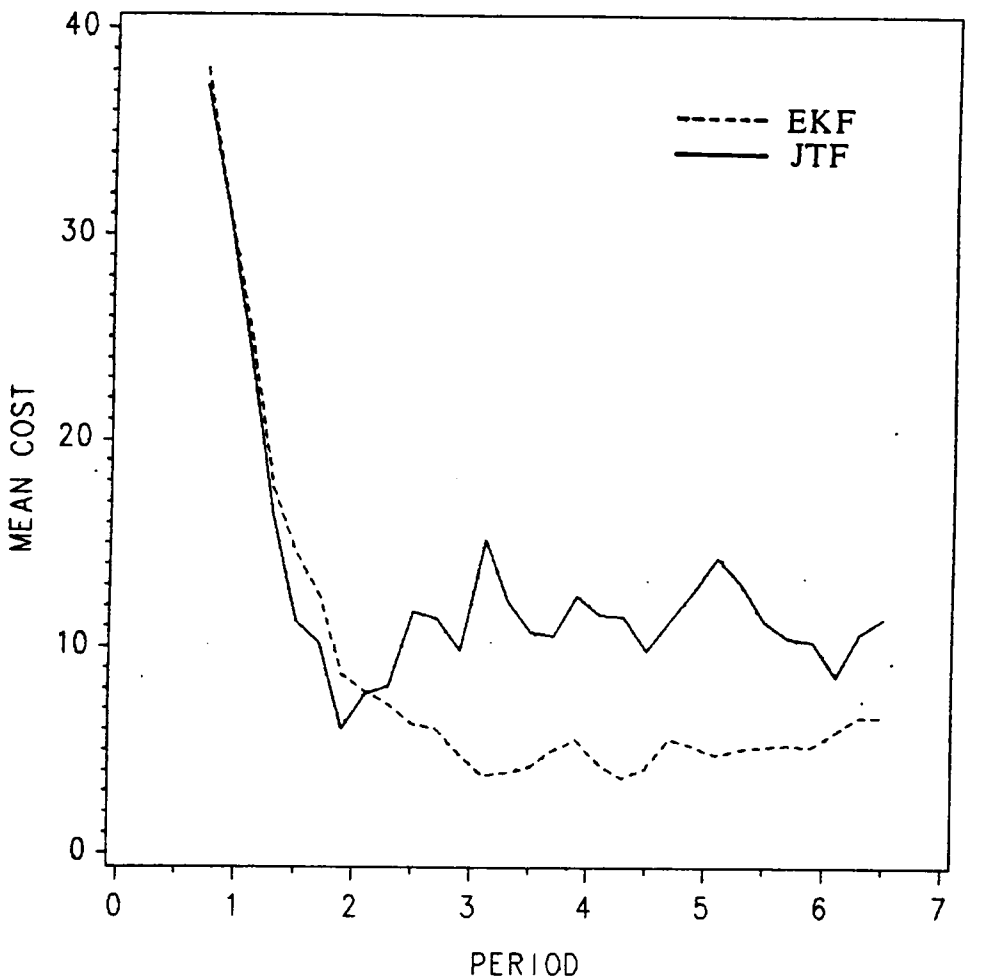

Figure 4. Cost (EHITS) vs. Period Plot for Case No. 139, Sinusoidal Wave.

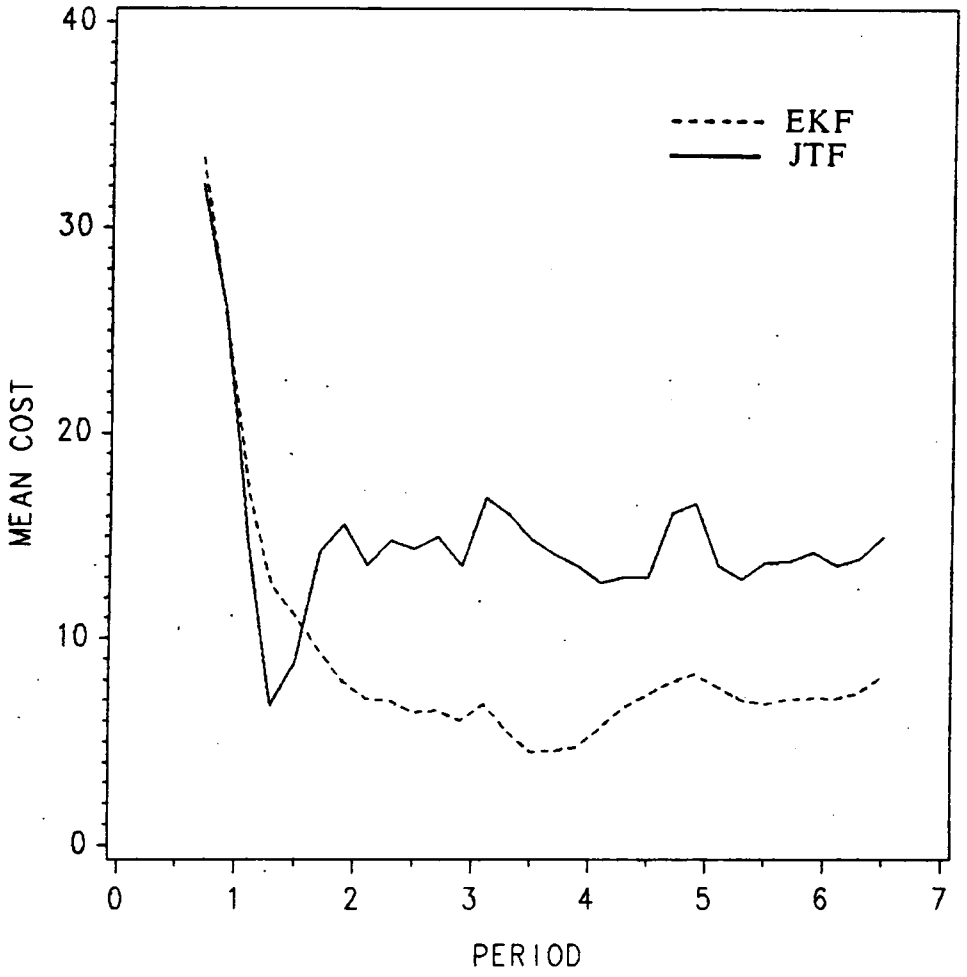

Figure 5. Cost (EHITS) vs. Period Plot for Case No. 145, Sinusoidal Wave.

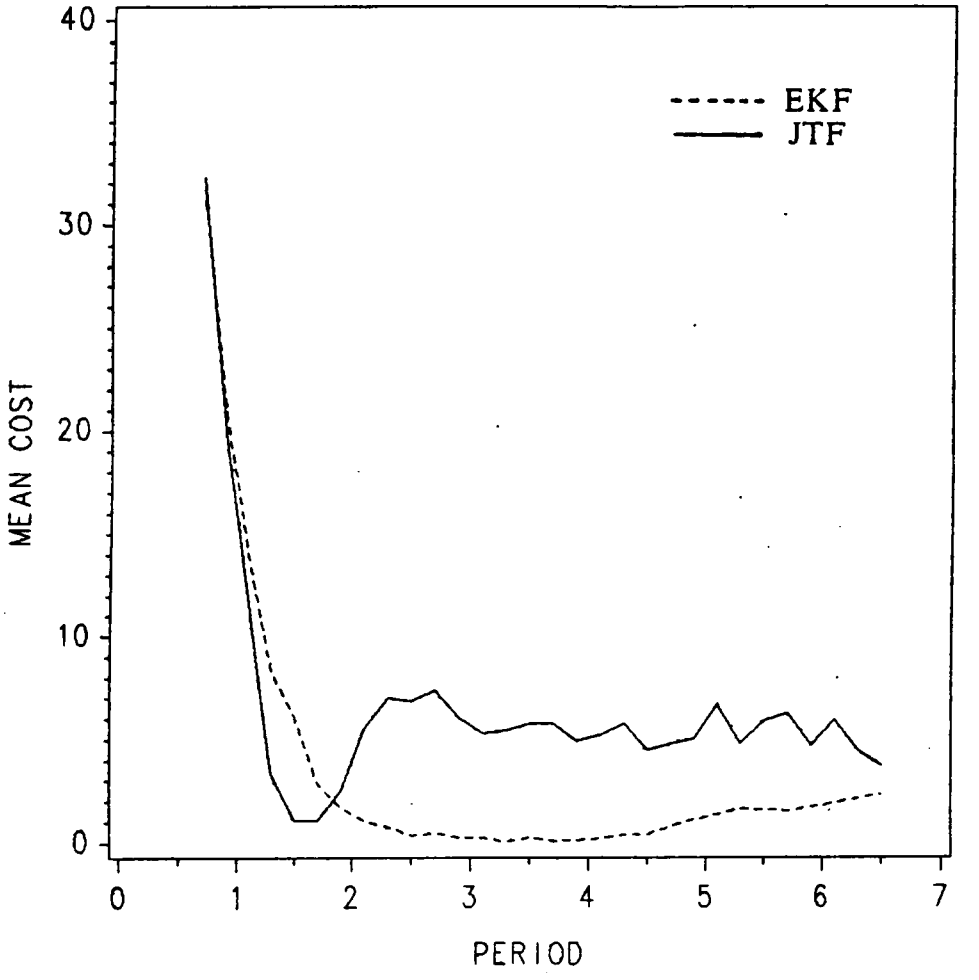

Figure 6. Cost (EHITS) vs. Period Plot for Case No. 147, Sinusoidal Wave.

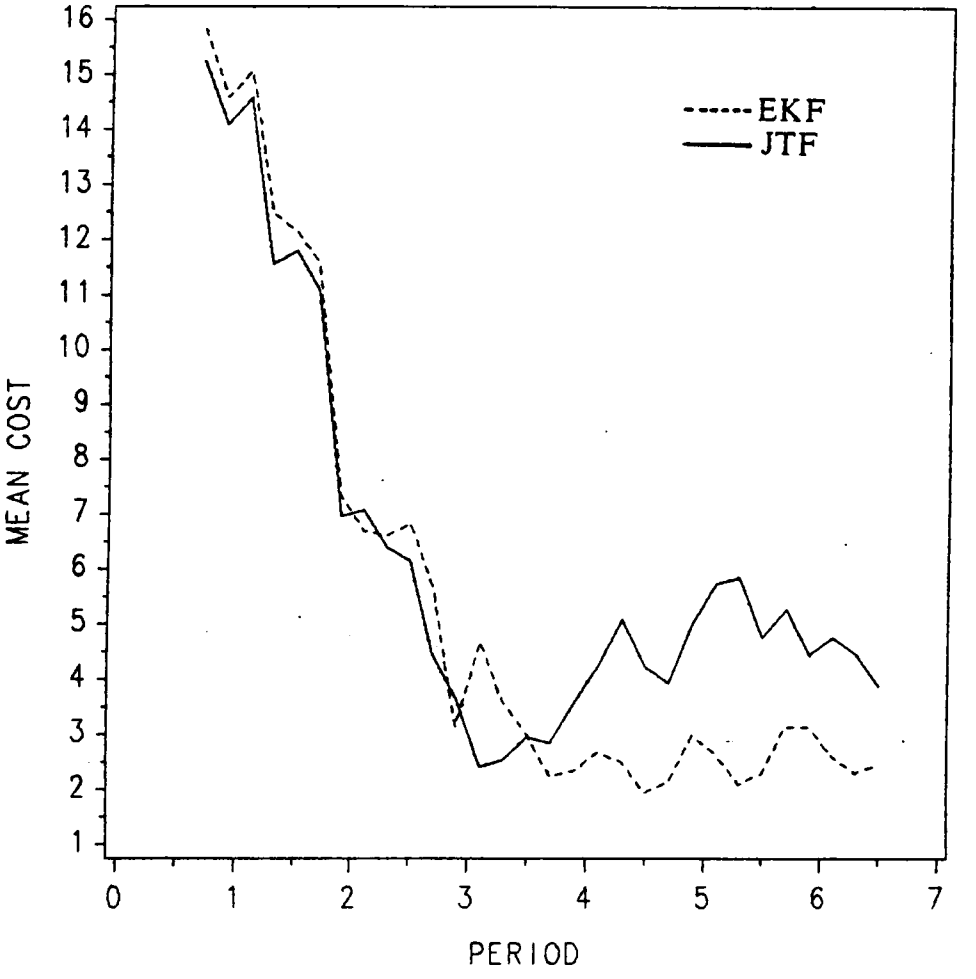

Figure 7. Cost (EHITS) vs. Period Plot for Case No. 163, Sinusoidal Wave.

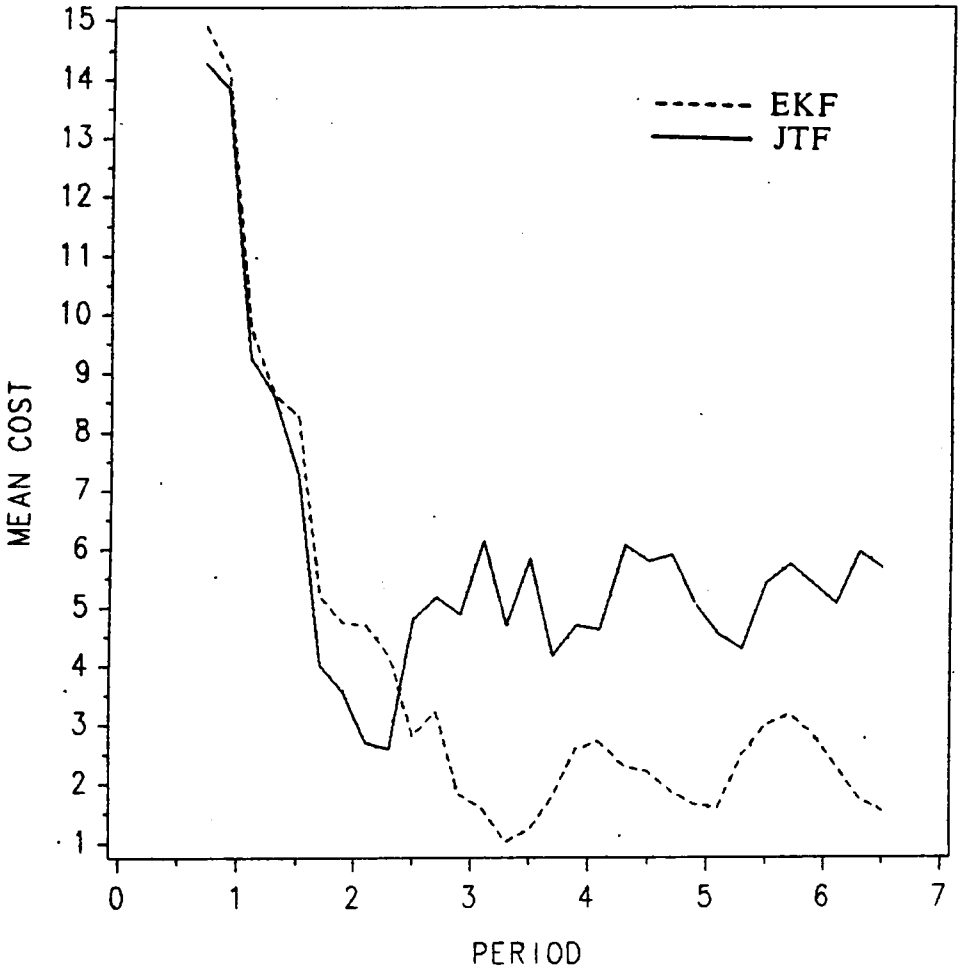

Figure 8. Cost (EHITS) vs. Period Plot for Case No. 169, Sinusoidal Wave.

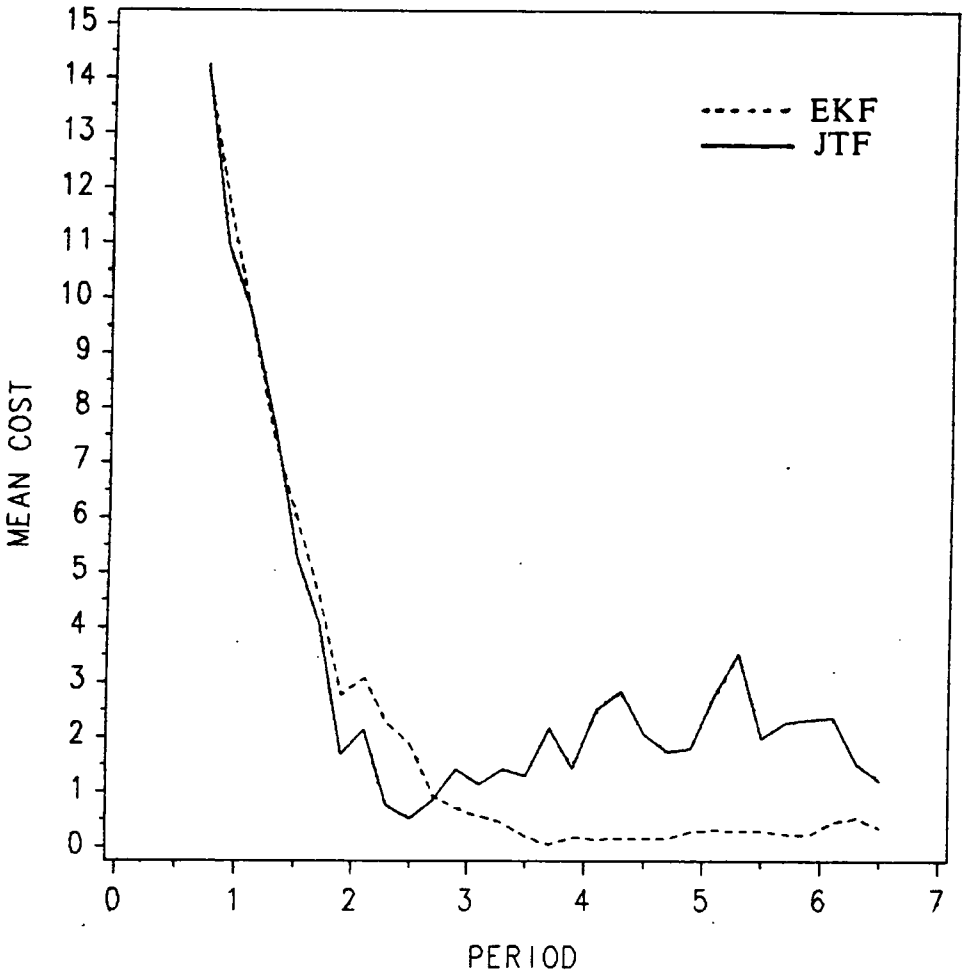

Figure 9. Cost (EHITS) vs. Period Plot for Case No. 171, Sinusoidal Wave.

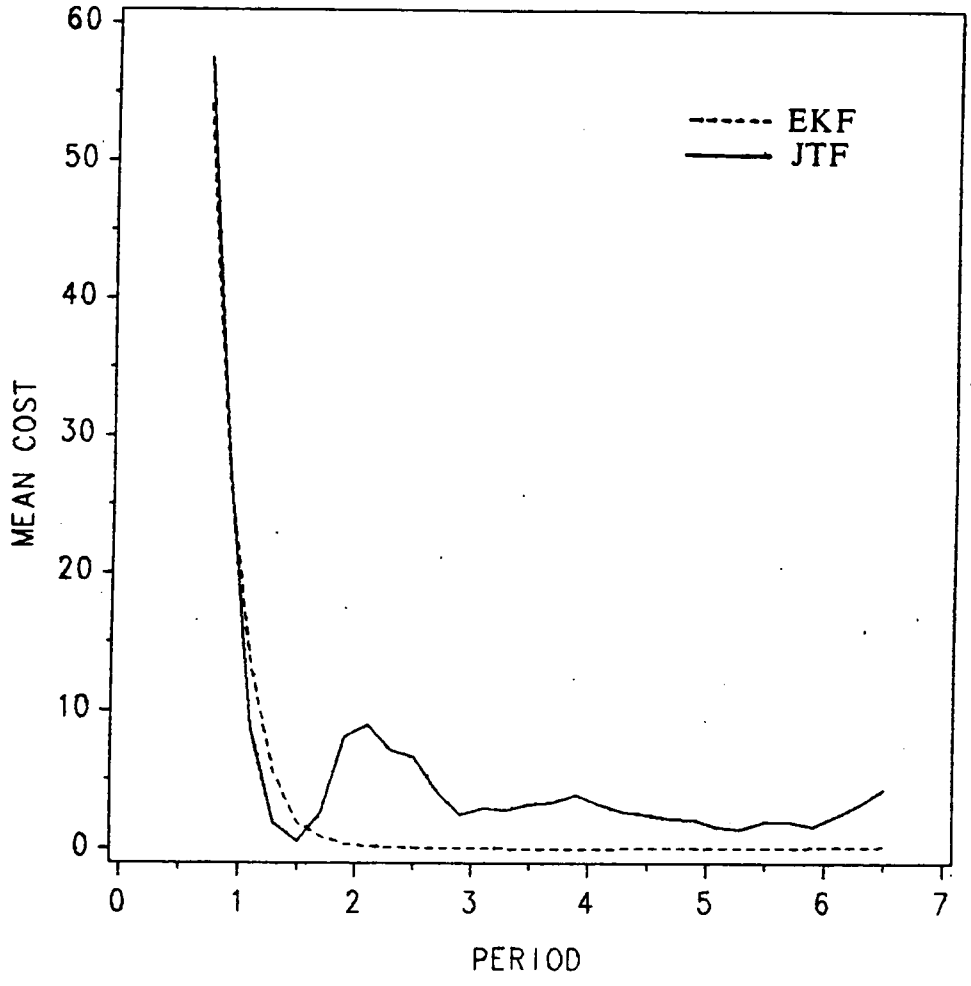

Figure 10. Cost (EHITS) vs. Period Plot for Case No. 123, Square Wave.

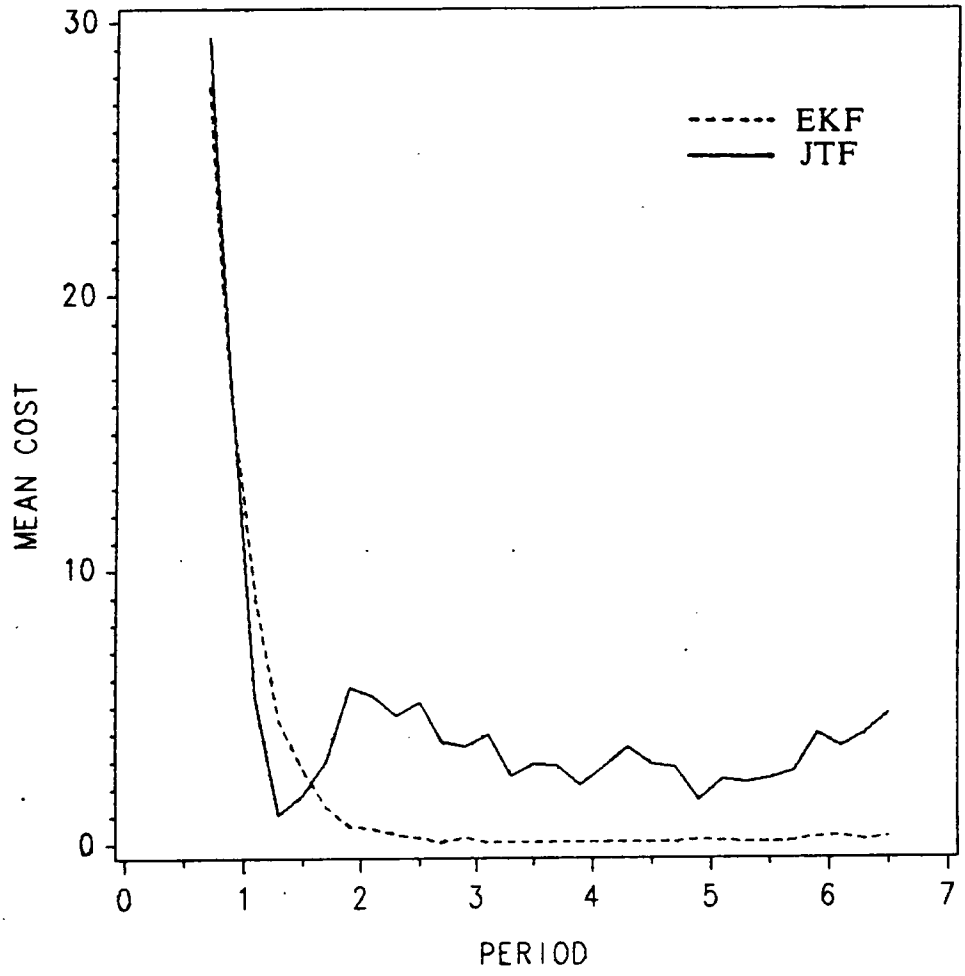

Figure 11. Cost (EHITS) vs. Period Plot for Case No. 147, Square Wave.

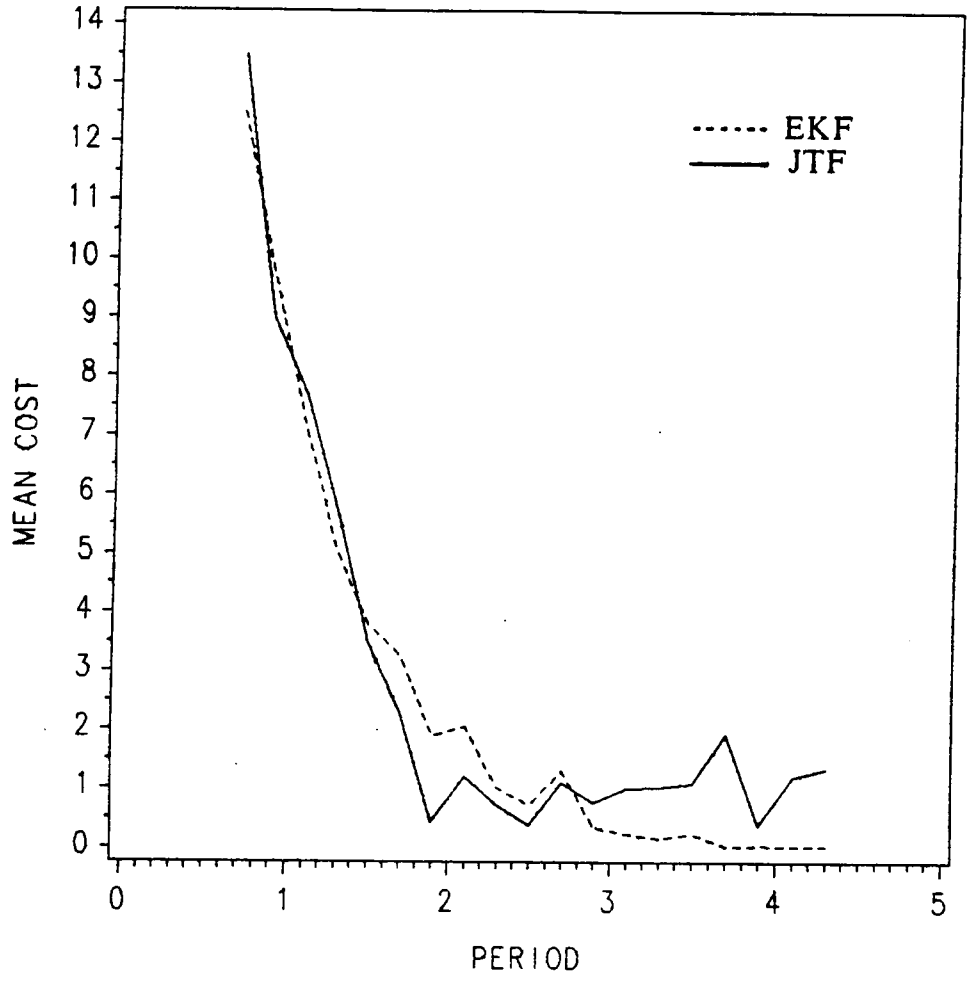

Figure 12. Cost (EHITS) vs. Period Plot for Case No. 171, Square Wave.

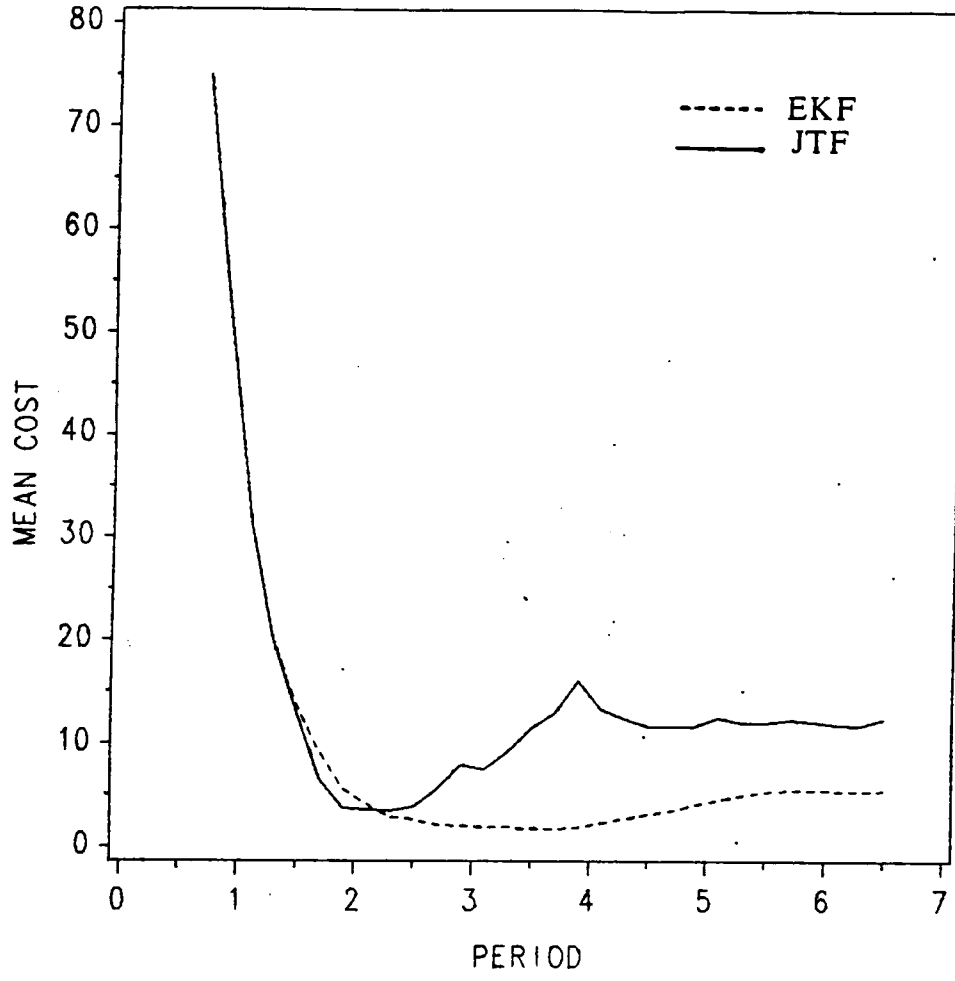

Figure 13. Cost (EHITS) vs. Period Plot for Case No. 123, Sawtooth Wave.

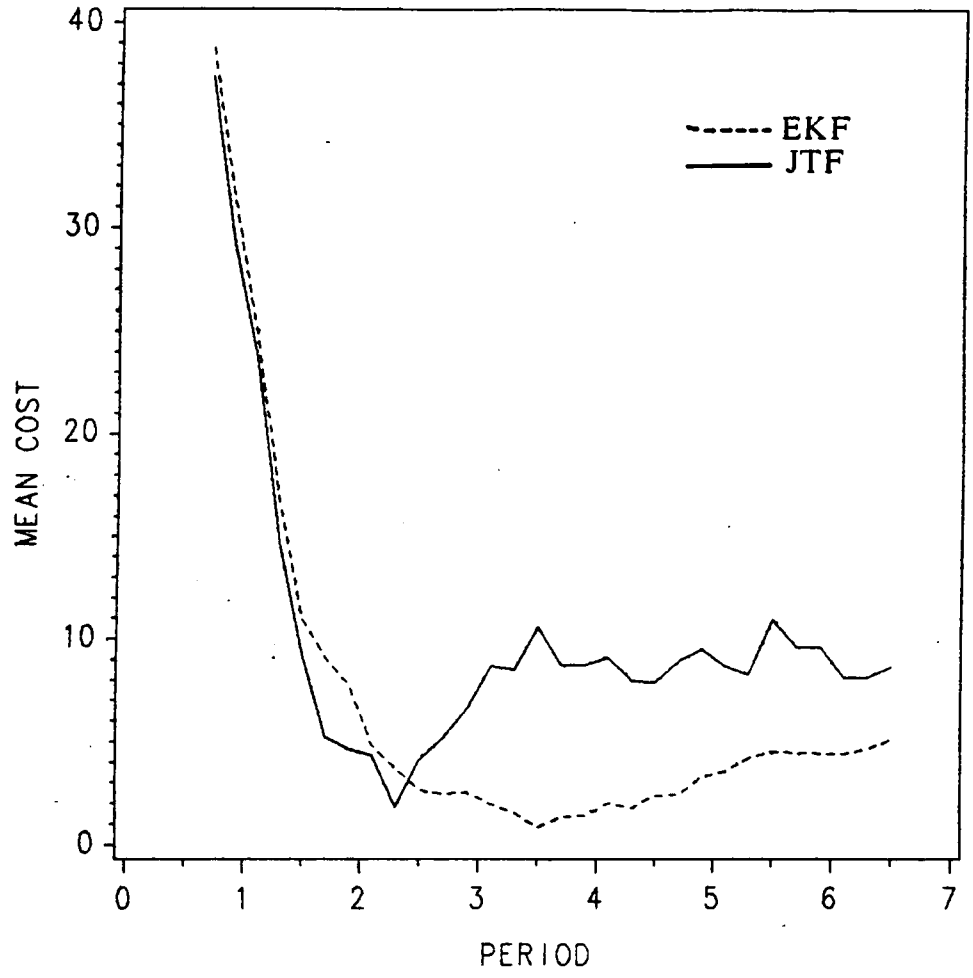

Figure 14. Cost (EHITS) vs. Period Plot for Case No. 147, Sawtooth Wave.

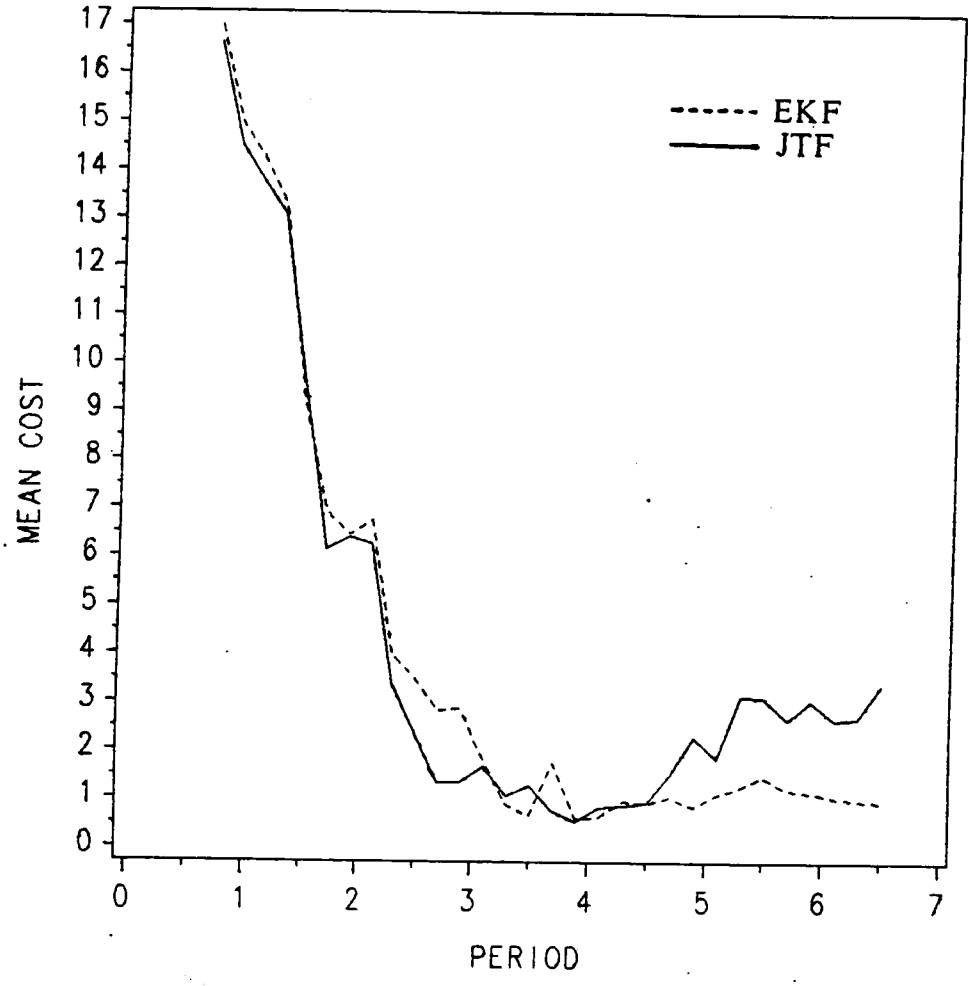

Figure 15. Cost (EHITS) vs. Period Plot for Case No. 171, Sawtooth Wave.

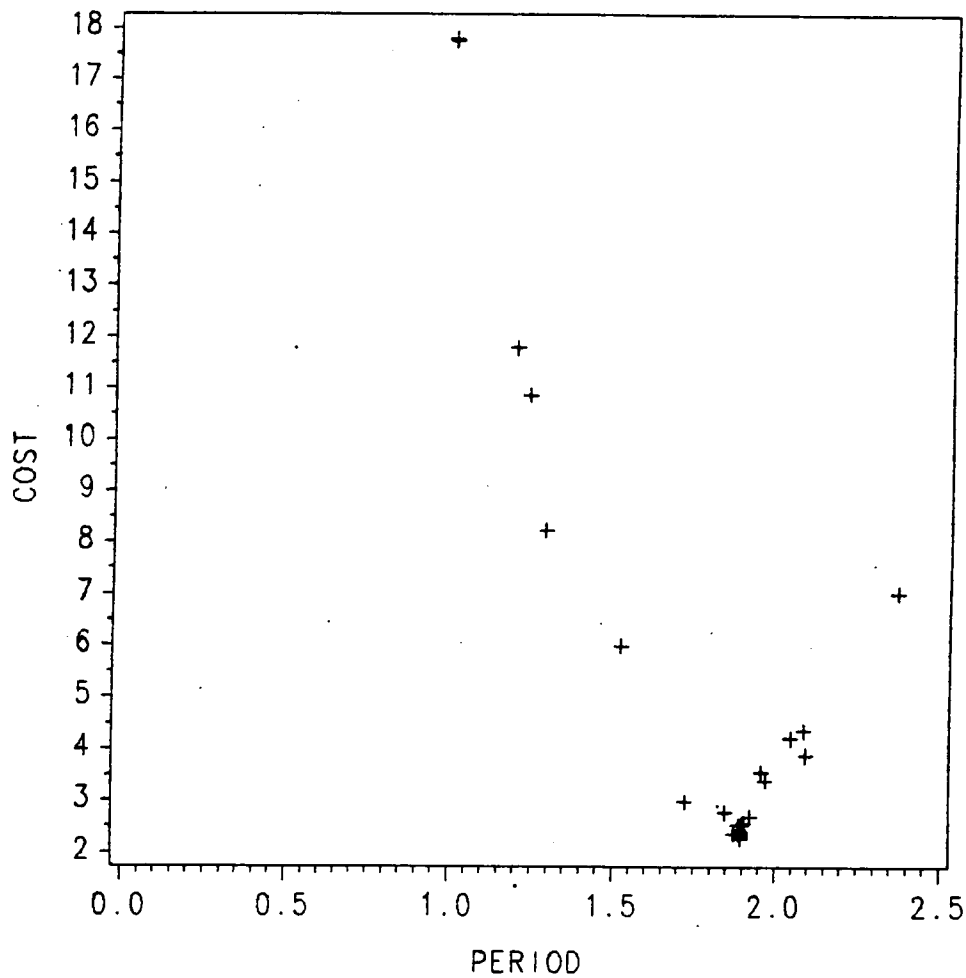

Figure 16. EHITS Points for Optimization Process, Case No. 147, Sinusoidal Wave.

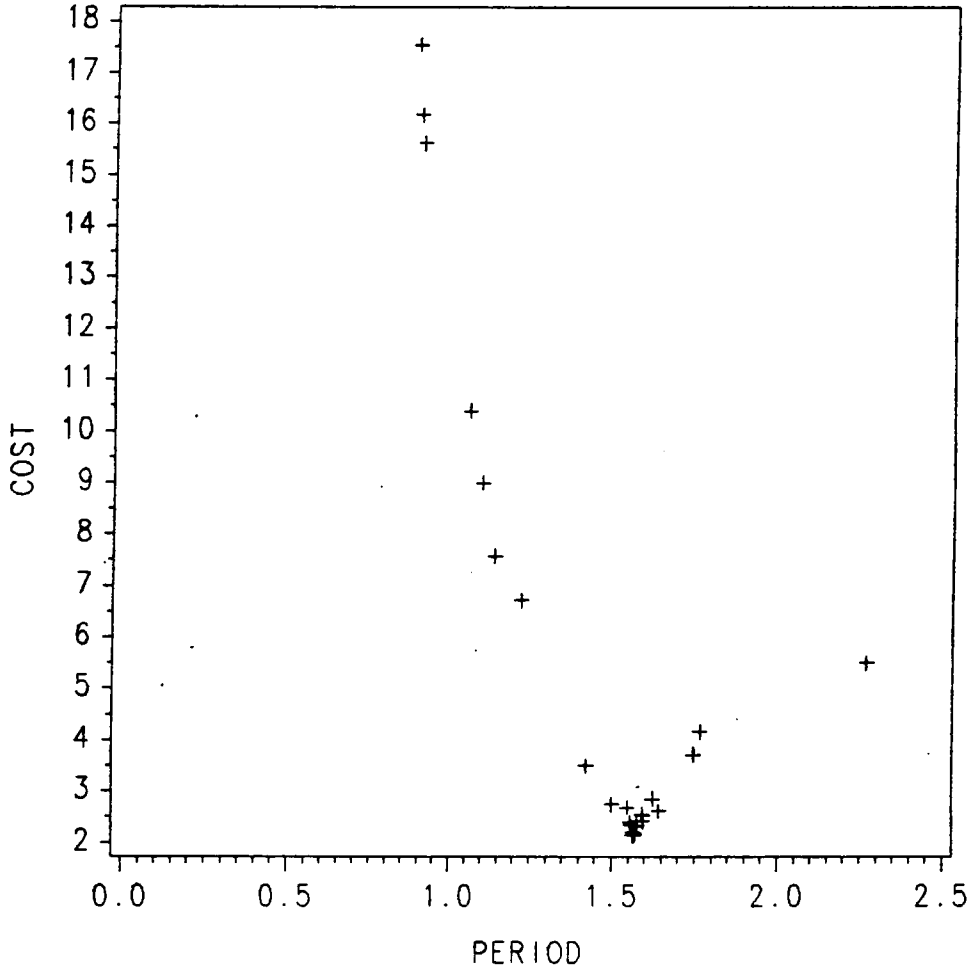

Figure 17. EHITS Points for Optimization Process, Case No. 147, Square Wave.

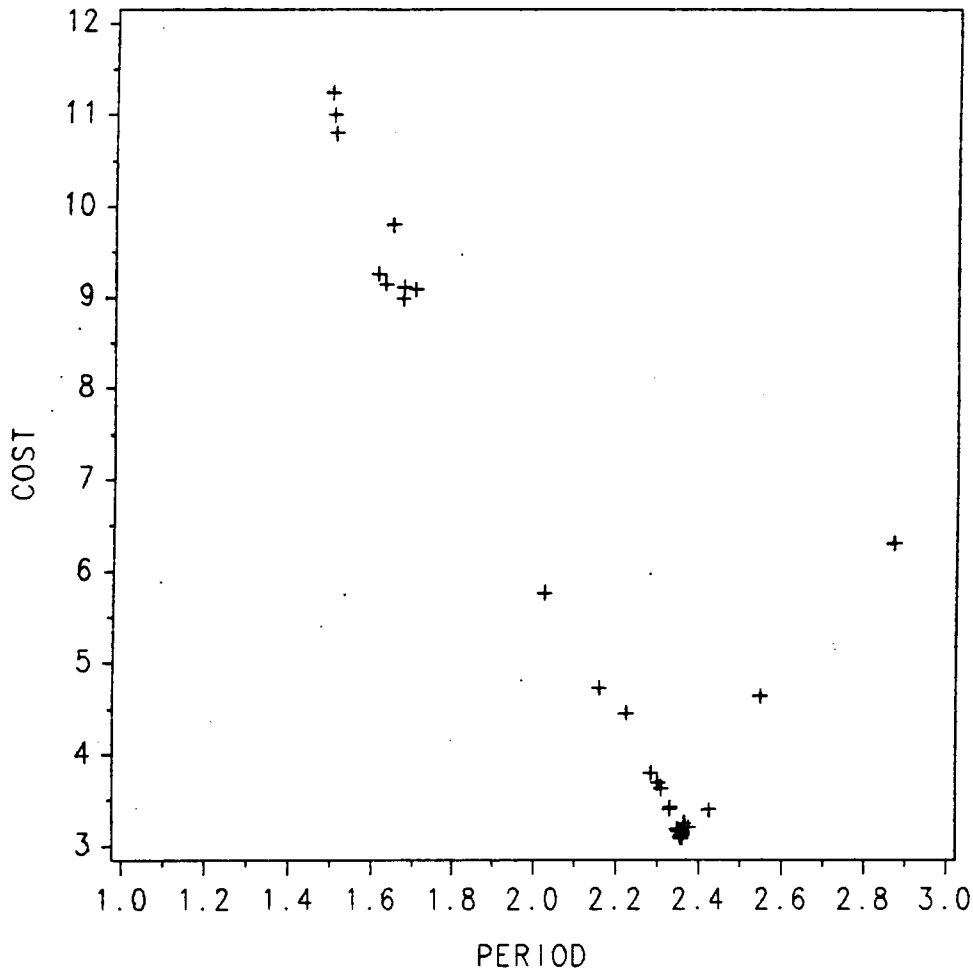

Figure 18. EHITS Points for Optimization Process, Case No. 147, Sawtooth Wave.

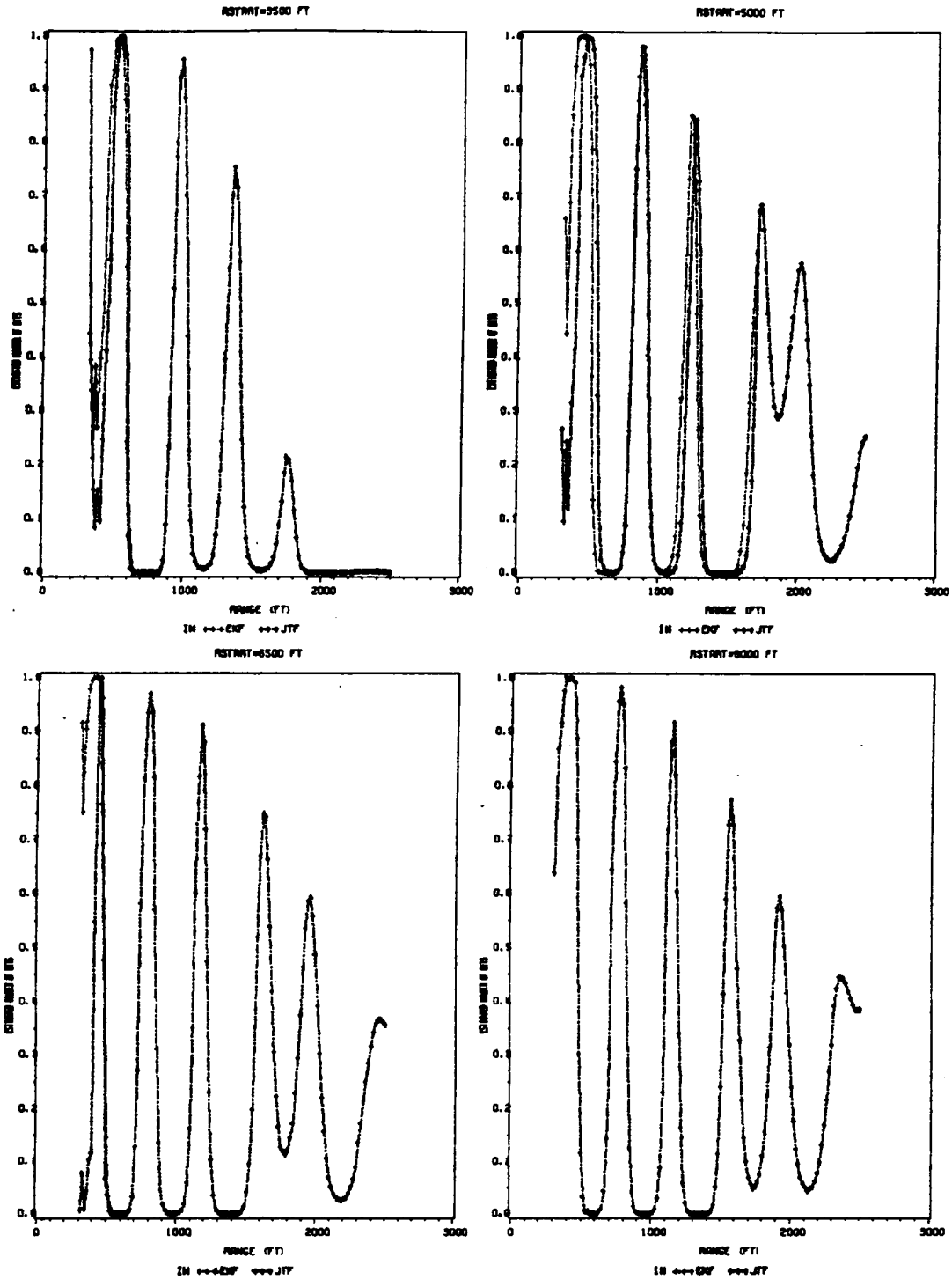

Figure 19. Probability of Hits vs. Range, Case No. 123, Period = 0.9, Sinusoidal Wave.

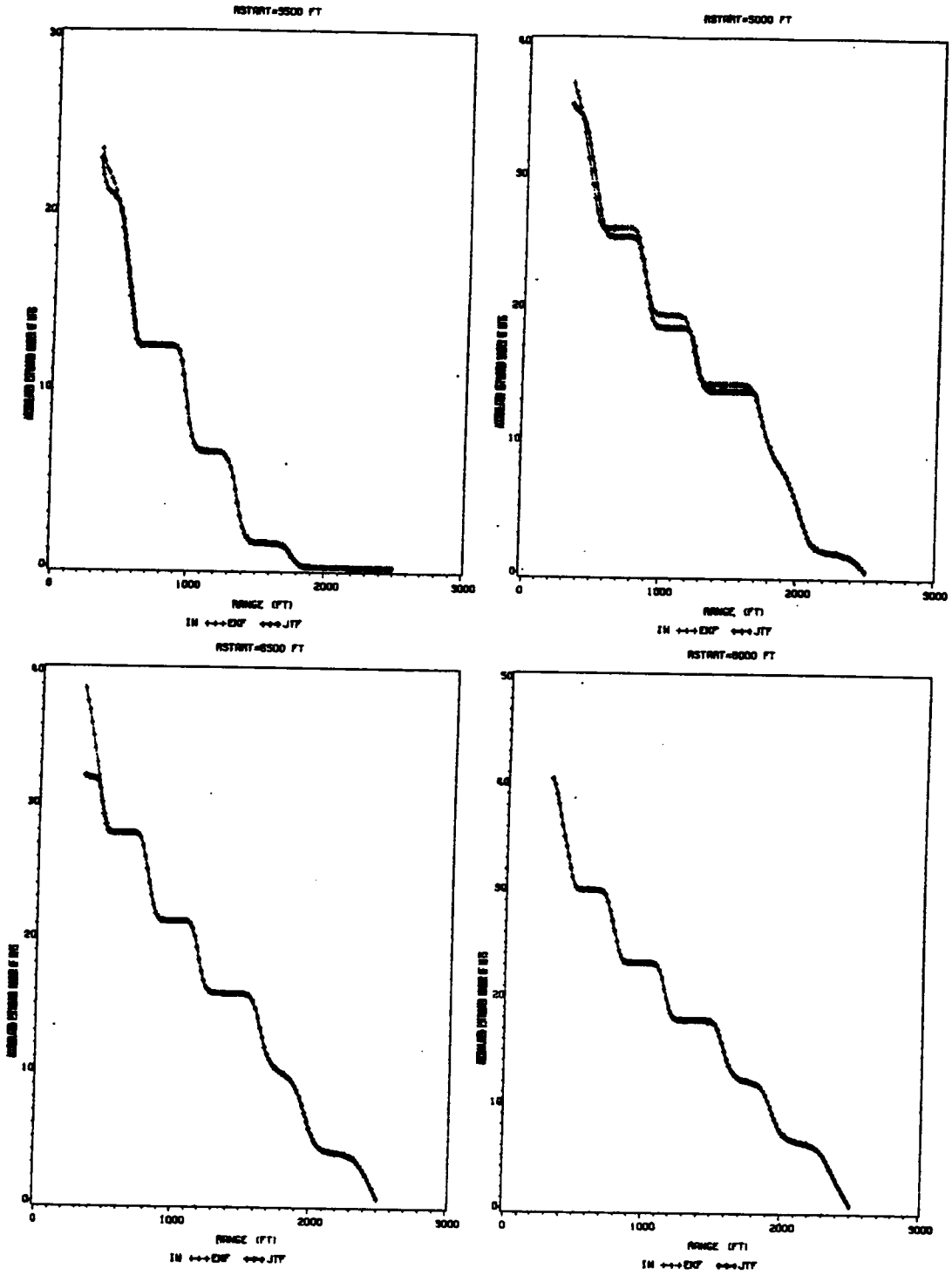

Figure 20. Accumulated Probability of Hits vs. Range, Case No. 123, Period = 0.9, Sinusoidal Wave.

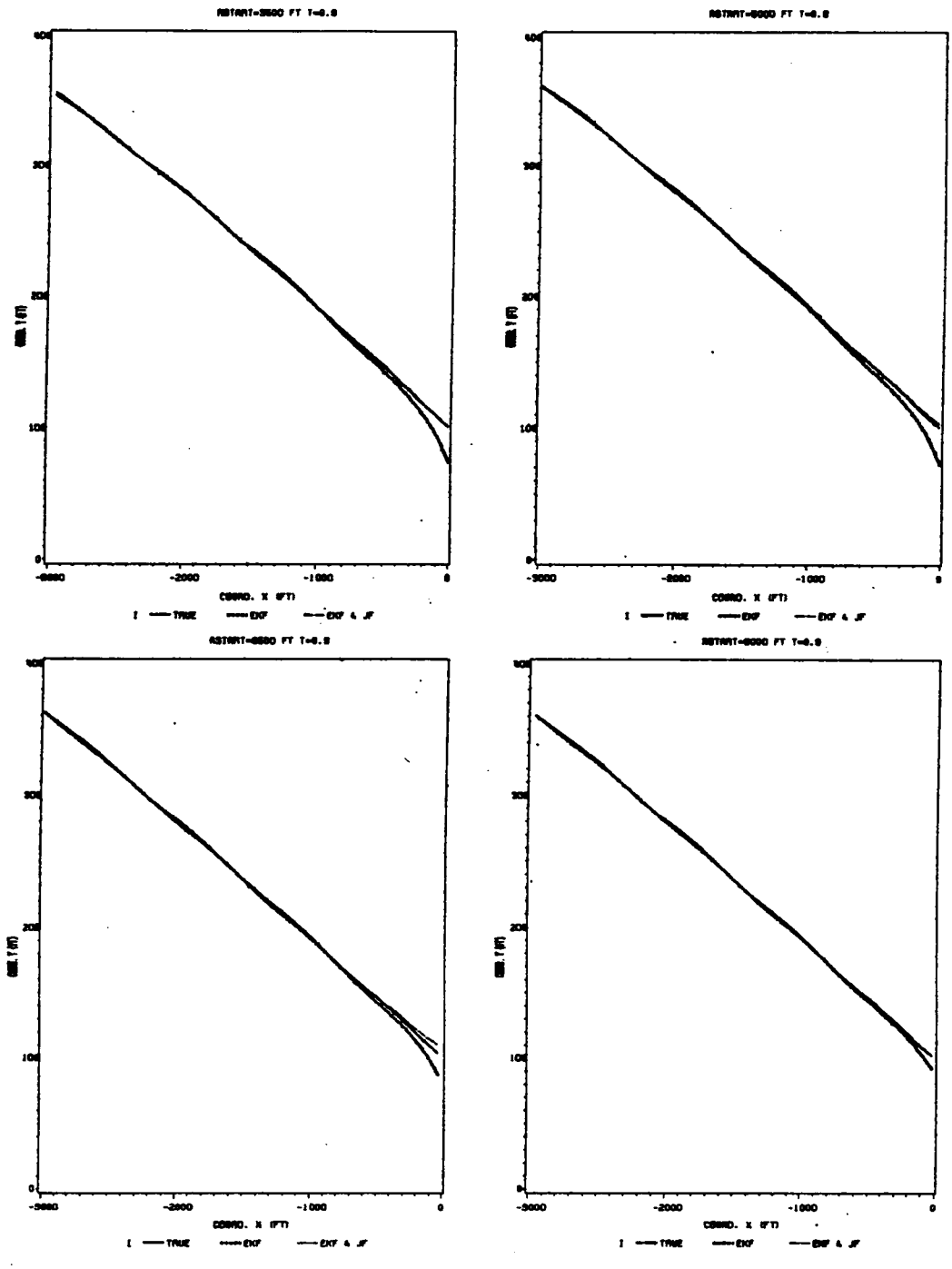

Figure 21. True and Estimated y vs. x, Case No. 123, Period = 0.9, Sinusoidal Wave.

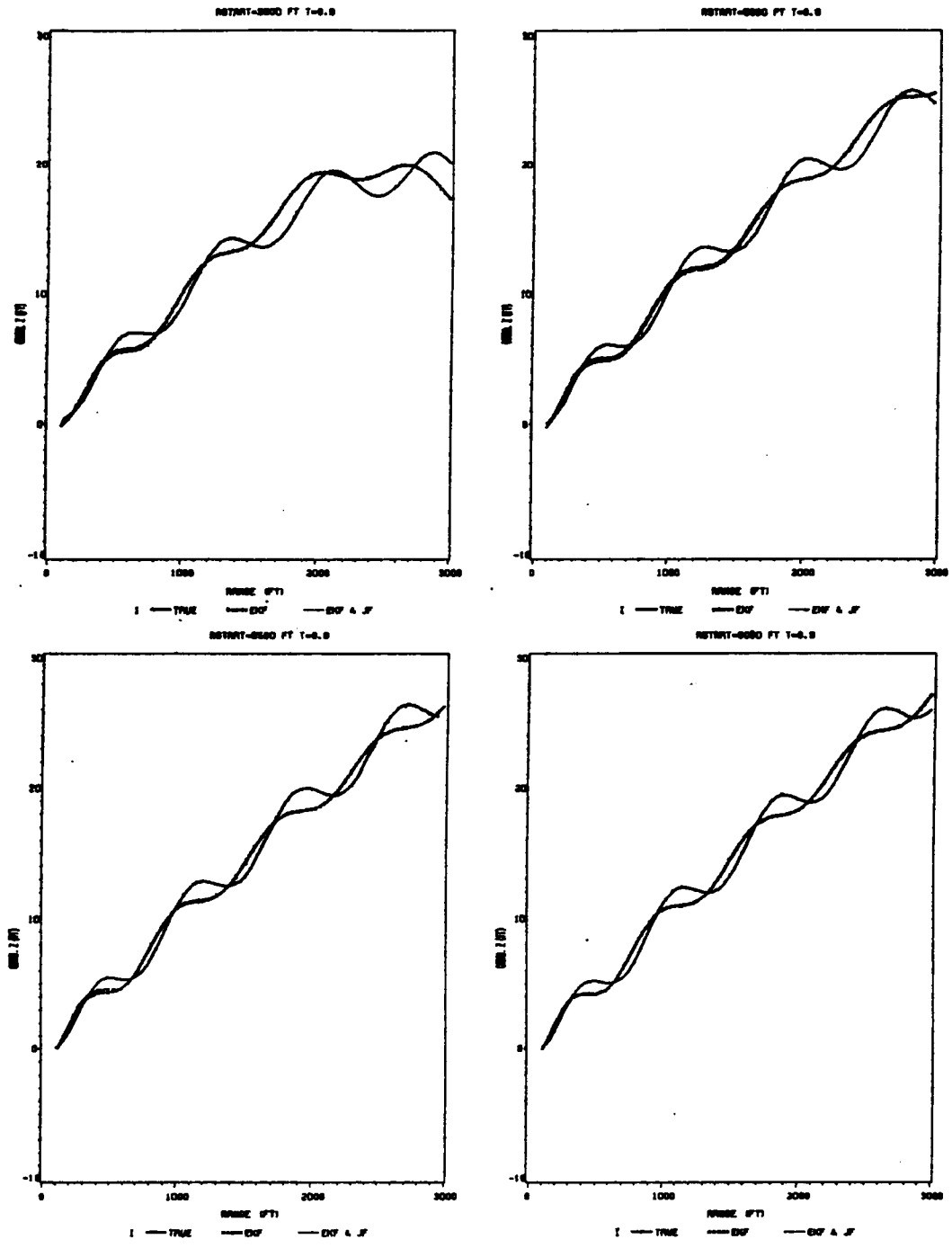

Figure 22. True and Estimated z vs. R, Case No. 123, Period = 0.9, Sinusoidal Wave.

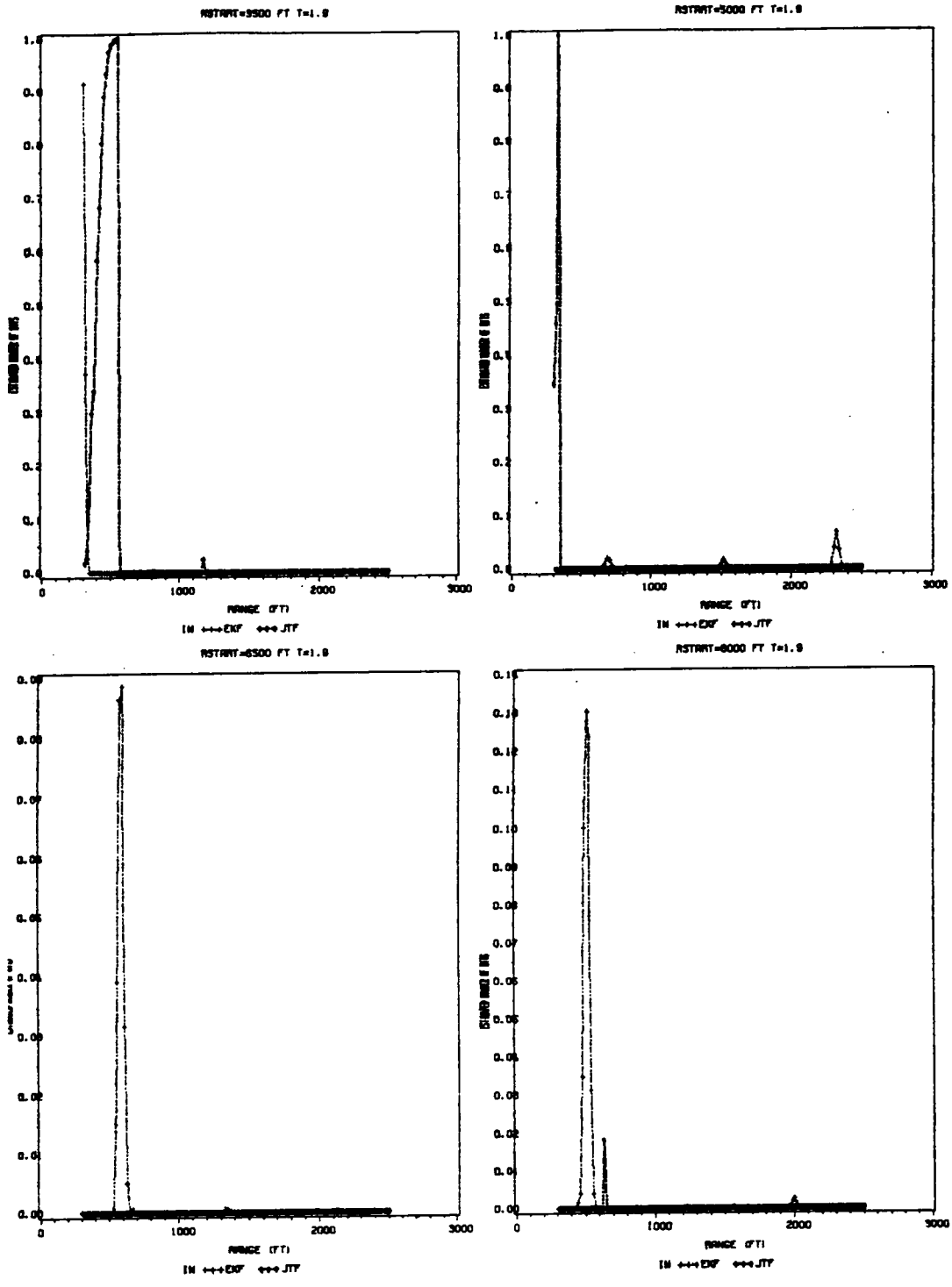

Figure 23. Probability of Hits vs. Range, Case No. 123, Period = 1.9, Sinusoidal Wave.

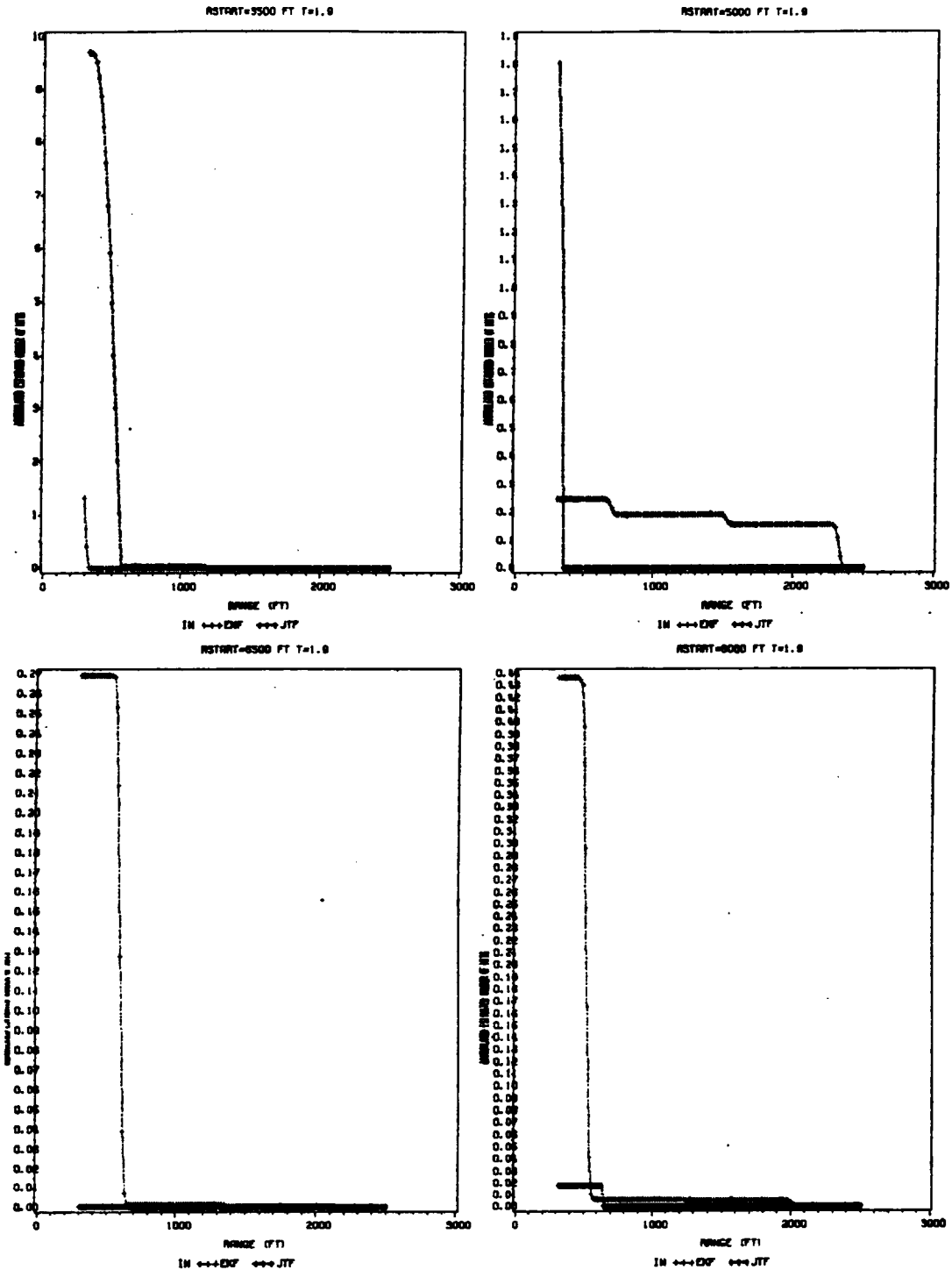

Figure 24. Accumulated Probability of Hits vs. Range, Case No. 123, Period = 1.9, Sinusoidal Wave.

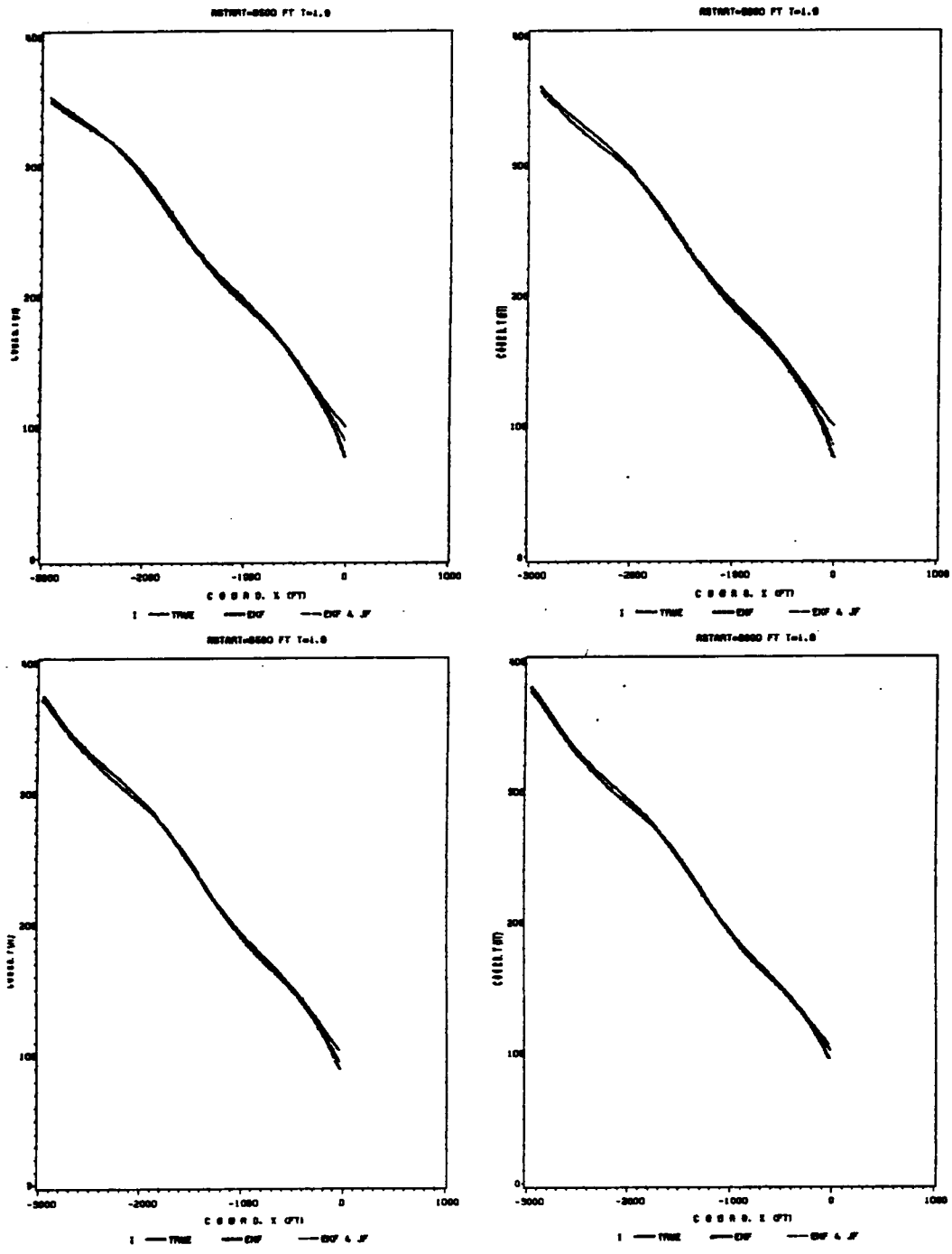

Figure 25. True and Estimated y vs. x, Case No. 123, Period = 1.9, Sinusoidal Wave.

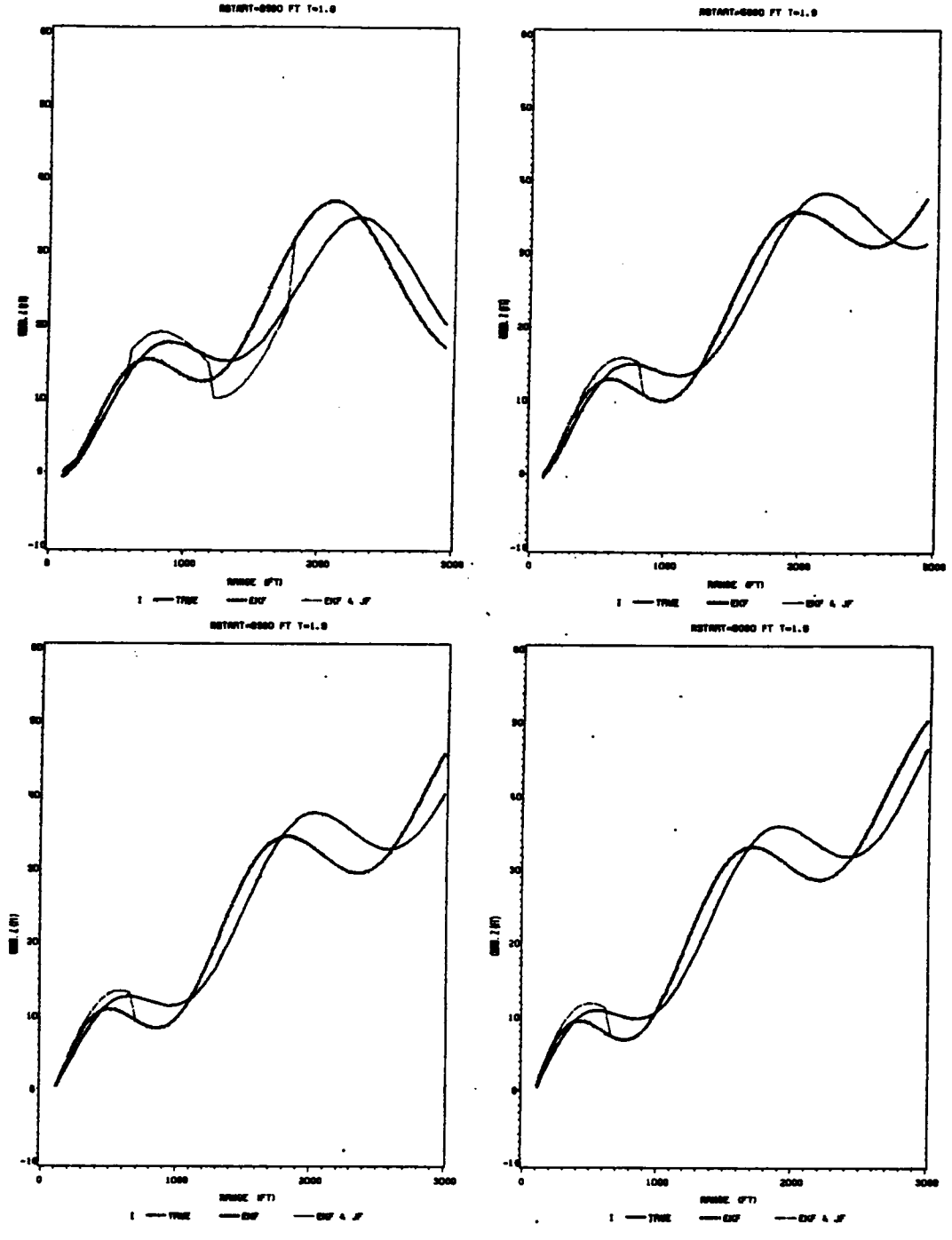

Figure 26. True and Estimated z vs. R, Case No. 123, Period = 1.9, Sinusoidal Wave.

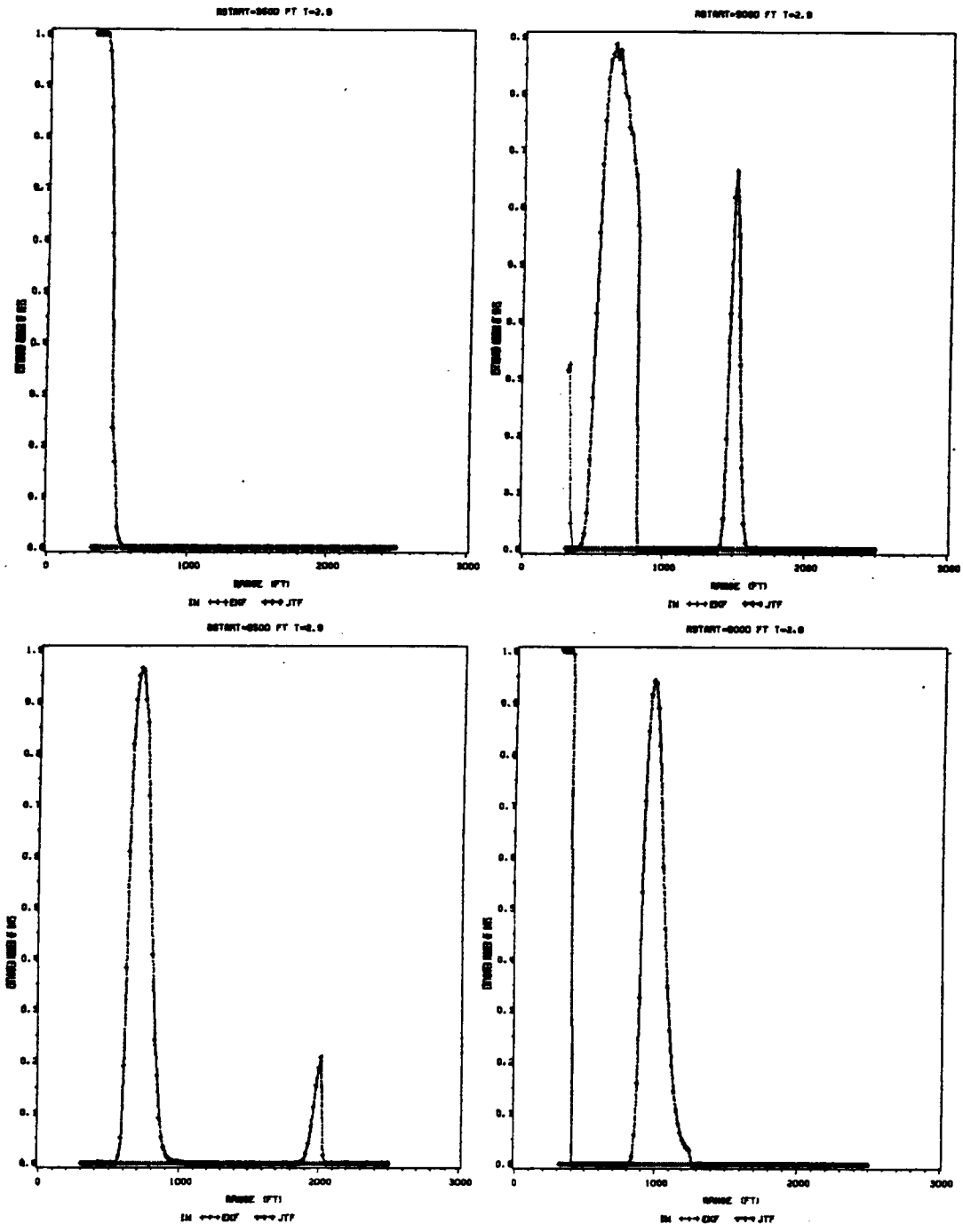

Figure 27. Probability of Hits vs. Range, Case No. 123, Period = 2.9, Sinusoidal Wave.

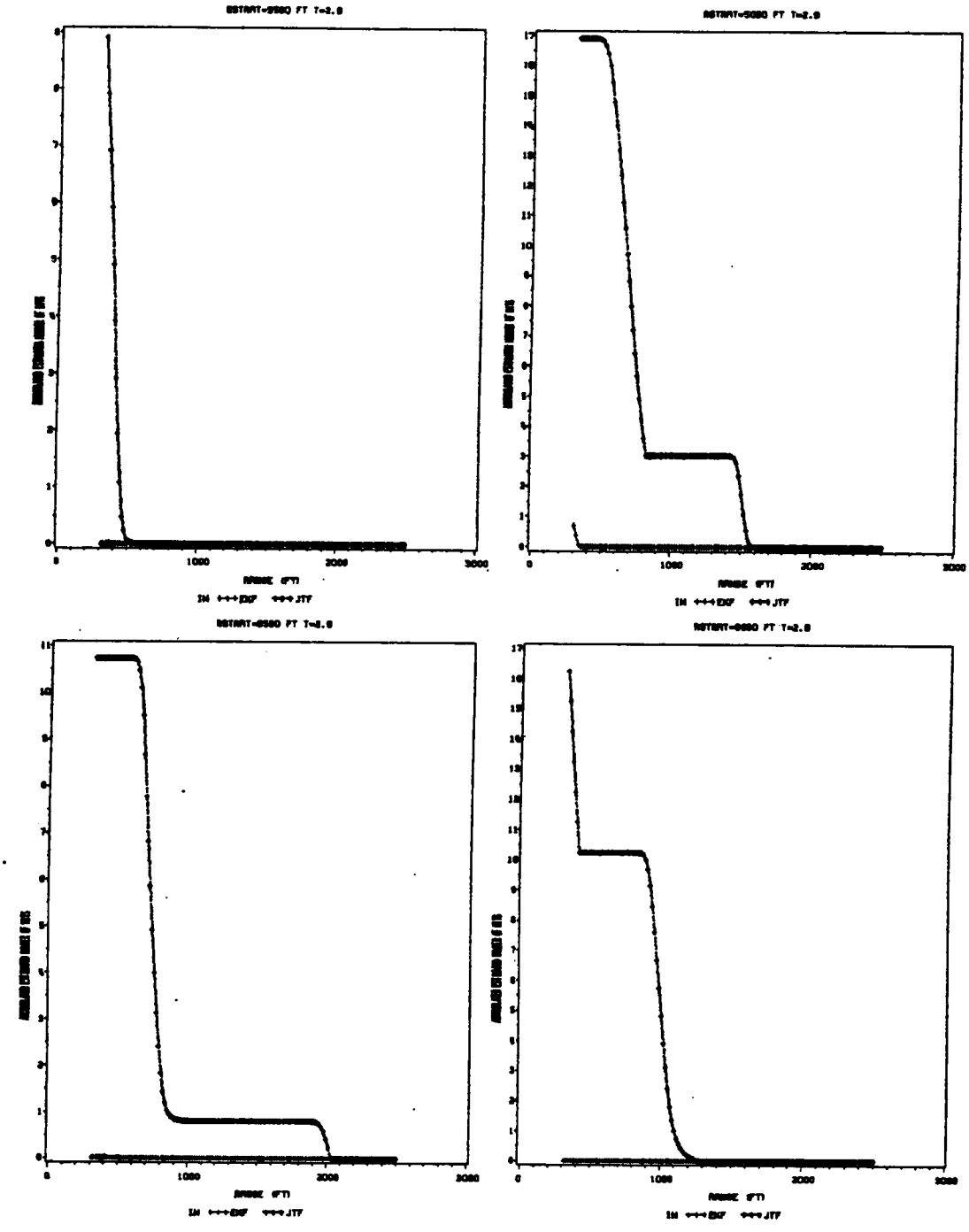

Figure 28. Accumulated Probability of Hits vs. Range, Case No. 123, Period = 2.9, Sinusoidal Wave.

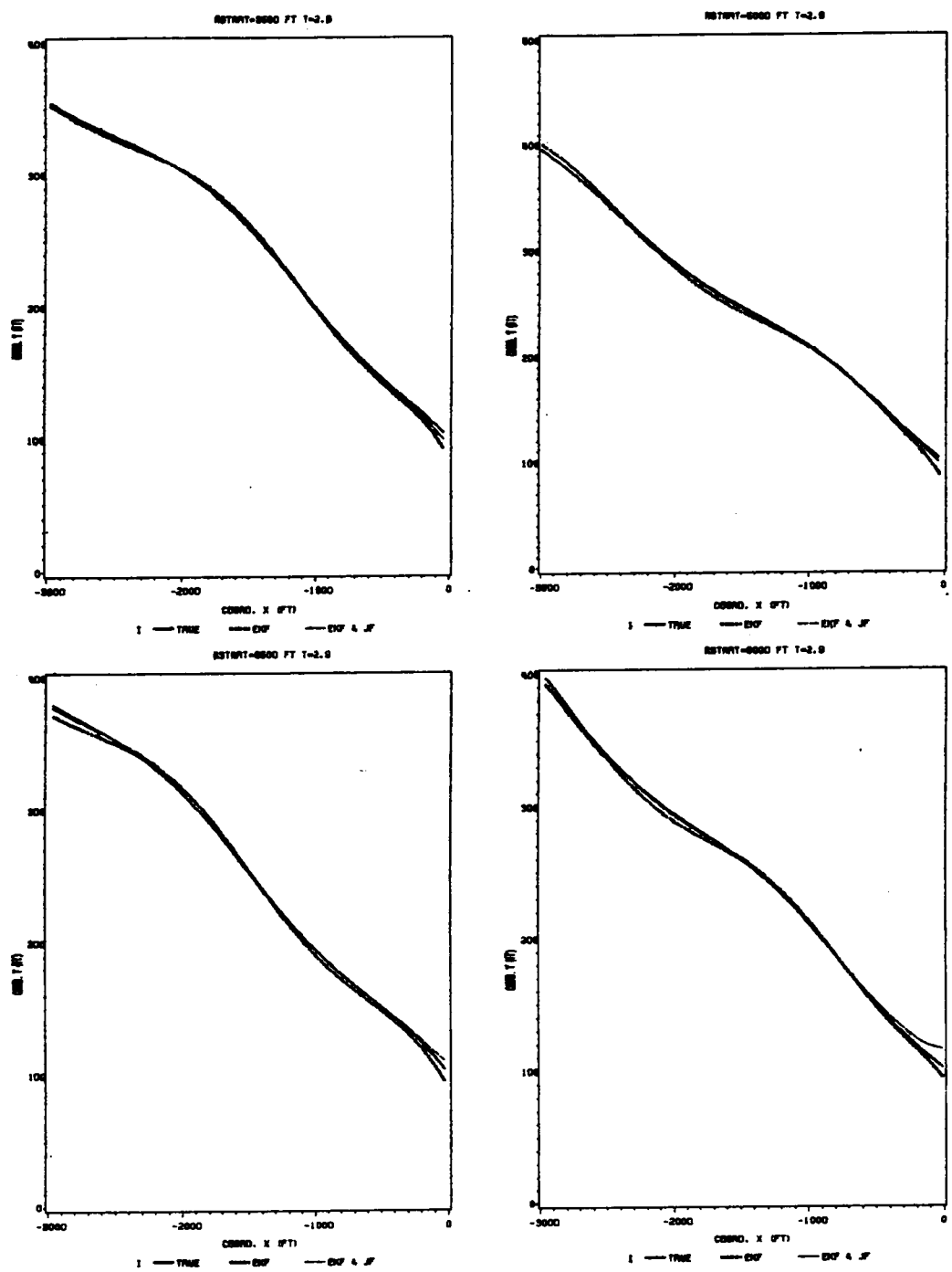

Figure 29. True and Estimated y vs. x, Case No. 123, Period = 2.9, Sinusoidal Wave.

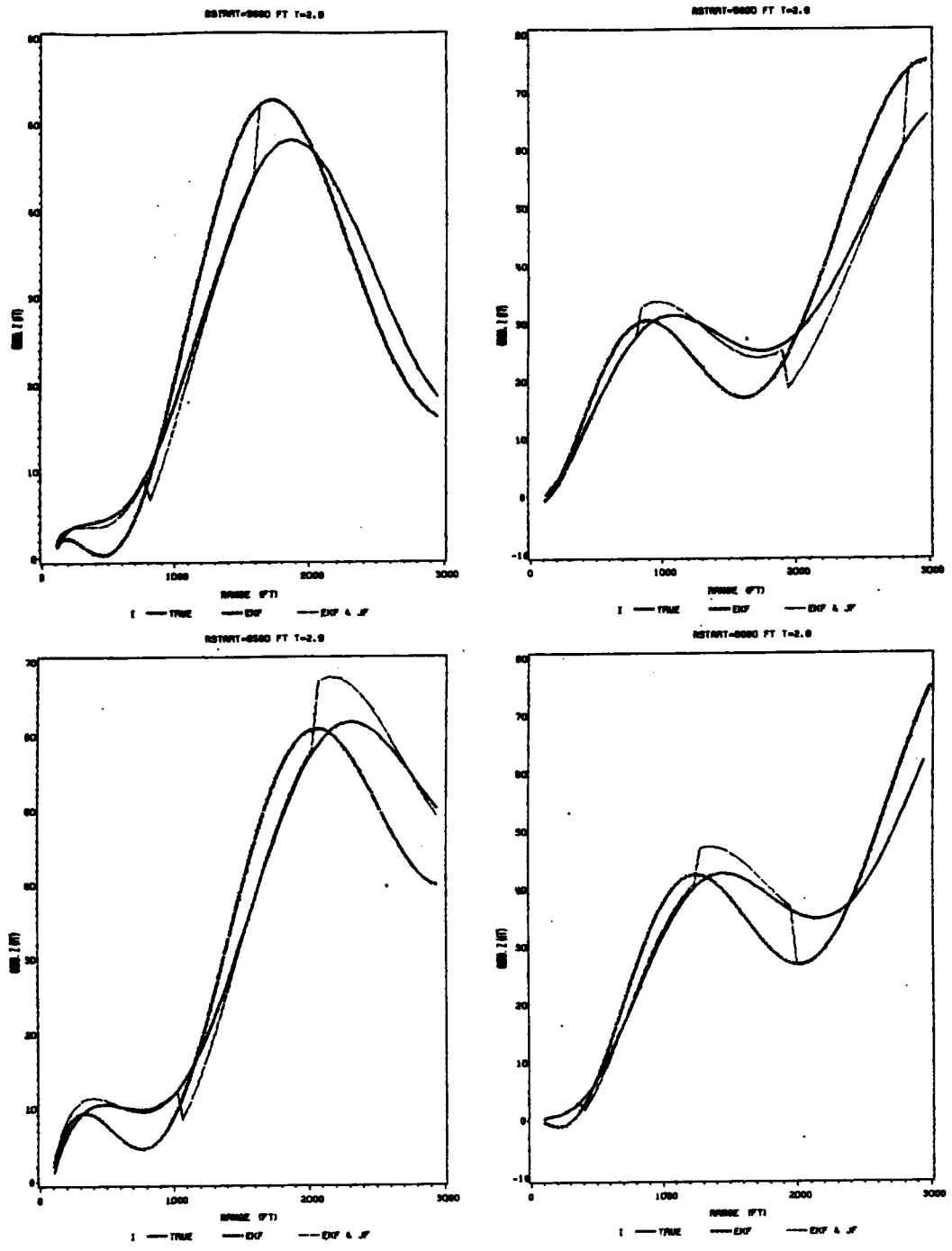

Figure 30. True and Estimated z vs. R, Case No. 123, Period = 2.9, Sinusoidal Wave.

Appendix A. Program Description

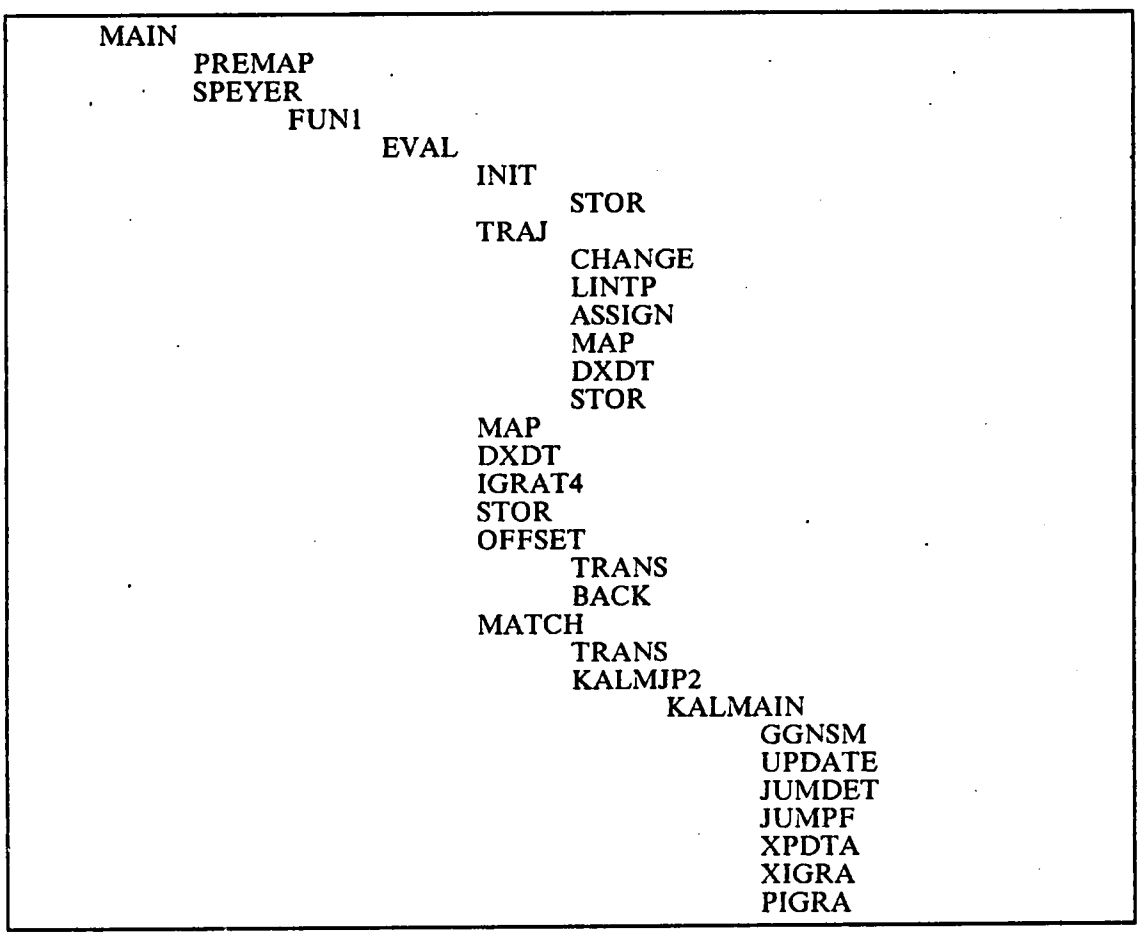

MAIN Main program.

PREMAP Sub. to preset some variables according to different IMAP.

SPEYER The optimization process entry sub.

FUN1 Sub. to supply the cost and its gradient for the opt. process.

EVAL Sub. to evalute the cost (EHITS) for given opt. parameter (period).

INIT Sub. to assign init. cond. to some parameters.

STOR Sub. to store the state vector of the missile at each time step.

TRAJ Sub. to compute the state vector history of the missile's trajectory.

CHANGE Sub. to recalculate states when the controls switch.

LINTP Linear interpolation sub.

ASSIGN Sub. to assign states & controls to the corresponding variables.

MAP Sub. to match proper waveforms of the controls due to different IMAP.

DXDT Sub. to calculate the derivatives of states.

IGRAT4 Fourth order Runge-Kutta method sub. for the integration of states,X.

OFFSET Sub. to add y offsets of missile homing-in position from radar.

TRANS Sub. to transform R, E, & A into X, Y, & Z coordinates.

BACK Sub. to transform X, Y, & Z into R, E, & A coordinates.

MATCH Sub. to prepare for the input data to sub. TSTPGM; called only when ICHG = 2.

KALMJP2 Sub. to set up init. values for filter(s), the EKF and the JTF.

KALMAIN The entry sub. for the EKF and the JTF.

GGNSM IMSL sub. to generate normal distributed noise data.

UPDATE Sub. to do the update part of EKF.

JUMDET Sub. to check the possibility of a jump.

JUMPF Sub. to calculate the jump amp. and correct the states in that filter after a jump is detected.

XPDTA Sub. to calculate the derivatives of states and the e'ement of the covariance matrix, P.

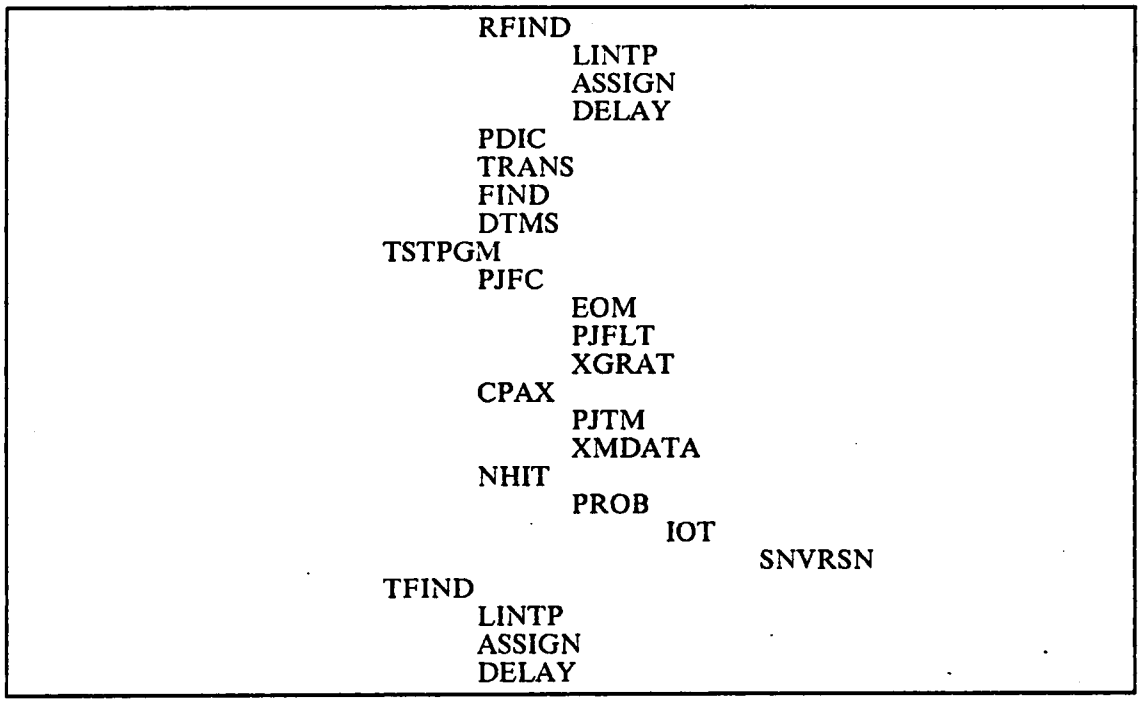

XIGRA Fourth order Runge-Kutta method sub. for the integration of states,X

PIGRA Fourth order Runge-Kutta method sub. for the integration of the elem. in the covariance matrix.

RFIND Sub. to find the first firing time of projectiles and the corresponding position of the missile.

DELAY Sub. to interpolate delayed time and position of missile from the given ones; called only when IDLY = 1.

PDIC Sub. to predict true position of missile for a given prediction time; called only when ICHG = 1

FIND Sub. to predict position of missile based on measured data for a given prediction time; called only when ICHG = 1

DTMS Fun. to calculate the distance between the two position evaluated in sub. PDIC & FIND; used only when ICHG = 1

TSTPGM The entry sub. to evaluate the probability of a hit on the missile by the projectile; called only when ICHG = 2.

EOM Sub. to compute equation of motion of the missile.

PJFLT Sub. to compute the elevation angle of the projectile.

XGRAT Fourth order Runge-Kutta integration subroutine.

CPAX Sub. to compute the closest point of approach of the missile and the projectile.

PJTM Sub. to compute the projectile's velocity and position vectors.

XMDATA Sub. to compute the missile's velocity and position vectors.

NHIT Sub. to compute the endpoints of the rectangle counted for the effect of the missile's geometrty on the POH.

PROB Sub. to accumulate the probabilities over the rectangle area.

IOT Sub. to compute the probability at specific point of the rectangle area.

SNVRSN Sub. for computing sin(h) vs. h.

TFIND Sub. to find the next firing time of the projectiles and the corresponding position of the missile.

Appendix B. Program Input Variables Description

XOPT	The init. guess-value(s) for the opt. parameter(s),X.	5.0
RSTAR	The beginning range(ft) to start changing control of N_2 and N_4	3500.
DN2	The amp. of ΔN_2	1.5
DN4	The amp. of ΔN_4	1.0
IDATA	= 1 : Read the traj. data from Disk 3	2
	= 2 : Use EKF and JTF before evaluating cost	
ITRJ	= 1 : Regenerate the traj. data; otherwise use the previous one	1
IWIGL	= 1 : Use $\tilde{N}_2$ and $\tilde{N}_4$ in eom for both the true and the est. traj.; otherwise Use N_2 and N_4 in eom for both the true and the est. traj.	
ILOOP	The no. of DO LOOP for different values of X = 1 whenever using the opt. process	
ICHG	= 1 : Use the simplified prob. fun.	2
	= 2 : Use the more realistic prob. sub.	
IDLY	= 1 : Use the delayed values of true traj. data as the approx. for the filters	0
DT	The integration time interval of the true traj. data	0.05
VM	The projectile's velocity(m/s).	900.
RNEAR	The beginning range(ft) to evalute the EHITS	2500.
RLAST	The ending range(ft) to evaluate the EHITS	300.
TPROJ	The time interval for the firing of projectiles	0.02
T	The init. value for time(s) used for both true traj. and the filters	0.
R	The init. value for range(ft) used for both the true traj. and the filters	9963.26
E	The init. value for the elevation angle(rad)	0.0042
A	The init. value for the azimuth angle(rad)	3.09
V	The init. value for the missile vel.(ft/s)	936.35
PHI	The init. value for the angle(rad) ϕ	-0.003
PSI	The init. value for the angle(rad) ψ and the filter	0.025

YOFF	The y-coord. offset of missile homing-in target from the position of radar	0 or 100 ft
ZOFF	The z-coord. offset of missile homing-in target from the position of radar	0.
P1	Constant defined in equation (2.29).	0.0117
	for international unit used in sub. EOM	1.07279EE-4
P2I	Constant defined in equation (2.29).	2.136752
PI2	for international unit used in sub. EOM	335.48472
P3G	= thrust/weight used for both the true traj. and the filter	0.41
RN1	Proportional navigation parameter in elevation	3.15
RN2	Vertical maneuver (gravity bias) parameter (pop-up)	1.0
RN3	The proportional navigation parameter in azimuth	3.0
RN4	Horizontal maneuver parameter (pop-over)	0.
IMAP	= 1 : ΔN_2 has the form of sin. wave with teh amp. DN2; = 2 : Both the ΔN_2 and ΔN_4 have the form of sin. wave; = 3 : ΔN_2 has the form of square wave with the amp. DN2; = 4 : Both the ΔN_2 and ΔN_4 have the form of square wave; = 5 : ΔN_2 has the form of square wave. with 2 opt. parameters. X(1) = time interval of switching X(2) = the amp. of the change of N_2 = 6 : Both the ΔN_2 and ΔN_4 have the form of saw tooth wave;	
DELT	The time interval for switching of N_2 & N_4 in the case IMAP = 4	0.5
LC	The max. no. of opt. process cycle	5
N	The no. of opt. parameter(s)	1
ME	The no. of equality constraint(s)	0
MI	The no. of inequality constraint(s)	0
PERT	The perturbation used for evaluating gradient	0.001
EPS1	Absolute specification of norm of the projected gradient required for convergence	0.01
EPS2	Relative specification of norm of the projected gradient required for convergence (relative to the norm at the first iteration)	0.001
EPSO	Factor applied to the internal 1-D search	1.
SPEPS	Tolerance on fun. values for 1-D search	0.001
RODG	Init. step size when performing the 1-D search	0.2
IPPR	The printout level (0-5)	4
LP	(LP-1) is the interpolation no. of data between two measurements to refine the data set for better estimation	1
INDP	= 1 : no measurement noise; otherwise measurement noise exists	1
P	The error covarance matrix for three filters	225., 4*0., 4. 9.e-6, 4*0., 4. 1.e-6, 4*0., 4.
GR	gravity constant (ft/s^2)	32.2
G	gravity constant (m/s^2)	9.807
RO0	The air density constant at the sea level ($lb\text{-}s^2/ft^4$	.23769e-2
RHOSEA	Th air density constant at the sea level (Kg/m^3)	1.226
C	The constant in English unit	.327e-4
	The constant in International unit	1.07279e-4
TRAD	The diameter of the cross-section of missile (m)	0.5
TLNGTH	The length of missile (m)	6.0

The vita has been removed from the scanned document